

UCSF

UC San Francisco Electronic Theses and Dissertations

Title

The interaction of a series of aprindine derivatives with cardiac sodium channels

Permalink

<https://escholarship.org/uc/item/1mn937sw>

Author

Moyer, James Worden

Publication Date

1985

Peer reviewed|Thesis/dissertation

The Interaction of a Series of Aprindine Derivatives
with Cardiac Sodium Channels

by

James Worden Moyer

DISSERTATION

Submitted in partial satisfaction of the requirements for the degree of

DOCTOR OF PHILOSOPHY

in

Comparative Pharmacology and Toxicology

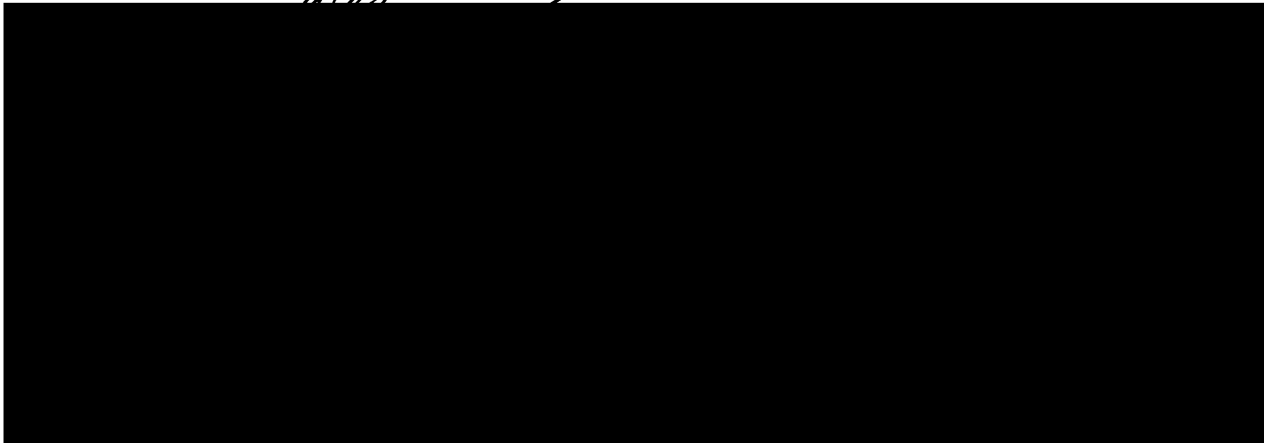
in the

GRADUATE DIVISION

of the

UNIVERSITY OF CALIFORNIA

San Francisco



M. L.
Date *4-24, 1986* *David D. Suley*
University Librarian

Degree Conferred: MAR 31 1985

Dedicated to Lane and Pricilla Moyer
With Much Love

Acknowledgements

I would like to thank Dr. Luc Hondeghem and Dr. Bert Katzung for their patient instruction during this project.

I would also like to thank my colleagues Dr. George Ehring and Mr. Charles Cotner for their help and support.

In addition I would like to thank the following people for their support and inspiration over the years: Peter Boyer, Les Brooks, Janet Forrester, Lynn Forrester, Jill Gacey, C. Hine, Harold Hodge, V. Pascucci, Ernie Vasquez, and many others.

Abstract

The Interaction of a Series of Aprindine Derivatives with Cardiac Sodium Channels

James Worden Moyer

Block of sodium current by antiarrhythmic drugs is an important mechanism underlying the efficacy of these drugs in the treatment of arrhythmias. The phenomenon of use-dependent block has been described in terms of a kinetic model known as the modulated receptor hypothesis (MRH).

This study examines the kinetics of block of a series of ten aprindine derivatives in term of the MRH model. Guinea pig papillary muscles mounted in sucrose gap were used in all the experiments. Microelectrode impalements of cells were used to measure the kinetics of drug-induced block. Voltage clamp circuits were used to modify the shape of action potentials.

Use-dependent block was assessed by stimulating the preparation at various rates in the presence of micromolar doses of drug. Time constants of block at 2 Hz varied among the ten compounds from 1.08 seconds in the fastest compound to 10.6 seconds in the slowest. Time constants of recovery from block also varied widely from 0.35 to 4.9 secs. The kinetics of block during the plateau of the action potential

was assess by voltage clamping during the plateau of the action potential. In the absence of drug a slowly developing block was found which had a time constant of onset of about 3 seconds. All the aprindine derivatives produced an exponential increasing block during depolarization. Time constants for this block varied from 100 msec to 2500 msec.

An attempt was made to correlate the physical properties of molecular weight, lipid solubility, and pKa of the ten compounds with the kinetics of block. pKa was found to correlate most strongly with the kinetics of onset and recovery from block. There was also a significant correlation between molecular weight and the onset of block.

The blocking properties of the compounds were analyzed in terms of the MRH model. A modified computer implementation of this model was developed which allows rapid determination of model parameters. With this model it becomes possible to describe and compare antiarrhythmic drugs in terms of these parameters.

Table of Contents

INTRODUCTION	1
1.1 Historical Background	2
1.2 Site of Action	5
1.3 Modulated Receptor Model	6
1.4 Voltage dependence	8
1.5 Structure-Activity Relationships	9
1.6 APRINDINE	12
2 METHODS	14
2.1 Preparation & Experimental Setup	14
2.1.1 Sucrose Gap	14
2.1.2 Animals	16
2.2 Electronics	17
2.3 Solutions	19
2.4 Experimental Protocols	19
2.5 Compounds Used in the Study	23
2.6 Physical-Chemical Constants.	27
2.7 Data analysis	30
3 USE-DEPENDENCE RESULTS	31
3.1 Use-dependence. Control	36
3.2 Use-dependence of aprindine derivatives	39
3.2.1 Aprindine use-dependent block	39
3.2.2 Moxaprine use-dependent block	41
3.2.3 A-777 use-dependent block	44

3.2.4 B-1704 use-dependent block	47
3.2.5 B-1622 use-dependent block	47
3.2.6 A-1800 use-dependent block	50
3.2.7 A-2077 use-dependent block	50
3.2.8 B-1400 use-dependence	53
3.2.9 B1401 use-dependence	53
3.2.10 B1404 use-dependence	53
3.3 Summary of use-dependence	55
4 RECOVERY RESULTS	58
5 VOLTAGE CLAMPED EXPERIMENTS	64
5.1 Slow inactivation	64
5.2 Plateau clamps in the presence of drug	67
5.2.1 Aprindine Plateau Clamp	67
5.2.2 A-1800 Plateau Clamp	72
5.2.3 A-1622 Plateau Clamp	72
5.2.4 A-777 Plateau Clamp	72
5.2.5 B-1704 Plateau Clamp	76
5.2.6 Moxaprine Plateau Clamp	76
5.2.7 B-1400 Plateau Clamp	76
5.2.8 B-1401 Plateau Clamp	76
5.2.9 B-1404 Plateau Clamp	76
5.3 Voltage dependence of plateau	82
6 DISCUSSION	86
6.1 Physical properties and use-dependence	86
6.1.1 Rate of development of block	86
6.1.2 Recovery from block	91

6.1.3 Block during the plateau	95
6.2 Models of sodium channel block	96
6.2.1 Modulated receptor model	100
6.3 Computer Implementation of the MRH	101
6.4 Simplification of the model	102
6.4.1 Rested state equilibrium	102
6.4.2 Modification of the open state model	104
6.4.3 Derivation of analytical solution	105
6.4.3.1 The Closed States Model	106
6.4.3.2 Open State Model	107
6.4.4 Least square error search	109
6.4.5 Comparison of MRH models	110
6.5 Fit of experimental data	117
6.6 Model parameters and Physical Properties	121
6.7 Conclusions	122

Table of Figures

1.1	Modulated receptor model.....	7
2.1	Sucrose gap diagram.....	15
2.2	Voltage clamped action potential.....	22
2.3	Compounds used in this study.....	24
2.4	Structural fragments of aprindine derivatives....	25
3.1	Aprindine vs A-777.....	32
3.2	Wash-in of aprindine.....	35
3.3	Use-dependence of control.....	37
3.4	Aprindine use-dependent block.....	40
3.5	d-cis-moxaprine.....	42
3.6	l-cis-moxaprine use-dependent block.....	43
3.7	A-777 use-dependent block.....	45
3.8	B-1704 use-dependent block.....	46
3.9	C-1622 use-dependent block.....	48
3.10	A-1800 use-dependent block.....	49
3.11	A-2077 use-dependent block.....	51
3.12	B-1400 use-dependent block.....	52
3.13	B-1401 use-dependent block.....	54
3.14	B-1404 use-dependent block.....	56
4.1	The recovery process.....	59
4.2	Recovery of B-1704.....	60
4.3	Fast and slow recovery.....	62

5.1	Aprindine plateau clamp.....	68
5.2	A-1800 plateau clamp.....	73
5.3	C-1622 plateau clamp.....	74
5.4	A-777 plateau clamp.....	75
5.5	B-1704 plateau clamp.....	77
5.6	Moxaprine plateau clamp.....	78
5.7	B-1400 plateau clamp.....	79
5.8	B-1401 plateau clamp.....	80
5.9	B-1404 plateau clamp.....	81
5.10	A-2077 plateau clamp.....	83
6.1	Beat constant vs molecular weight.....	88
6.2	Beat constant vs pKa.....	90
6.3	Tau recovery vs pKa.....	93
6.4	Plateau time constants vs mol. wt.....	97
6.5	Plateau time constants vs log Q.....	98
6.6	Modified modulated receptor model.....	108
6.7	Model simulation of lidocaine rate data.....	113
6.8	Model simulation of lidocaine voltage data.....	114
6.9	Model simulation of quinidine rate data.....	115
6.10	Model simulation of quinidine voltage data.....	116

Table of Tables

2.1	Buffered solutions.....	20
2.2	Structural codes for aprindine derivatives.....	26
2.3	Table of physical constants.....	29
3.1	Summary of use-dependent experiments.....	57
4.1	Recovery time constants.....	63
5.1	Slow inactivation time constants.....	65
5.2	Summary of plateau clamp data.....	84
5.3	Zero time intercepts.....	85
6.1	Physical characteristics of compounds.....	87
6.2	Time constants of recovery.....	94
6.3	Model constants used.....	112
6.4	Parameters for modified model.....	120

CHAPTER 1

INTRODUCTION

"The optimal antiarrhythmic therapy has not yet been developed. However, as we gain more knowledge about the genesis of cardiac arrhythmias, we can foresee the time when a specific drug will be tailored to a specific disorder of cardiac rate and rhythm." (Lucchesi 1982)

Block of sodium current by antiarrhythmic drugs is an important mechanism underlying the efficacy of these drugs in the treatment of cardiac dysrhythmias (Weidmann 1955b, Hauswirth & Singh 1979). The complexity of drug effects, which depend on rate, action potential duration, and resting membrane potential, have frustrated attempts to systematically compare these drugs and to arrive at rational choices in selecting an agent to fit a particular dysrhythmia. In recent years many studies, both in nerve and heart, have revealed important aspects of the mechanism of action of this class of agents that has brought closer the goal of rational drug design and use.

Design of optimal antiarrhythmic drugs will require a deeper understanding of the structural correlates which determine blocking kinetics as well as voltage selectivity, and pH dependence. Further clarification of the role of molecular structure would hopefully allow the design of safer, more specific antiarrhythmic compounds.

The purpose of this work was to determine what structural properties of molecules might be responsible for the kinetic behavior of compounds in the aprindine series.

1.1. Historical Background

The rising phase (phase 0) of the action potential in nerve and heart is due to a rapid increase in the permeability of the cell membrane for sodium ions (Hodgkin 1951, Draper & Weidmann 1951). In a pioneering study Weidmann (1955b) demonstrated that local anesthetics decreased the maximum rate of rise of the action potential (V_{max}) without affecting the resting membrane potential. He also noted that this blocking action could be reduced by passing hyperpolarizing current. Weidmann interpreted these observations as an indication that the drugs act by shifting inactivation kinetics to more negative potentials.

The first report describing the kinetics of block development by these compounds in cardiac tissue was made by Johnson & Mckinnon (1957). They showed that quinidine applied to guinea pig ventricular fibers produced a progressive decline in the maximum rate of depolarization of the action potential (V_{max}) upon repetitive stimulation. The rate of the beat-by-beat decline of V_{max} as well as the eventual steady-state level of block was dependent on the rate of stimulation. At sufficiently slow rates the

drug appeared to have no effect. Moreover a change in stimulation rate produced a change in the level of block, which took several beats to achieve. Like Weidmann, Johnson and Mckinnon assumed V_{max} to be proportional to sodium permeability and thus a valid indicator of the level of sodium channel block.

Heistracher (1971) showed similar rate dependent effects on V_{max} for quinidine and procainamide and demonstrated that recovery from block was an exponential process insensitive to drug concentration.

Chen, Gettes, & Katzung (1975), demonstrated that recovery from block was also voltage dependent. In potassium depolarized guinea pig ventricular tissue, recovery from lidocaine-induced block was slower than recovery at more negative potentials.

Similar observations on the relationship between channel use and local anesthetic block were made by Strichartz (1973) in nerve. He applied the quaternary lidocaine derivative QX-314 to single frog nodes of Ranvier. Using a voltage clamp protocol, he found that block by QX-314 was enhanced by repetitive depolarizations. Larger depolarizations produced greater levels of block. If depolarizations were preceded by strong hyperpolarizations block was relieved. This "use-dependent" blocking and unblocking demonstrated a voltage-dependent equilibrium

between blocked and conducting channels. The steady-state could be reached only after repetitive opening of the channels. Strichartz suggested that the drug could enter or leave its blocking site only when the channel was conducting.

Courtney (1975) showed that similar use-dependent blocking effects were produced by the tertiary amine local anesthetic GEA-968. He also reported a shift in inactivation kinetics of blocked channels that developed with use. This voltage shift, similar to that seen by Weidmann, was incorporated into the Strichartz model. It seemed clear that not only may closed gates prevent access to and from the receptor, but presence of the drug may also modify gating by shifting the voltage dependence of inactivation to more negative potentials.

Courtney also observed, but didn't include in his model, recovery from block in the absence of channel opening. This closed-channel unblocking was much faster with the tertiary amine than that seen by Strichartz for quaternary compounds.

Khodorov (1976) further explored these closed channel interactions. In the frog node, long depolarizing pulses produces a slowly developing block in the presence of tertiary amines. This slowly developing block was not seen with quaternary compounds. He also demonstrated closed-

channel voltage-dependent unblocking. From his results Khodorov developed a model which incorporated separate receptors for tertiary and quaternary compounds.

1.2. Site of Action

The site of action and active form of local anesthetics has been the subject of some controversy. Physical theories of membrane fluidity (Metcalf et al. 1971), membrane expansion (Seeman 1972) and surface-charge modulation (Ritchie 1975) have been invoked as well as a specific channel receptor (Hille 1966).

Experiments in various nerve preparations measuring block as a function of internal and external pH (Ritchie et al. 1965, Narahashi et al. 1970, Strobel & Bianchi 1970) led to the conclusion that local anesthetics are most potent from inside the cell in the cationic form. Similar results have been obtained in cardiac tissue (Gliklich & Hoffman 1978, Grant et al. 1980, Gintant et al. 1983). It is also clear that the uncharged form is capable of producing block both in nerve and cardiac tissue. (Ritchie & Ritchie 1968, Hille 1977, Hondeghem et al. 1978).

1.3. Modulated Receptor Model

The observations cited above indicate that local anesthetic block depends on stimulation pattern, voltage, pH and dose in a complex way. In an attempt to synthesize these effects into a coherent model Hille (1977b) and Hondeghem and Katzung (1977) presented a model for the interaction of local anesthetics with the sodium channel. They extended the Strichartz-Courtney model to include closed channel interactions. The model known as the "Modulated Receptor Hypothesis" (Figure 1.1) includes the following propositions.

- 1) Drugs bind to a receptor associated with the transmembrane ionic channel.
- 2) The affinity of the drug for the receptor is modulated by the state of the channel (rested, activated, or inactivated).
- 3) Drug-associated channels do not conduct.
- 4) The inactivation kinetics of drug-bound channels are shifted in the hyperpolarizing direction.
- 5) Drugs may interact with the channel either through a hydrophilic pathway (charged drug), when the channels are open, or a hydrophobic pathway (uncharged drug) through the cell membrane at any time.

The modulated receptor model has been quite successful in describing and predicting behavior of numerous

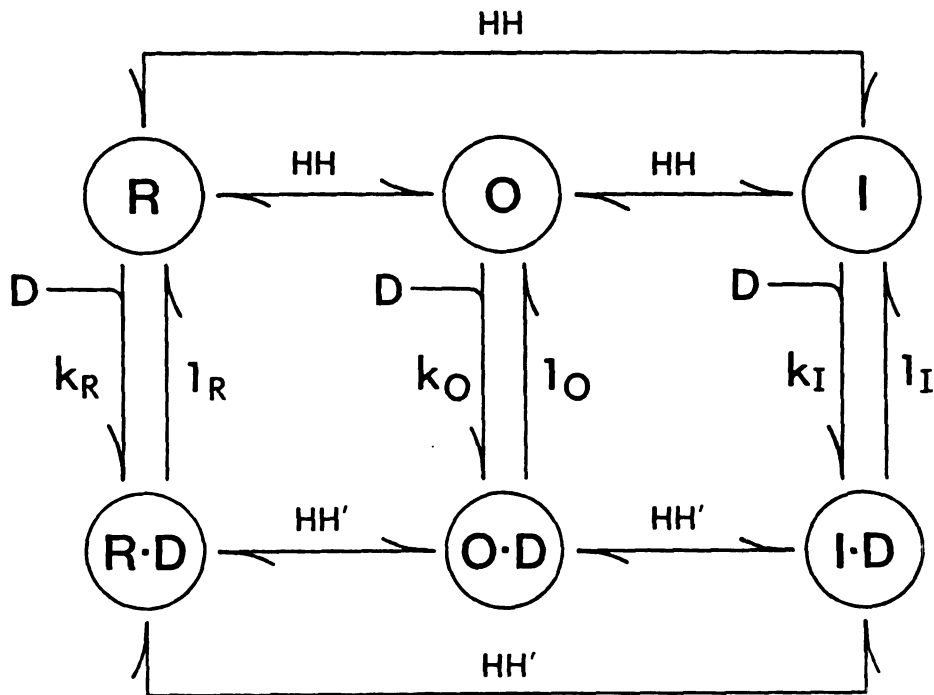


Figure 1.1 Modulated receptor model.

Drug-free channels (R , O , I) bind drug (D) with rate constants k_R , k_A , and k_I . Drug associated channels ($R \cdot D$, $O \cdot D$, $I \cdot D$) disassociate with rate constants l_R , l_O , and l_I . Channel gating (HH) is shifted in the hyperpolarizing direction for drug associated channels (HH').

sodium and calcium channel blockers . In the years since its introduction more than 100 studies have referred to the modulated receptor hypotheses to describe the action of sodium and calcium channel blockers (Hondegem & Katzung 1984).

With the advent of this model it became possible to describe the behavior of local anesthetic drugs for any rate or rhythm and any membrane potential in terms of a voltage shift and affinities of the drugs for three channel states. In contrast, comparisons between drugs such as "half-blocking potency" are valid only in the context of a single set of rate, rhythm, and potential conditions.

1.4. Voltage dependence

Since voltage dependent channel kinetics modulate receptor affinity blocking is a priori voltage dependent. Whether the affinities for a particular state of the channel are voltage dependent is a question that remains unanswered.

Strichartz (1973), Courtney (1975) and Cahalan (1978) have shown that clamp pulses to progressively higher potentials increase open channel block. Cahalan (1978) and Yeh & Narahashi (1977), and Starmer et al.(1983) have developed models that explain voltage dependence of open channel block. The models attempt to predict the effect

of an electric field on the action of a charged local anesthetic.

Voltage dependence of block of closed channels is more controversial. Although their analysis has been questioned (Courtney 1983), Weld et al. (1982) reported voltage dependent inactivation block in the presence of quinidine. Hondeghem and Matsubara (1984) have reported similar results. They reported a time constant and voltage dependence similar to "slow inactivation" (Clarkson et al. 1983) and proposed that quinidine somehow promotes slow inactivation. Closed channel interactions are presumably with the uncharged form of the molecule, dissolved in the membrane. The mechanism by which the membrane electric field would influence receptor binding in this case is not as apparent as for open channel interactions. Studies with other local anesthetics have not demonstrated this voltage dependence (Mason et al. 1983, Sanchez-Chupula et al. 1983). Whether quinidine is unique in this regard remains to be seen.

1.5. Structure-Activity Relationships

Sodium channels can be blocked by a great variety of chemical structures. Amino-esters, amino-ethers and many other chemical types show blocking behavior (Seeman 1972). The success of the specific drug-receptor interactions

inherent in the modulated receptor hypothesis is perhaps surprising in light of the very diverse range of drugs which show local anesthetic and antiarrhythmic effects.

In 1948 Lofgren proposed a general structure for local anesthetic compounds: consisting of an aromatic structure linked to an amine residue by an intermediate chain. If we broaden the definition to a hydrophobic residue-intermediate chain-hydrophilic residue, we include most of the compounds that are in clinical use as local anesthetic or antiarrhythmic agents.

The sodium channel blocking kinetics of antiarrhythmic drugs vary greatly. Quinidine, under normal conditions, develops use-dependent block over many action potentials whereas lidocaine reaches a steady-state level of block within a few beats. Likewise, the time constant of recovery of block at normal potentials for quinidine is more than ten times that for lidocaine.

In nerve preparations a global parameter, half-blocking potency, correlates well with lipid solubility (Overton 1896, Meyer 1901, Seeman 1972, Courriere 1978). For cardiac tissue, Courtney (1983b) has shown a good correlation between blocking during the action potential and the lipid distribution coefficient (Q) of a series of amide-linked local anaesthetics. The correlation between lipid solubility and block may result from the effect of

molecular charge on the rate of development of block. Permanently charged molecules develop use-dependent block slowly and recover slowly. Uncharged molecules exhibit rapid blocking and unblocking. Tertiary amines have intermediate blocking rates that can be modified by pH (Grant et al. 1980).

Recovery from block has been shown to be related to the molecular weight of a blocking agent (Courtney 1980, Ban & Sada 1980). This correlation is improved by also considering lipid solubility. Apparently there is a size-sensitive step involved in closed channel unblocking that is the rate-limiting process. Although size and solubility seems to be important structural parameters determining the kinetics of unblocking, exceptions can be found (Ehring et al. 1980, Sada et al. 1980, Moyer & Hondeghem 1982, Campbell & VaughanWilliams 1983).

Physical parameters, though apparently important in comparing different compounds, cannot explain the differences in the kinetics of block and unblock seen with optical isomers of quinidine, disopyramide (Mirro et al. 1981), and RAC-109 (Yeh 1980). These studies showed significant differences between isomers in rates of block as well as changes in action potential duration. Differences in potency of up to ten fold have also been shown for optical isomers of local anaesthetic drugs in nerve (Akerman

et al. 1969, Akerman 1973, Nelson et al. 1980).

From these studies it is clear that although the physical parameters of size, lipid solubility, and charge are important there also appears to be a stereoselective component of block that modulates the kinetic behavior of these compounds.

The kinetic behavior of a drug can have important implications for its suitability in a particular arrhythmia (Hondeghe & Katzung 1984). Indeed, it has been suggested that division of sodium channel blockers by blocking rate into slow, fast or intermediate categories might serve as a secondary classification system for these drugs (Campbell 1983).

1.6. APRINDINE

Aprindine hydrochloride (N-[3-diethylamino)propyl]-2-indamine) is a new antiarrhythmic agent that has been extensively used in Europe and is available in this country as an investigational drug. It has been used for the treatment of ventricular and supraventricular tachyarrhythmias (Zipes et al. 1978, Fasola et al. 1977). Its electrophysiological effects include slowing of phase 0 and phase 4 depolarization rates, reduction of action potential duration, and an increase in the refractory periods of the atrium, AV node, and His-Purkinje system

(Verdonck et al. 1974, Carmeliet et al. 1974, Steinberg & Greenspan 1976, Gilmour et al. 1981). Use of aprindine has been limited due to serious side effects - especially agranulocytosis, which occurs at a rate of 1 in 400-1000 patients (VanLeeuwen & Meyboom 1976, Pisciotta & Cronkite 1983). Recently, the aprindine derivative moxaprine, which appears to be less toxic, has begun trials in Europe (Staessen et al. 1981).

Initial studies with aprindine demonstrated slow rate-dependent blocking with a time course similar to quinidine (Moyer & Hondeghem 1978). Studies of derivatives of aprindine showed that these closely related compounds had a large range of blocking and unblocking rates (Moyer et al. 1982). The availability of a large series of aprindine derivatives, as well as their intriguing differences in kinetics of block, suggested that this series could offer important clues as to what structural characteristics are important in determining the kinetics of sodium channel block.

CHAPTER 2

METHODS

2.1. Preparation & Experimental Setup

2.1.1. Sucrose Gap

All experiments were performed using the single sucrose gap preparation (Beeler and Reuter 1970, New and Trautwein 1972). A schematic diagram of this preparation is shown in Figure 2.1. The tissue chamber consisted of three compartments formed from a block of Plexiglas. The front and rear chambers were identical reservoirs with a volume of 1.5 ml. The center sucrose chamber was 1.5 mm wide and was separated from the other chambers by a thin sheet of rubber on each side. Holes were punched in the rubber to provide a snug fit on the muscle without damaging it. Solutions flowed in from one side of each chamber and were removed from the opposite side. The flow was adjusted so that a complete exchange of solution in the front chamber took about 20 sec. The inflow and outflow ports were positioned to insure adequate mixing and temperature control. Temperature in the front chamber was monitored by a temperature probe (Yellow Springs instrument Co.) positioned close to the preparation. Temperature was maintained between 36° and 37° C. Pre-heated

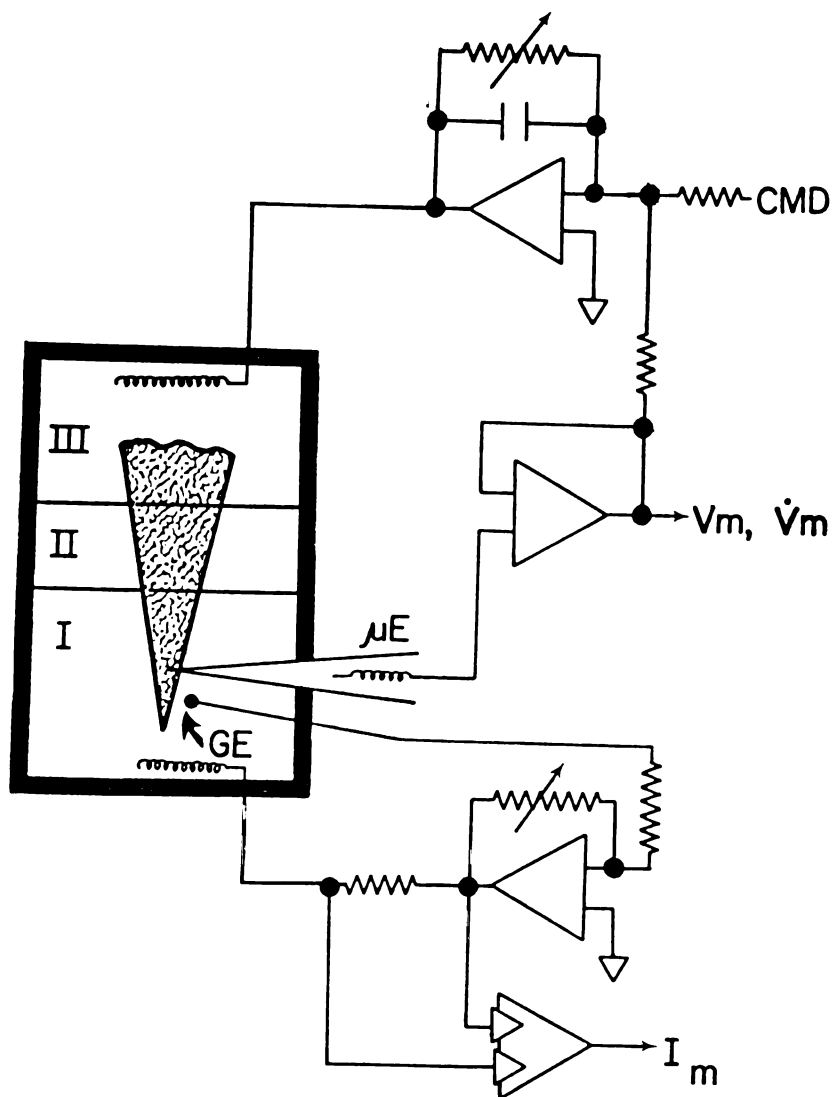


Figure 2.1 Sucrose Gap

Experimental chamber was divided into three sections. Normal salt solution (I), sucrose compartment (II), and a high potassium chamber. Current was passed from the silver electrode (III) through the muscle when a command potential (CMD) is given to the clamp amplifier. Current passing through the gap (I_m) is measured by the ground clamp circuit, which also keeps the ground reference electrode (GE) at zero.

oxygenated solutions were mounted above the experimental table and gravity-fed to drip chambers where the flow rate was controlled. The solutions were heated to their final temperature in a water bath directly below the muscle chambers.

2.1.2. Animals

Young albino guinea pigs of either sex weighing between 250-400 g were used in these experiments. The animals were housed in our animal care facilities according to USDA federal guidelines for a duration of 1 day to 2 weeks before experiment. Their diet consisted of standard diet (Wayne Guinea Pig Diet). Animals were killed by a blow to the neck. The hearts were removed and transferred to cold (10° C) oxygenated Tyrode's solution. Under a dissecting microscope, papillary muscles were removed from the right or left ventricle. Muscles with irregular morphology or improper size (greater than 0.7 mm or less than .4 mm) were discarded. Care was taken during the dissection to relieve tension on the papillary and prevent stretching. Excised papillary muscles were placed in a petri dish filled with cold HEPES buffered Tyrode's solution bubbling with 100% oxygen and allowed to come to room temperature before the experiment. The muscles were securely tied by a short length of surgical

thread around the chorda tendineae extending from the tip of the muscle in preparation for mounting in the sucrose gap.

2.2. Electronics

Current was passed through the muscle from a silver wire electrode positioned in the rear chamber to an identical silver electrode in the front chamber. The reference electrode in the front chamber was kept at virtual ground by a ground clamp circuit which also measured the current flowing through the preparation. A silver-silver chloride pellet served as the sensing electrode for the ground clamp circuit.

Membrane potential was recorded by means of a microelectrode filled with 3 M KCl. 1 mm o.d. conventional pyrex glass tubing or 1.2 mm Omega Dot tubing were pulled on a vertical electrode puller (David Kopf Instr.). Electrodes were selected with resistances of 15-20 M-Ohm (conventional) or 25-30 M-Ohm (Omega Dot). These resistances correspond to tip diameters in the range of 0.5 - 1.0 microns or less (Geddes 1972). Electrodes were inserted into a microelectrode holder (WPI Co.) filled with 3M KCl, and attached directly to the microelectrode pre-amplifier (input resistance 10^{15} ohms) mounted on a micromanipulator.

Membrane potential measurements were displayed on a storage oscilloscope (Tektronics 564B) and recorded on a Grass polygraph. Action potentials were also captured in an A-to-D converter and dumped, by D-to-A conversion, at a slow speed on the polygraph. The membrane signals were electronically differentiated and were displayed on the storage oscilloscope to allow monitoring and control of stimulus-upstroke latencies. The differentiated signal (dV/dt), linear from 10 V/sec to 750 V/sec, was also sent to a peak detector which provided as output the peak dV/dt for a period of 70 msec for recording by the polygraph (Hondeghe and Cotner 1978).

Clamp protocols were created as files on a Digital Equipment Corp. PDP-11/34A computer and compiled using a special compiler developed as part of this dissertation research. This compiler allowed clamp durations and potentials to be easily specified and changed. Clamp mode (current, or voltage) as well as automatic branching between protocols was also provided by the compiler. Compiled protocols were then loaded into a Kim microprocessor (MOS Technology Inc.) that controlled the voltage clamp amplifier. The Kim operating system, also developed as part of this dissertation, allowed two-way communication between the microprocessor and the minicomputer. The microprocessor was equipped with a timer board (MDC Inc.)

that allowed timing of pulses to an accuracy of 1 microsecond. The digitally stored pulse amplitudes were sent to a separate, optically coupled, digital-to-analog converter that provided the command potentials to the clamp amplifier.

2.3. Solutions

All buffered solutions were buffered with HEPES (N-2-Hydroxethyl Piperazine-N-2-Ethanesulfonic Acid). This buffer was chosen to avoid the divalent cation interactions and other problems associated with commonly used buffers (Spitzer & Hogan 1979, Wiggins 1980, Courtney 1981). Solutions were made in two-liter batches as 20:1 buffered stock. These were diluted, and the glucose added, on the day of the experiment. Buffered solutions were titrated, if necessary, with 1N NaOH to give solutions with a pH of 7.40 at 37° C. The composition of the buffered solutions is shown in table 2.1.

2.4. Experimental Protocols

After an initial equilibration period the papillary muscle was impaled with a glass microelectrode. Only cells that possessed adequate resting membrane potentials (< -80 mV) and showed healthy action potentials (duration > 150 msec) were used.

BUFFERED SOLUTIONS

	Normal Na+ (mM)	High K+ (mM)
Na+	145.0	6.0
K+	4.0	145.0
Ca++	1.8	1.8
Mg++	1.1	1.1
Cl-	152.0	152.0
Glucose	5.5	5.5
HEPES	5.0	5.0

Table 2.1 Solutions Used in the experiments.

Preparations that had significant rate-dependent depression of V_{max} under control conditions were also discarded. For all experiments a one millisecond current-clamped stimulus was used to evoke the action potential. The stimulus strength was adjusted to provide a latency of less than 5 msec. The criteria of short latency is known to be important in insuring linearity of V_{max} measurement (Walton and Fozzard 1979). Only preparations that demonstrated a constant V_{max} over a range of at least 2 msec were used in experiments. During the experiments the stimulus strength was adjusted to keep V_{max} within this range. At least three preparations were used for each drug although not every protocol was used in all preparations.

Rate-dependent effects were elicited with a 10 second train of current-clamped stimulated action potentials at various frequencies. The cell was allowed to recover at least 20 seconds between successive determinations.

The kinetics of post-stimulation recovery were assessed by a single action potential invoked at variable intervals after the end of the last action potential in a train that produced a steady-state level of block. Trains with a 300 msec ISI (InterStimulus Interval) were used.

Voltage clamp experiments were used to assess the blocking effects of the drugs at depolarized potentials.

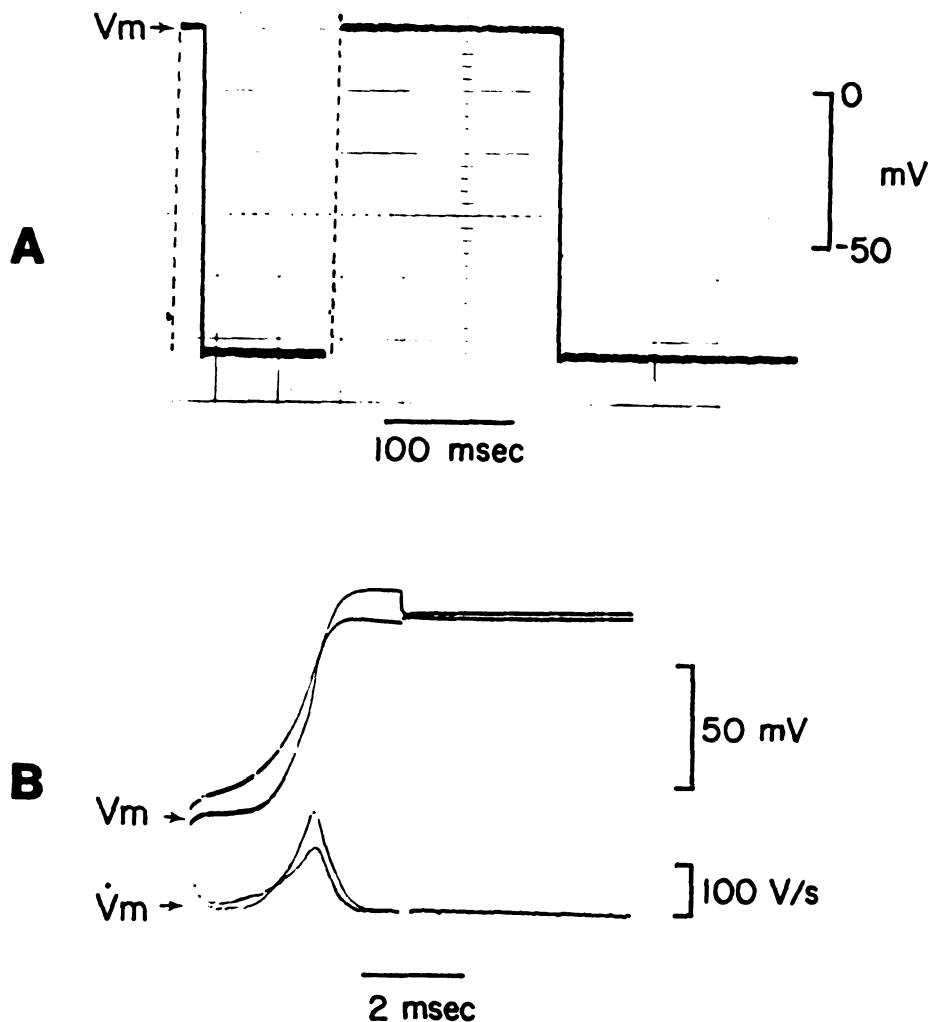


Figure 2.2 Voltage Clamped Action Potential

A) A clamp to +20 mV for 10 msec followed by a 180 msec clamp. Dashed lines indicate free running upstroke.

B) Two superimposed action potentials (V_m) show free running upstroke followed by the voltage clamp. This experiment, done in the presence of a sodium channel blocker shows a decline in V_{max} (V_m) during the second action potential.

The flexibility of the microprocessor controlled voltage clamp allowed control of the membrane potential soon after the upstroke (within 5 msec). The protocol consisted of voltage clamping the resting potential, stimulating the cell under current clamp, permitting a free running upstroke, and then voltage clamping the plateau (Figure 2.2). This new technique, developed for this research, allowed the study of drug effects at various potentials, with plateau durations ranging from 10 msec to several seconds.

2.5. Compounds Used in the Study

The compounds used in this study, all derivatives of the parent compound aprindine, are shown in Figure 2.3 (page 24). These compounds were synthesized and kindly provided by A. Christians S.A., Brussels, Belgium.

Aprindine and its derivatives fit the general model of local anesthetics proposed by Lofgrun (1948). That is, an aromatic moiety, a connecting chain and a terminal amino group. Figure 2.4 (page 25) divides the compounds used in this study into these three parts. These compounds have been given a code corresponding to the fragment used to make up its structure (see Table 2.2, page 26). The code simplifies the description of structural similarities and differences between compounds.

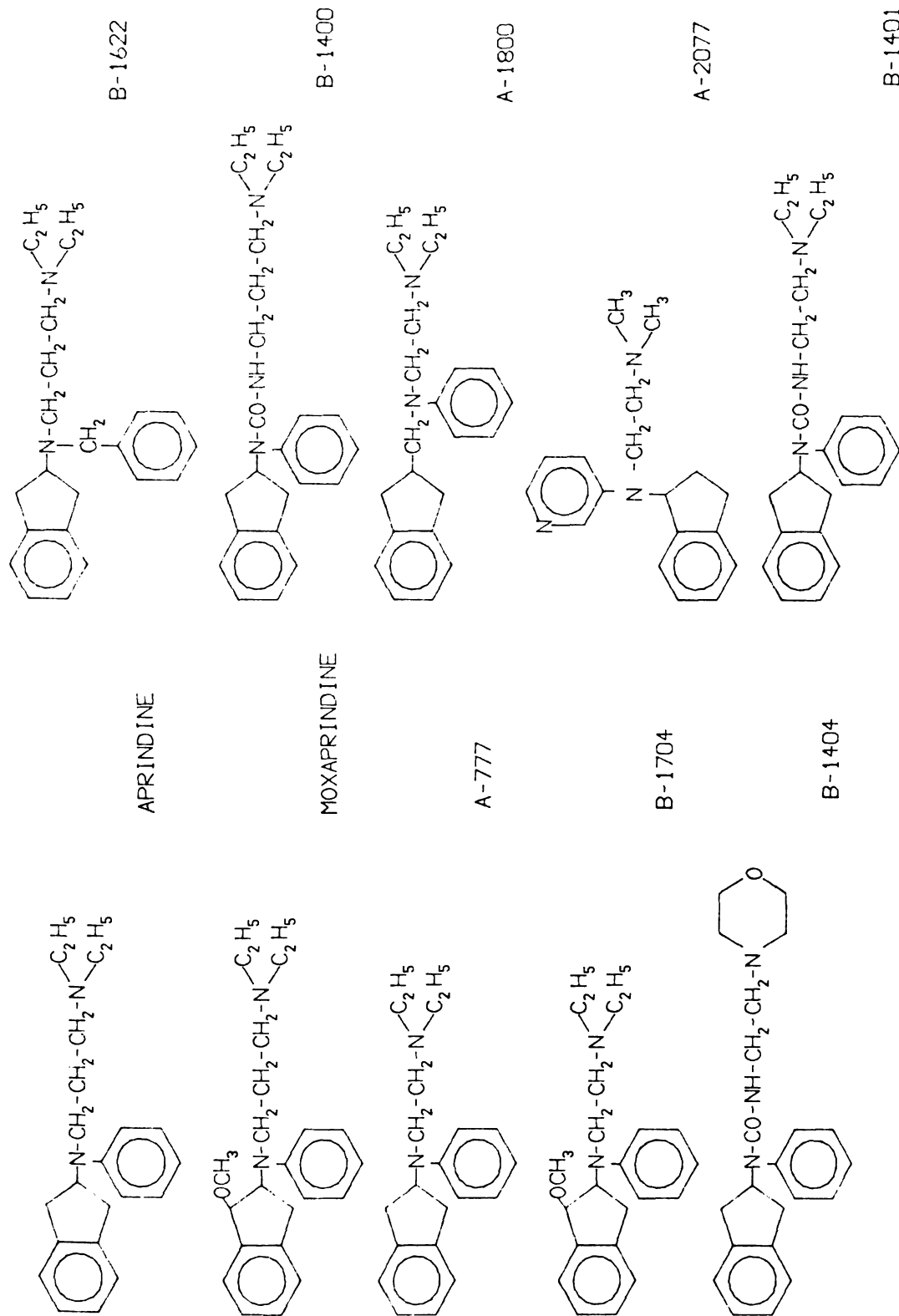


Figure 2.3 Compounds used in this study.

AROMATIC-----CONNECTING CHAIN ----- AMINO GROUP

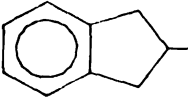
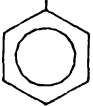
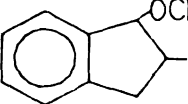
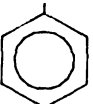
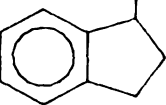
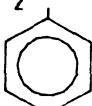
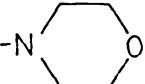
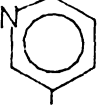

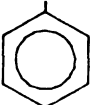
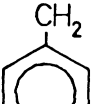
 1	$-\text{N}-\text{CH}_2-\text{CH}_2-\text{CH}_2-$  1	$-\text{N}(\text{C}_2\text{H}_5)_2$ 1
 2	$-\text{N}-\text{CO}-\text{NH}-\text{CH}_2-\text{CH}_2-\text{CH}_2-$  2	$-\text{N}(\text{CH}_3)_2$ 2
 3	$-\text{CH}_2-\text{N}-\text{CH}_2-\text{CH}_2\text{N}$  3	 3
	 $-\text{N}-\text{CH}_2-\text{CH}_2-$ 4	
	$-\text{N}-\text{CO}-\text{NH}-\text{CH}_2-\text{CH}_2-$  5	
	$-\text{N}-\text{CH}_2-\text{CH}_2-$  6	
	$-\text{N}-\text{CH}_2-\text{CH}_2-\text{CH}_2-$ CH_2  7	

Figure 2.4 Structural Fragments for Aprindine Derivatives

Compound	Code	Molecular Weight (Free Base)
Aprindine	1-1-1	322.49
Moxaprine	2-1-1	352.52
A-777	1-6-1	308.47
B-1704	2-6-1	338.49
B-1404	1-5-3	365.47
B-1622	1-7-1	336.52
A-1800	1-3-1	322.49
A-2077	3-4-2	281.40
B-1401	1-5-1	351.49
B-1400	1-2-1	365.42

Table 2.2 Structural Codes for Aprindine Derivatives

The compounds used in this study are all indane-amine derivatives. 2-Indane is the basic hydrophobic group for eight out of the ten derivatives. The two alternate structures are methoxy-indane and 1-indane. The hydrophobic fragments in column A have chiral centers at the 2 and 3 positions. Unless noted, all experiments were done with the racemic mixture.

The seven different connecting-chains fragments are shown in column B. Chain 2 and 5 contain a urea group; all others are tertiary amines with aliphatic chains.

Eight out of ten of the compounds contain the diethyl terminal amino group. The other terminal amino groups are the dimethyl amine and the morpholine group. Table 2.2 lists the codes used to describe each of the compounds. The first number in the code corresponds to the hydrophobic fragment in column A of Figure 2.4 (page 25) the second number indicates the connecting chain and the third number the terminal amino group.

2.6. Physical-Chemical Constants.

The pKa's and partition coefficients were determined, in collaboration with Dr. Wayne Settle, by simultaneous potentiometric titration (Koski et al. 1975). A 12x75 mm glass test tube was used as the sample cell. A teflon cuvette stirring bar mixed the sample solution. The cell

was maintained at 37° C with a Haake water bath circulator. Carbon dioxide-free air blanketed the sample to prevent CO₂ absorption from the air. A Markson model 90 pH meter with a combination microelectrode was used for measuring the pH. The output was recorded on an Omniscribe chart recorder.

The titrant was delivered into the cell by means of a 100 microliter Hamilton syringe driven by a Palmer slow injection apparatus. The major modification of the published technique was to reduce the volume of the sample to 1 ml for the titration, because of the limited sample available.

Prior to the analysis of the ten compounds, a preliminary study using lidocaine was carried out to validate the technique. Tests were also performed to determine proper rates of addition of the titrant and mixing of the solution to maintain equilibrium in the two phase system.

For each determination 0.004 mmole of the compound was added to the test cell. Titration rates were adjusted to require approximately two hours to complete each sample. The pKa was determined by measuring the apparent pKa in three ethanol concentrations and extrapolating to zero percent.

Determination of the partition coefficients was done in the presence of 2.4%, 4.7%, 6.9% octanol by volume.

Compound	pKa (\pm S.D.)	Log P (\pm S.D.)	Log Q
B-1404	6.38 \pm .12	2.65 \pm .05	2.61
A-2077	8.43 \pm .05	3.14 \pm .12	2.07
A-777	8.80 \pm .07	3.63 \pm .05	2.21
A-1800	8.13 \pm .12	4.34 \pm .04	3.54
A-1704	8.73 \pm .17	3.43 \pm .05	2.08
Aprindine	9.18 \pm .04	4.20 \pm .08	2.41
Moxaprine	9.63 \pm .02	4.32 \pm .10	2.09
B-1401	8.82 \pm .11	3.36 \pm .08	1.92
B-1400	9.45 \pm .15	3.02 \pm .12	.966
C-1622	9.26 \pm .10	4.34 \pm .18	2.36

Table 2.3 Physical constants determined in this study. For Log P (logarithm of the partition coefficient), N=3. For pKa, N=4. Values are shown plus or minus one standard deviation. Log Q, the distribution coefficient at pH 7.4 is also shown.

The results of the pKa and Log P determinations are shown in Figure 2.5.

2.7. Data analysis

Vmax values were measured from strip chart records by use of a digitizing tablet connected to the computer. Data for each experiment was stored in separate files for later analysis.

A graphics package, written as part of this research, was used to plot most of the figures seen in this dissertation. This graphics package included non-linear least-square exponential fitting routines. These routines were used in the exponential fits shown in the results section.

A separate regression program was written to perform the multiple regressions shown in the results section. This program was tested against several sets of published data with identical results (Wonnacott & Wonnacott 1977).

CHAPTER 3

USE-DEPENDENCE RESULTS

Under appropriate conditions all commonly used sodium channel blocking agents produce a beat-by-beat decline in V_{max} until a steady-state level of block is reached (Hondeghe & Katzung 1984). This phenomenon, known as frequency- or use-dependence, is thought to be important to the therapeutic usefulness of these compounds.

The kinetics of frequency-dependent block can vary greatly between drugs. At equivalent doses during a train of action potentials at the same potential lidocaine reaches a steady state level of block in a few beats while quinidine may take tens of beats to reach steady state (Heistracher 1971, Hondeghe & Katzung 1980).

During the preliminary experiments with aprindine derivatives we noticed a large range in the rate of the onset of block for these compounds.

Figure 3.1 shows a typical experiment demonstrating use-dependent effects. After a 20 second period of rest the preparation was stimulated at a rate of 2 Hz. The membrane potential for both experiments was -85 mV. The figure shows the decline in V_{max} until a steady-state is reached. The solid lines in the figure show the beat-by-

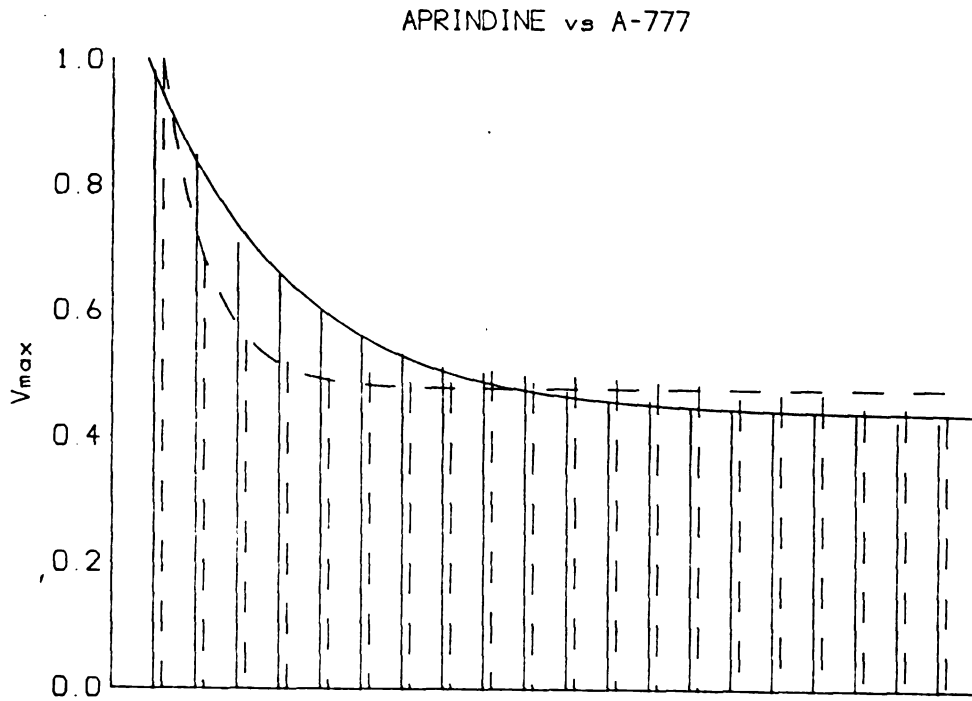


Figure 3.1 Aprindine vs A777

Vmax values of a 2 Hz train of action potentials in the presence of 1.0µg/ml aprindine (solid lines) and 1.0µg/ml A-777 (dashed lines) is shown. Least-square exponential fits of the Vmax values connect the points. Time constant for aprindine was 6.8 beats and 2.1 beats for A-777.

beat decline in V_{max} at a rate of 2 Hz in the presence of 1.0 $\mu\text{g/ml}$ [2.79 μM] aprindine. The dashed lines show the same experiment in the presence 1.0 $\mu\text{g/ml}$ [2.90 μM] of compound A-777.

The increment of block produced by each successive beat decreases as the train progresses. The block produced by each beat apparently depends on the previous history of the cell. The kinetics of the block produced by these two compounds are obviously different. With A-777 the steady-state level of block is achieved within four beats, whereas aprindine required ten beats to achieve steady-state level of block.

In terms of the modulated receptor hypothesis, block increases during the upstroke (activation) and/or the plateau (inactivation) and declines during diastole. That is, drugs appear to have a lower affinity for channels in the rested state as compared to open or inactivated channels. At steady-state, the amount of block occurring during each action potential equals the amount of unblocking that occurs during diastole. The rate of onset of block has been correlated with size (i.e. Molecular Wt.) and lipid solubility of the compound (Courtney 1980). The derivatives in Figure 2.3 (page 24) differ in structure by only a methylene group (5% change in molecular weight) and in lipid solubility (Log P) by 13% (Table 2.3, page

29). The differences seen between these two compounds suggest that some structural feature may be involved in sodium channel block that is not reflected in the physical properties of size and partition coefficient.

As stated above, the rate of onset of block is a function of potential, rate, dose, and action potential duration. Direct comparisons between different drugs at different doses is difficult without controlling all the parameters involved or by using a model that faithfully reproduces the interaction of the experimental parameters. Nevertheless, for a given potential and driving rate, drug concentrations that result in similar levels of block can be qualitatively compared by describing the rate of onset of block.

Figure 3.2 shows the wash-in of the drug effect upon the introduction of aprindine into the experimental chamber. During this wash-in period the preparation was stimulated at a rate of 2 Hz for a period of 20 sec followed by a 20 second rest period. The panels were selected at 5 minute intervals during the washing-in period. The delay in the onset of the response is presumably due to diffusion of the drug through the preparation to the active site. It is clear from this figure that as the drug concentration in the cell increases the steady-state level of block and the rate of block development

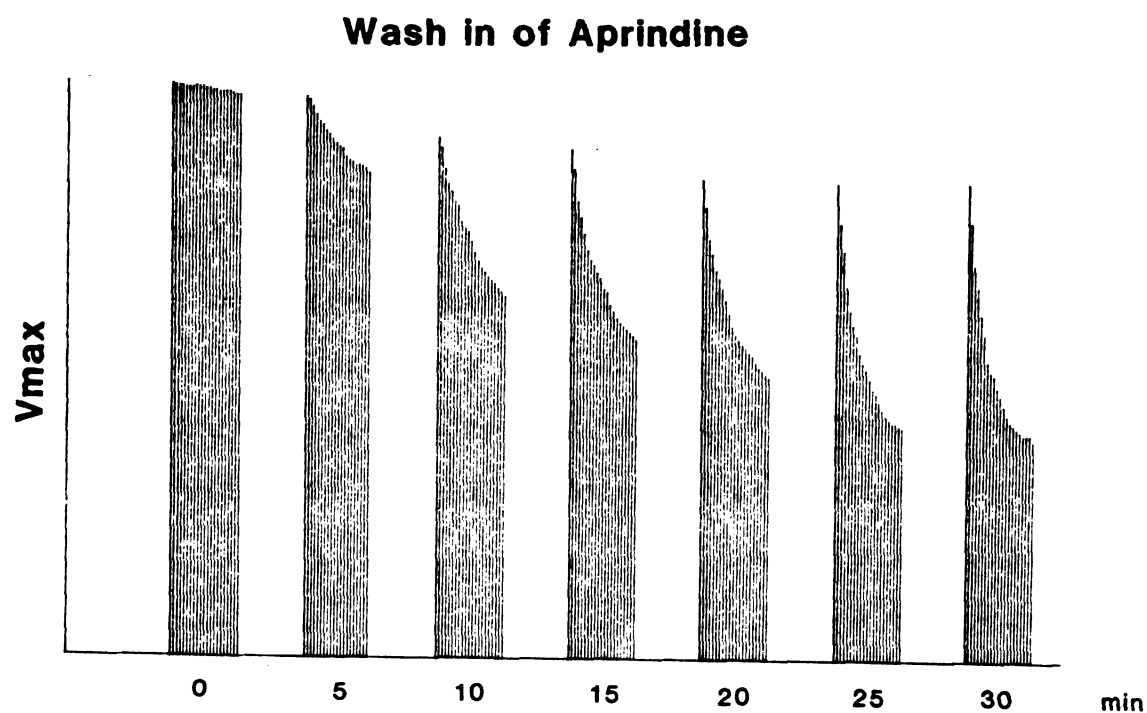


Figure 3.2 Wash-in of aprindine effects.

Vmax recorded from a representative muscle during 2 Hz trains of 20 beats at 0,5,10,15,20,25,30 minutes after the introduction of 5 $\mu\text{g/ml}$ aprindine into the test compartment. Use-dependence and, in this experiment, "tonic" block gradually increase over time until a quasi steady-state occurs. Upon removal of the drug Vmax recovered with approximately the same time course. However, Vmax never returned to control values and some use-dependence was apparent even after long (1 hr) wash-out periods.

increases.

The doses in this section were chosen to produce a significant (approximately 50%) block at a rate of 3.3 Hz. This criterion allows a qualitative comparison of the rates of onset of block.

3.1. Use-dependence. Control

In most preparations, at ISI's greater than 250 msec, control preparations exhibited little use-dependence. Those preparations with significant (> 10%) use-dependence at 250 msec ISI, which was usually accompanied by depolarization during the train, were rejected. Significant use-dependence in control may also be due to accumulation of slow-inactivation (see below). Selecting preparations with small control use-dependence may affect the measured drug response if indeed slow-inactivation and drug block are linked.

Figure 3.3 shows the use-dependence of a typical control experiment. The three dimensional graph shown in this and following figures provides a profile of kinetic behavior at various rates of stimulation. V_{max} (Y-axis) values are normalized to the first beat in a train after a long (> 20 sec.) rest. The X-axis plots the duration of the train in seconds starting at time zero. The Z-axis in these figures is the interstimulus interval (ISI) of the

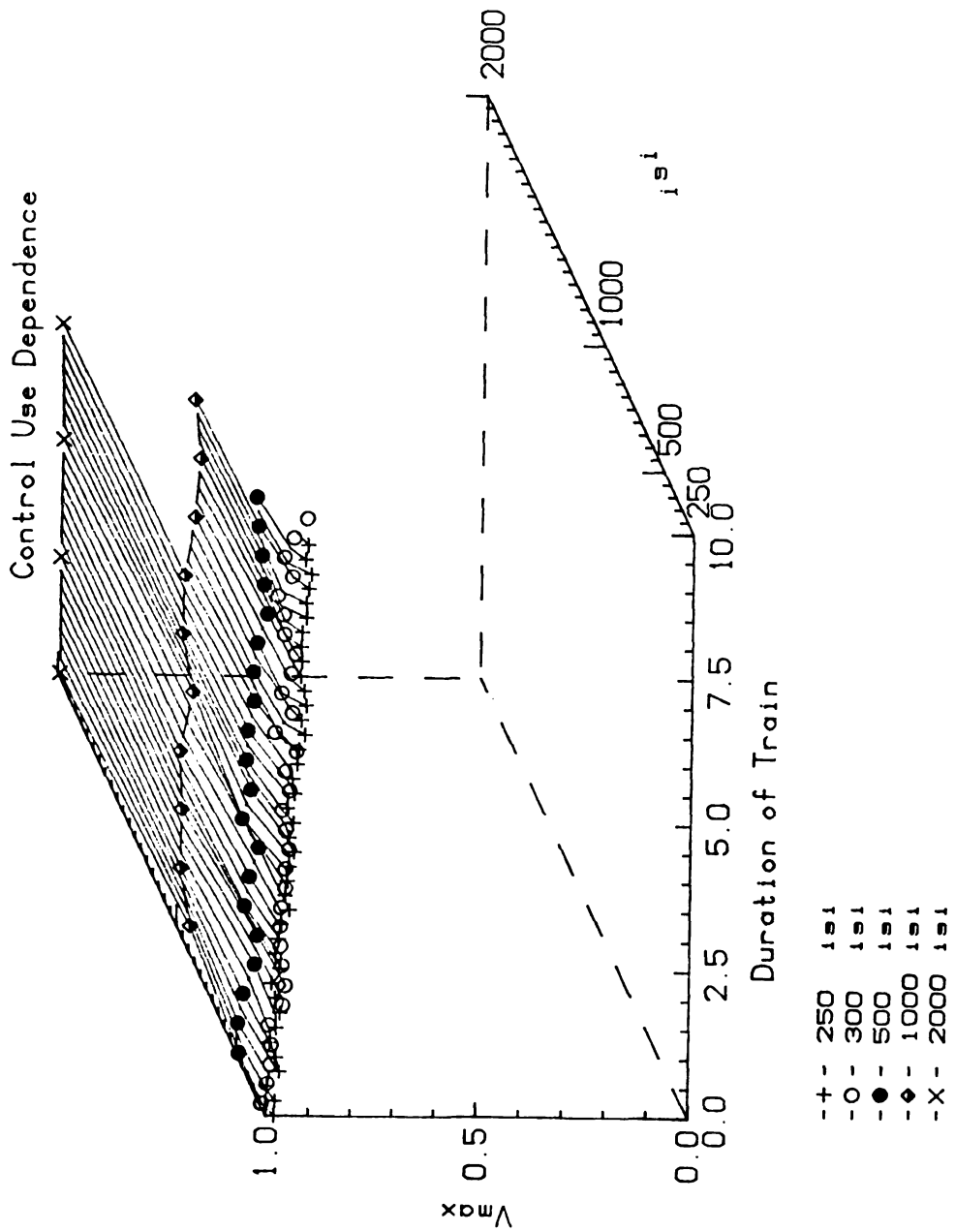


Figure 3.3 Use dependence of V_{max} in the absence of drug. V_{max} values are normalized to that of the first beat after a 20 sec. rest period. Train duration is in seconds and ISI in milliseconds.

train. The protocol used in this and the following graphs consisted of a 10 sec period of stimulation followed by a 20 second or longer period of rest.

Figure 3.3 shows a use-dependent decline in V_{max} of 9% after 10 seconds of stimulation at 5 Hz. This decline was accompanied by a decrease of membrane potential of about 4 mV in the experiment shown. The depolarization produced by fast rates of stimulation has been attributed to K^+ accumulation in the extracellular space (Kline et al.). However at potentials more negative than -80 mV the effect of a small depolarization on V_{max} should be less than 10% (Chen & Gettes 1976). Fast driving rates have also been shown to increase intracellular sodium due to a rate-induced resetting of the sodium-potassium ATPase system (Glitsch 1973, Eisner et al 1981). An increase in internal sodium ions will decrease the driving force for sodium ions and thus effect V_{max} . Fast driving rates are also associated with changes in action potential shape. These changes have been associated with intracellular and extracellular changes in Na^+ , Ca^{++} and K^+ ions (Attwell et al 1981). The shortening of the action potential duration may result in a decrease in the accumulation of slow-inactivation during the action potential as well as an increase in the time for recovery from this process between action potentials. At rates of 5 Hz with a vol-

tage clamped preparation, slow inactivation can result in as much as 20% decline in V_{max} (Clarkson et al. 1984).

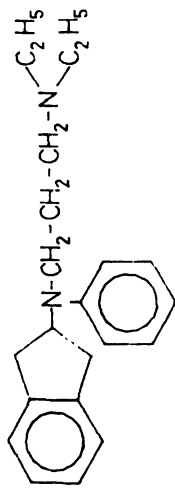
All these factors can contribute to changes in V_{max} seen during rapid stimulation in control conditions. The effect of these factors on the measured drug effect was minimized by selecting preparations with small (< 10%) control use-dependent block.

3.2. Use-dependence of aprindine derivatives

The following figures demonstrate the drug induced depression for the ten aprindine derivatives used in this study.

3.2.1. Aprindine use-dependent block

Figure 3.4 shows the use-dependent effect of 2.79 μM aprindine [1-1-1]. In this experiment the duration of the action potential was 170 msec. There was about 20% tonic block. Tonic block is defined as the difference between the control V_{max} and the first beat after a long rest in the drug situation at normal resting potential. Tonic block includes open channel block that occurs during the upstroke before V_{max} occurs and drug induced inactivation (trapping in ID state). The latter is strongly voltage dependent and thus varies from experiment to experiment depending on the resting potential of the cell. This type



APRINDINE

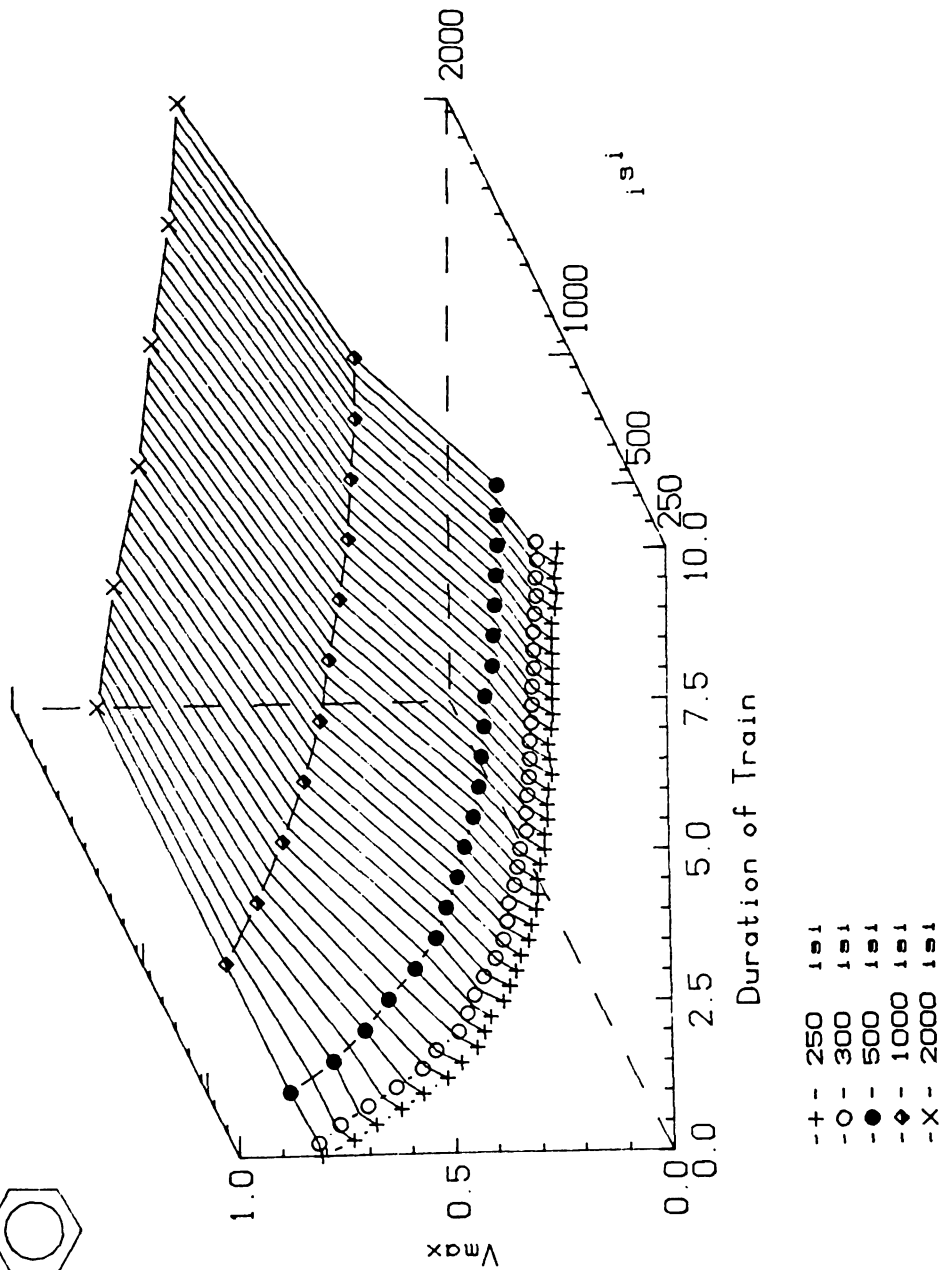


Figure 3.4 Use dependence of Aprindine

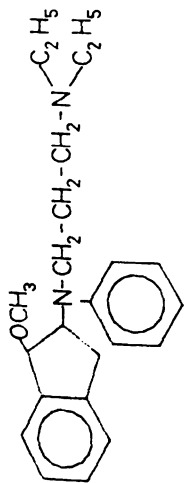
The effects of 1.0 $\mu\text{g/ml}$ [2.79 μM] of aprindine are shown on V_{max} values for a 10 sec train at various rates of stimulation. Z-axis gives the interstimulus interval (ISI) for each train.

of block can usually be partly reversed by preceding the upstroke by a hyperpolarizing prepulse. The block that occurs before the time of V_{max} will not be reversed by a hyperpolarizing prepulse and will thus contaminate our estimates of rested block for these compounds.

In this experiment the steady-state V_{max} was 0.31 that of control and was achieved within 12 beats at an ISI of 500 msec. The depression of V_{max} during a train followed an exponential course in all experiments. The exponential decline in V_{max} can be expressed as a "beat constant", i.e. the number of beats required to produce 1/e of the steady-state depression at a particular rate. The "beat constant" for this experiment was 4.62 beats at 2 Hz. The measured membrane potential was -85 mV. Use dependent block is apparent even at an ISI of 2000 msec.

3.2.2. Moxaprine use-dependent block

The use-dependent profile for 12.85 μM d-cis moxaprine is shown in Figure 3.5. Moxaprine ([2-1-1] page 24) differs from aprindine [1-1-1] by a methoxy group in the 2 position in the indane ring structure. In the cis configuration the methoxy group and the connecting chain project out from the same side of the indane structure. The addition of the methoxy group to aprindine changes the weight of the compound by about 5 %. Alkoxy



d-Cis MOXAPRINDINE

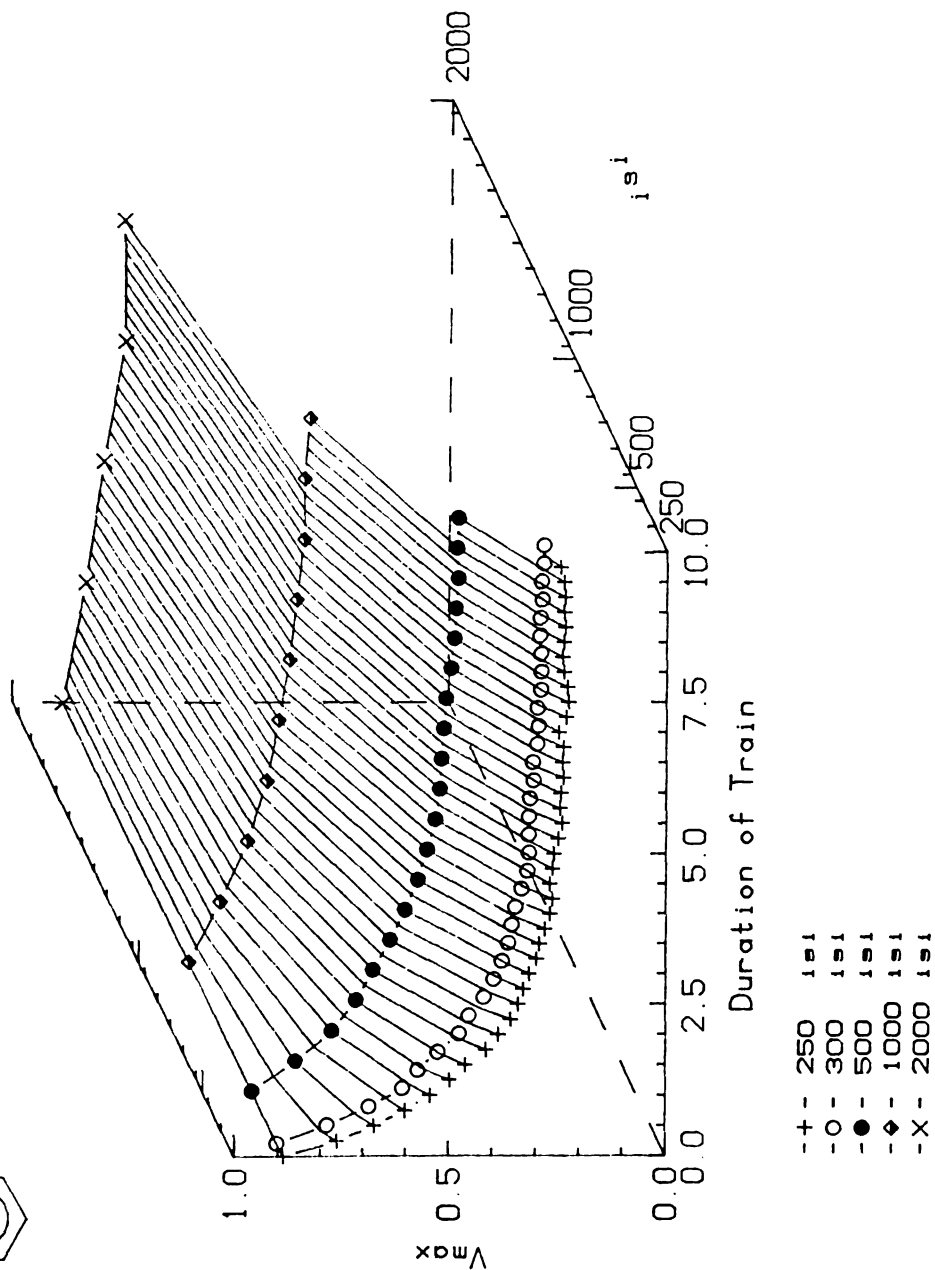


Figure 3.5 Use dependence of Moxaprine

A dose of 5.0 $\mu\text{g/ml}$ [12.9 μM] d-cis moxaprine produces a steady-state value of 0.23 at an ISI of 250 msec.

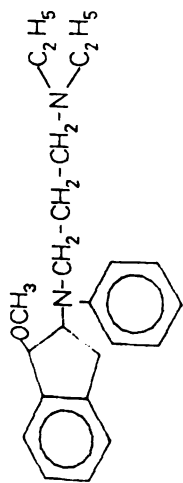
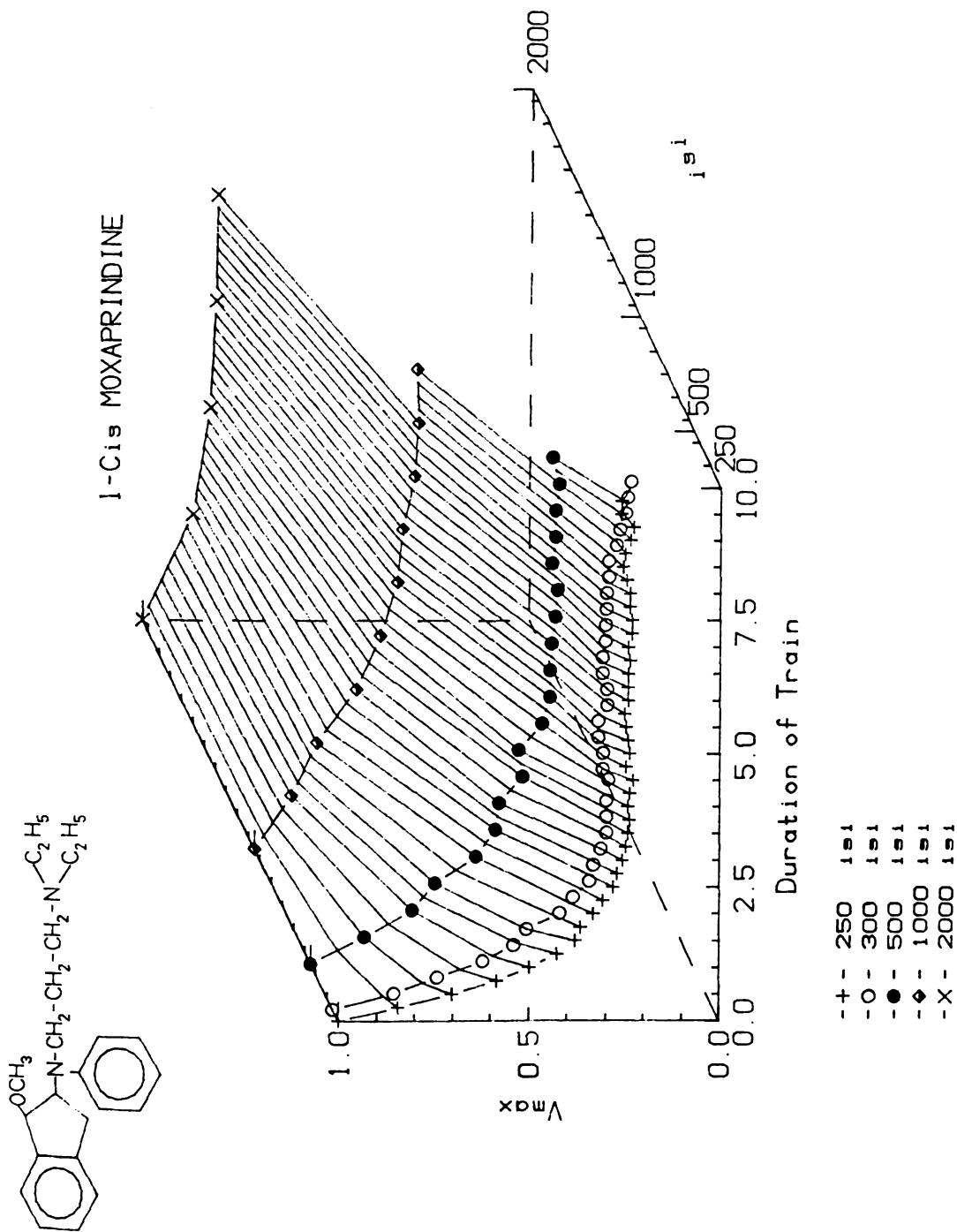


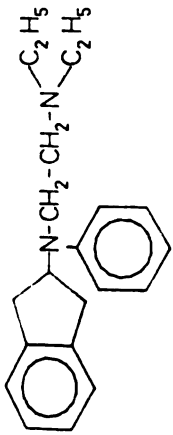
Figure 3.6 Use dependence of 1-cis Moxapridine. A dose of 5.0 µg/ml [12.9 µM] 1-cis moxapridine. produced a steady-state value of 0.26 at an ISI of 250 msec.

groups added to the aromatic portion of local anaesthetics have been reported to increase the potency of local anesthetics (Buchi and Perlia, 1971). The profile of use dependence for moxaprine is very similar to that of aprindine. A steady-state level of block (0.40) is achieved within 14 beats at 500 msec ISI. This corresponds to a "beat constant" of 4.42 beats. This is similar to a constant of 4.62 seen with a lower dose of aprindine.

The same dose of 1-cis moxaprine is shown in Figure 3.6. It is clear that there is little difference between the two isomers. In the experiments done with each isomer there was very little difference seen in the beat constants at each rate.

3.2.3. A-777 use-dependent block

The structure of A-777 [1-6-1] differs from aprindine by a single methylene group on the connecting chain. The two drugs differ by only 5% in molecular weight. As shown in Figure 3.7, this drug shows a quite different profile from that of aprindine. At ISI of 500 msec, 1 $\mu\text{g/ml}$ [2.90 μM] A-777 has a "beat constant" for depression of V_{max} of 1.56 beats as compared to 4.62 for the same dose of aprindine. Steady-state (0.78) is reached within 4 to 5 beats.



A-777

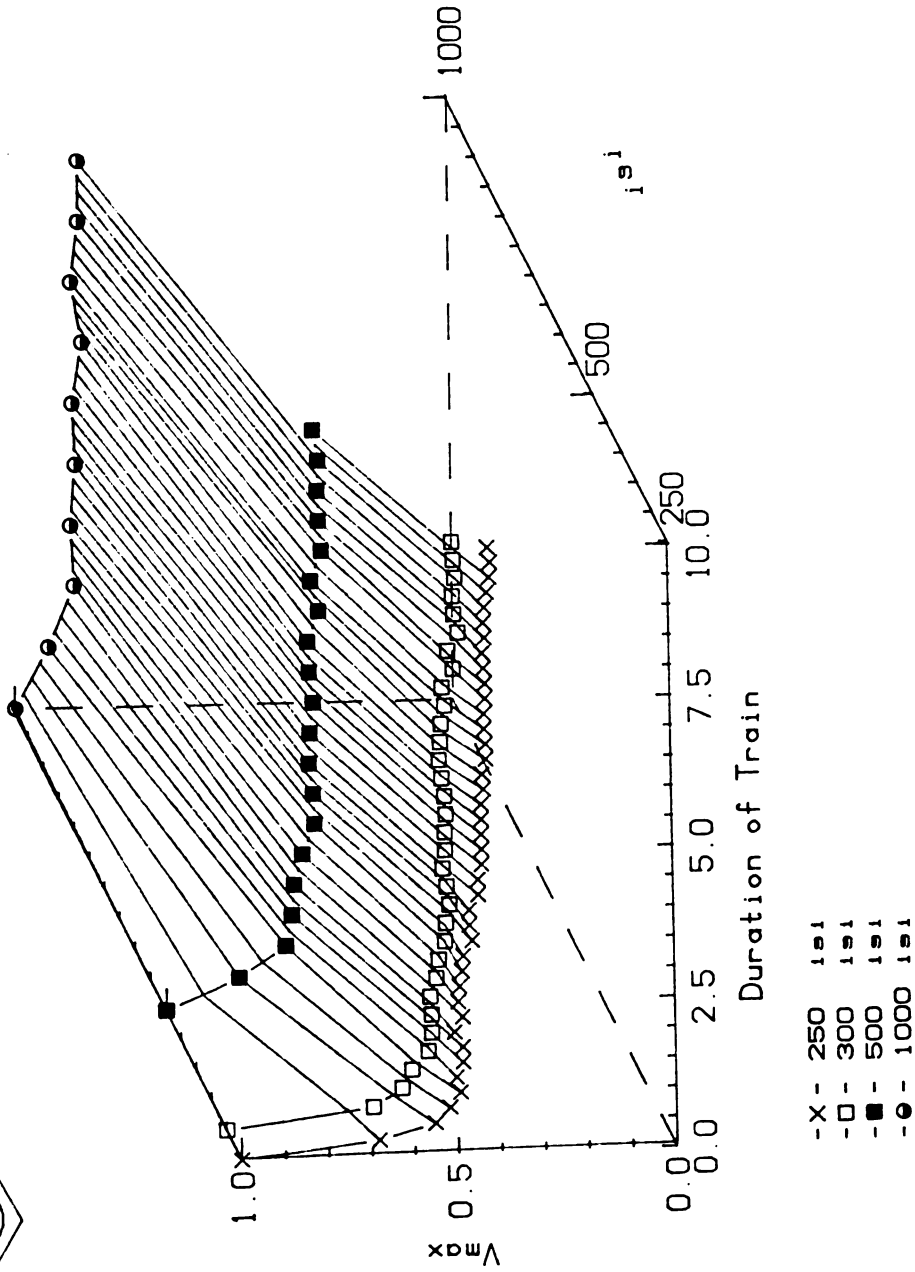
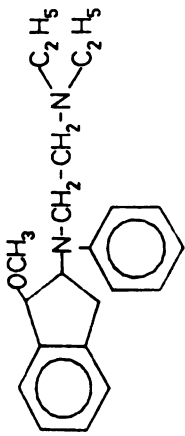


Figure 3.7 Use dependence of A-777

The effects of 1.0 µg/ml [2.90 µM] A-777 are shown. First beat was unchanged from control. Steady-state value at 250 ISI was 40 % of control.



B-1704

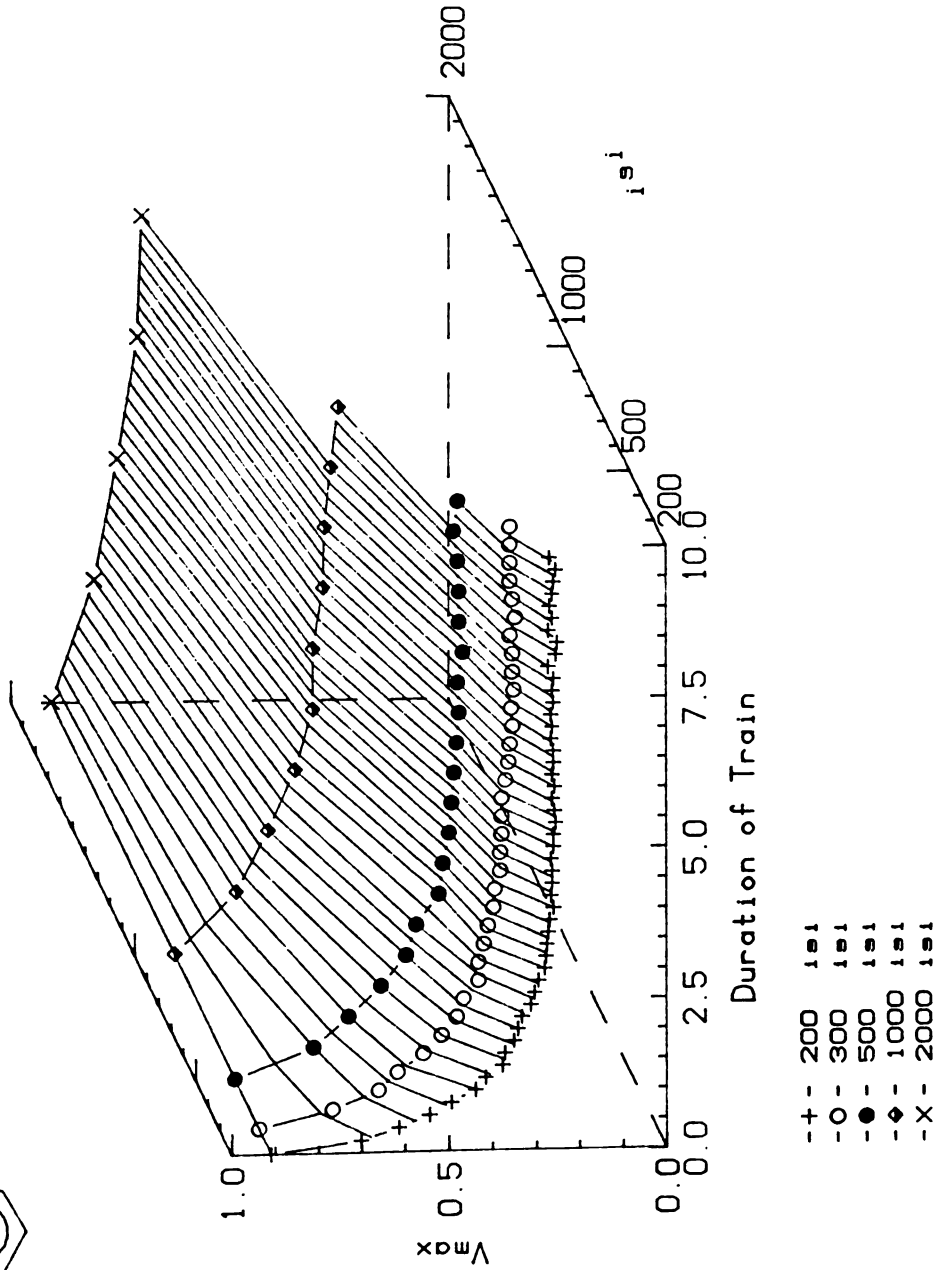


Figure 3.8 Use dependence of B-1704

The effects of 5.0 µg/ml [14.7 µM] B-1704 are shown. The first beat of each train is 90% of control. Steady-state level at 200 ISI is 27% of control.

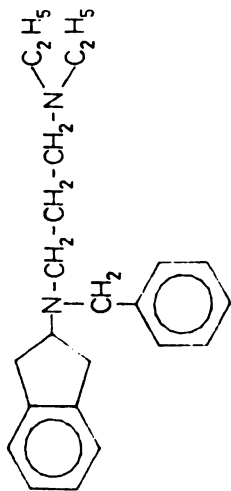
3.2.4. B-1704 use-dependent block

B-1704 [2-6-1] structurally is like A-777 [1-6-1] in that it has a short connecting chain and is like moxaprin-dine due to the presence of the methoxy group. The addition of a methoxy group to aprindine changed the kinetics very little. Therefore we might expect that B-1704 [methoxy-A-777] would show the same fast kinetics as A-777. Figure 3.8 shows that this is not the case. At 2 Hz 5 $\mu\text{g/ml}$ [14.77 μM] produced a steady state level of block of 0.39 with a constant of 2.78 beats. This constant is twice that of A-777 even though done at five times the dose.

3.2.5. B-1622 use-dependent block

B-1622 [1-7-1] differs from aprindine by the insertion of a methylene group between the indane-amine nitrogen and the phenyl side-chain. The change should decrease the delocalization of the nitrogen electrons making this nitrogen more basic.

Figure 3.9 shows the kinetic profile for 1.0 $\mu\text{g/ml}$ [2.44 μM] B-1622. This dose produces a steady-state decline to 0.72 at 2 Hz with a constant of 11.5 beats.



B-1622

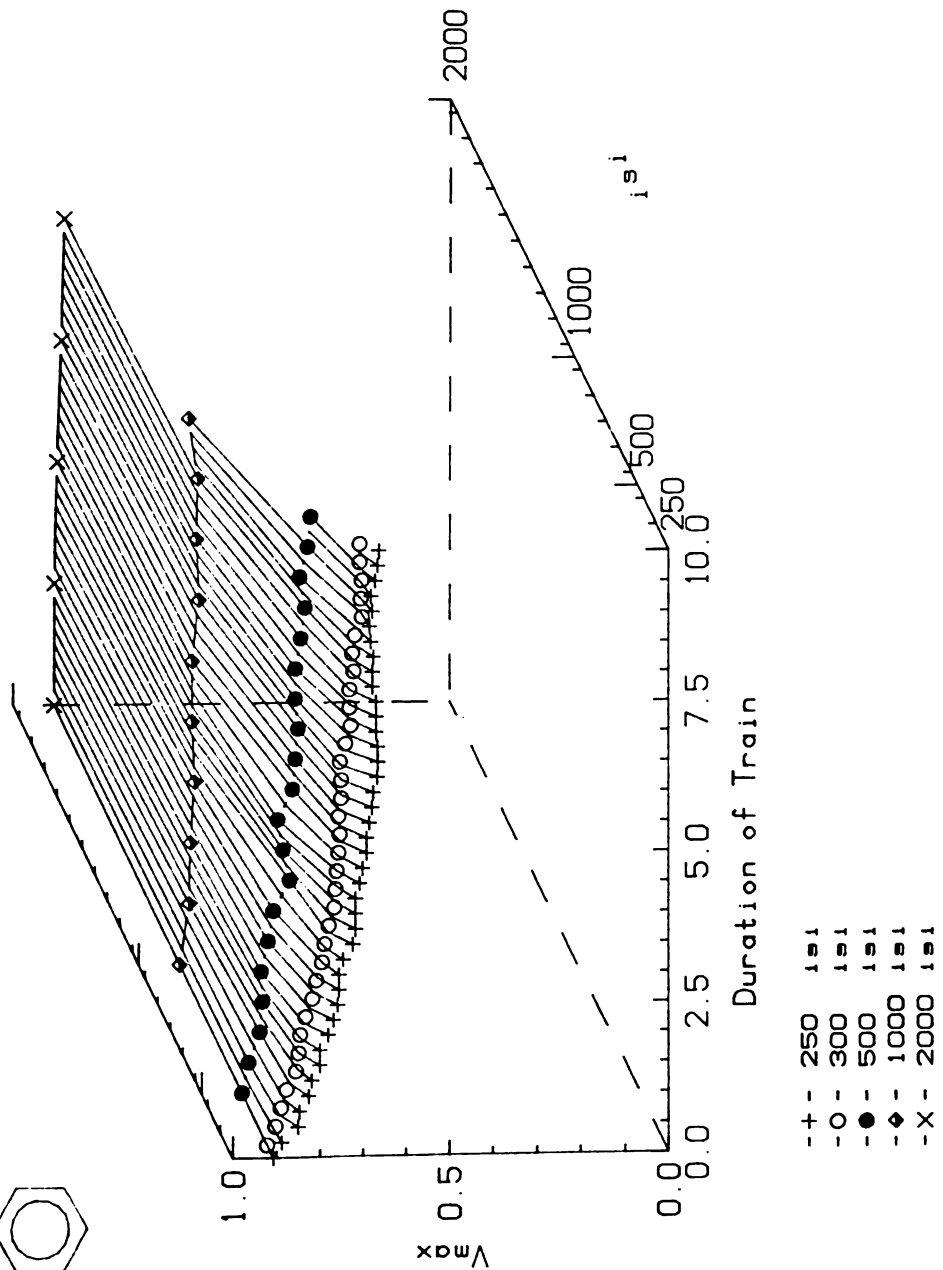
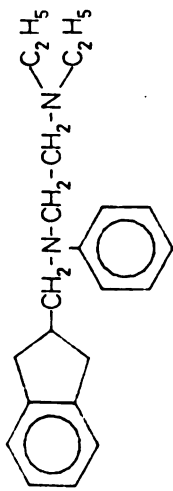


Figure 3.9 Use dependence of B-1622

The effects of 1.0 $\mu\text{g/ml}$ [2.44 μM] B-1622 are shown. The first beat of the train was 90% of control. Steady-state at 250 ISI was 67%. Control V_{max} was 295 V/sec.



A-1800

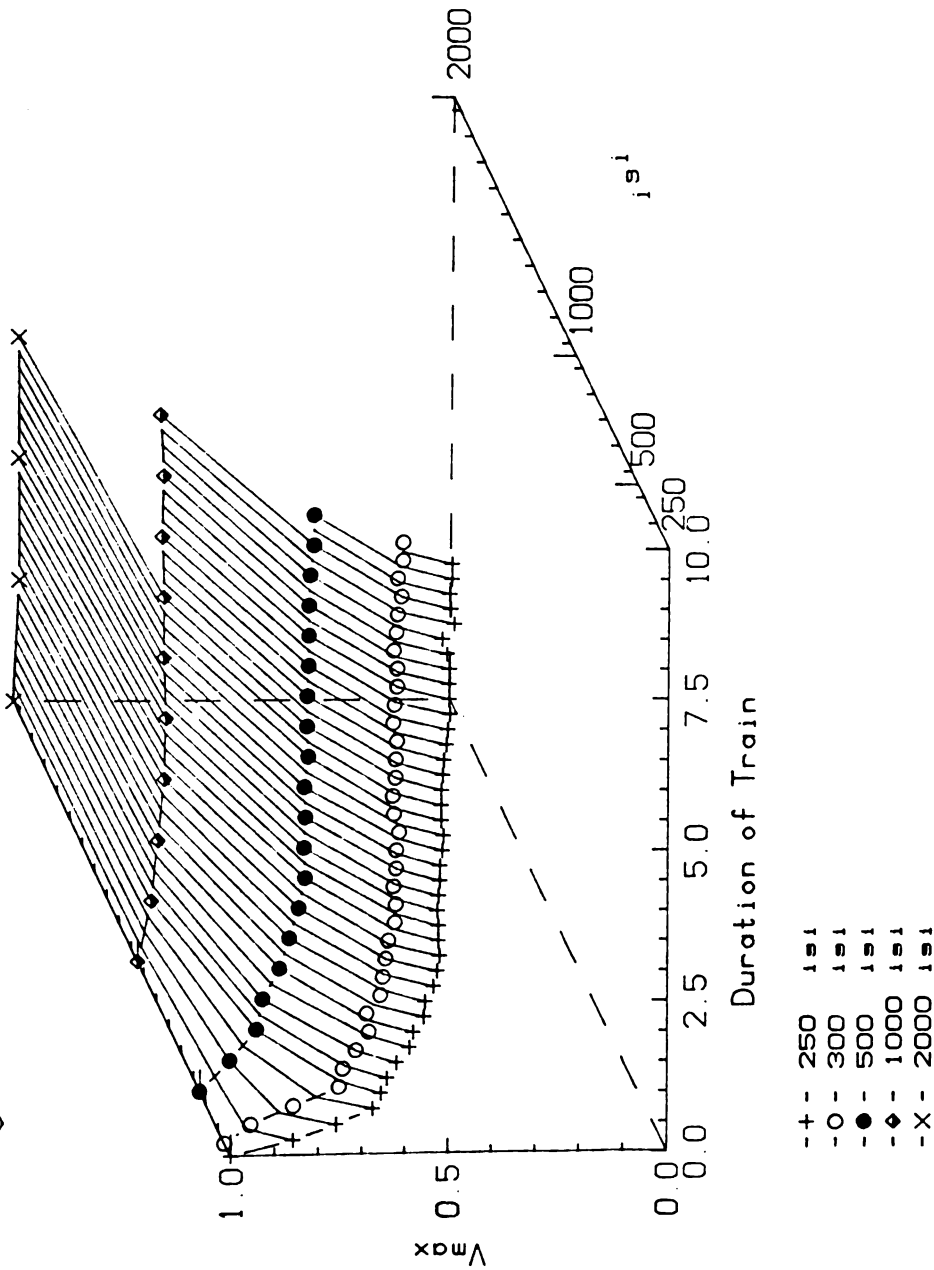


Figure 3.10 Use dependence of A-1800

The effects of 5.0 $\mu\text{g/ml}$ [11.4 μM] of A-1800 are shown. The first beat of train was the same as control. Steady-state level at 250 ISI was 49%.

3.2.6. A-1800 use-dependent block

A-1800 [1-3-1] is an isomer of aprindine. They differ in the position of the N-phenyl side-chain with the side-chain for A-1800 being separated from the indane moiety by a methylene group. Figure 3.10 (page 49) shows the rate-dependent effects of 5 $\mu\text{g/ml}$ [11.4 μM] A-1800. At this dose a 2 Hz train reaches a steady-state level of 0.75 with a constant of 2.97 beats. This rate of use-dependent block is faster than aprindine (constant = 4.62) even though the dose used for aprindine produced greater steady-state block (0.31). The beat constant of block is also slower than A-777 (1.56) at doses that produce similar levels of steady-state block.

3.2.7. A-2077 use-dependent block

The structure of A-2077 [3-4-2] is quite different from that of the other compounds studied. This compound is the only 1-indane-amine compound in this series. It is also the only compound with a heterocyclic ring on the side chain. A-2077 also has a shortened side chain and a dimethyl terminal amine group.

The effect of 5.0 $\mu\text{g/ml}$ [11.4 μM] A-2077 is shown in Figure 3.11. At 2 Hz a steady-state level of 0.67 is reached with a "beat constant" of 1.41. This is comparable to the speed of A-777.

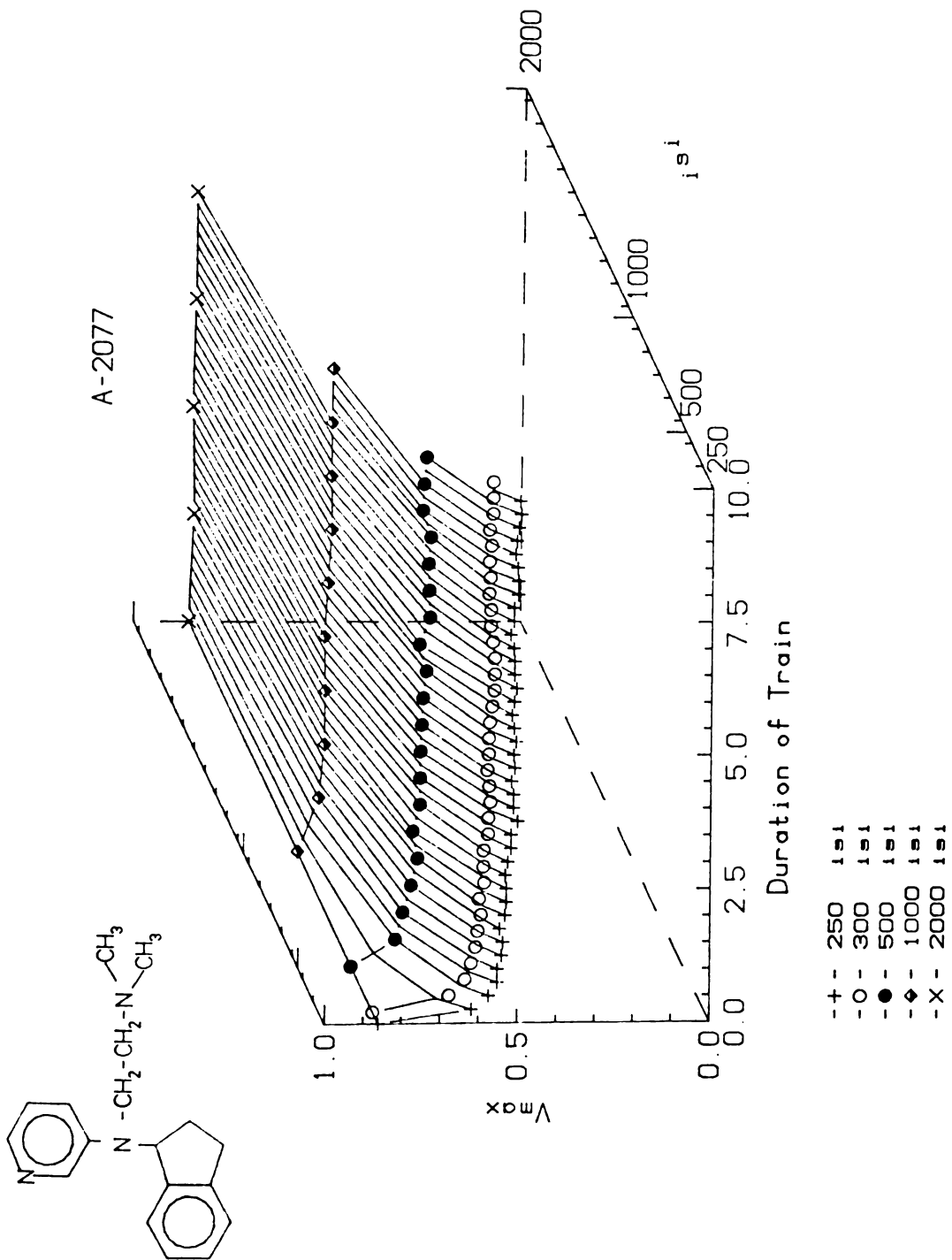
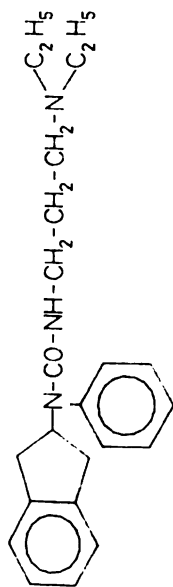


Figure 3.11 Use dependence of A-2077

The effects of 5.0 $\mu\text{g/ml}$ [11.4 μM] of A-2077 are shown. The first beat was 87% of control. Steady-state level at 250 ISI was 50% .



B-1400

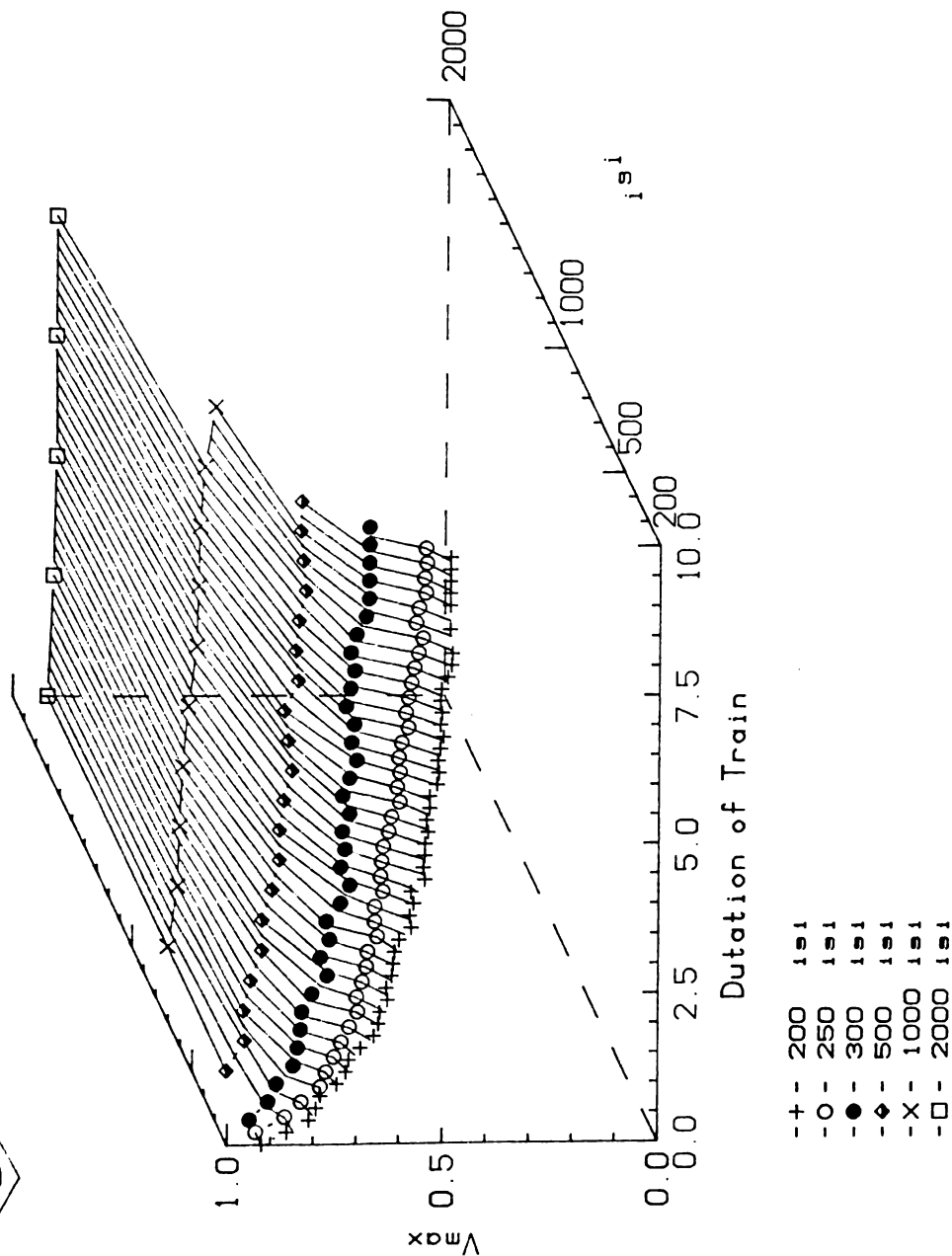


Figure 3.12 Use dependence of B-1400

The effects of 3.0 $\mu\text{g/ml}$ [7.5 μM] of B-1400 are shown. Steady-state value at 250 ISI was 0.4.

3.2.8. B-1400 use-dependence B-1400 [1-2-1] differs from the compounds presented so far by the presence of the urea group in the connecting chain.

3.12 shows the effects of 3 $\mu\text{g/ml}$ [$7.46\mu\text{M}$] B-1400. This experiment produced a steady-state level of 0.79 with the large "beat constant" of 8.13 beats.

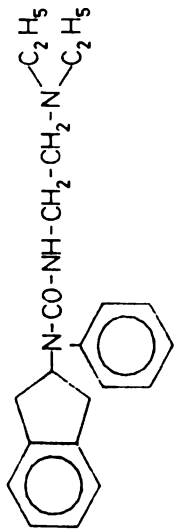
3.2.9. B1401 use-dependence

B-1401 is similar to B-1400 with the connecting chain shortened by one methylene group. The kinetic behavior of the two drugs is also similar.

Figure 3.13 profiles the behavior of 3.0 $\mu\text{g/ml}$ [$7.73\mu\text{M}$] B-1401. At this dose a 2 Hz train reaches steady-state level of 0.54 with a beat constant of 7.88 beats.

3.2.10. B1404 use-dependence

B-1404 [1-5-3] is similar in structure to B-1401. B-1404 has a terminal morpholine group rather than the diethylamine common to most of the other compounds. This compound was significantly less potent than the other compounds in this series. A dose of 1.0 $\mu\text{g/ml}$ [$2.5\mu\text{M}$] had no effect. Figure 3.14 shows the profile of 20 $\mu\text{g/ml}$ [$49.8\mu\text{M}$] B-1404. It is clear that this drug is one of the fastest of the drugs. At 2 Hz, steady-state of .78



B-1401

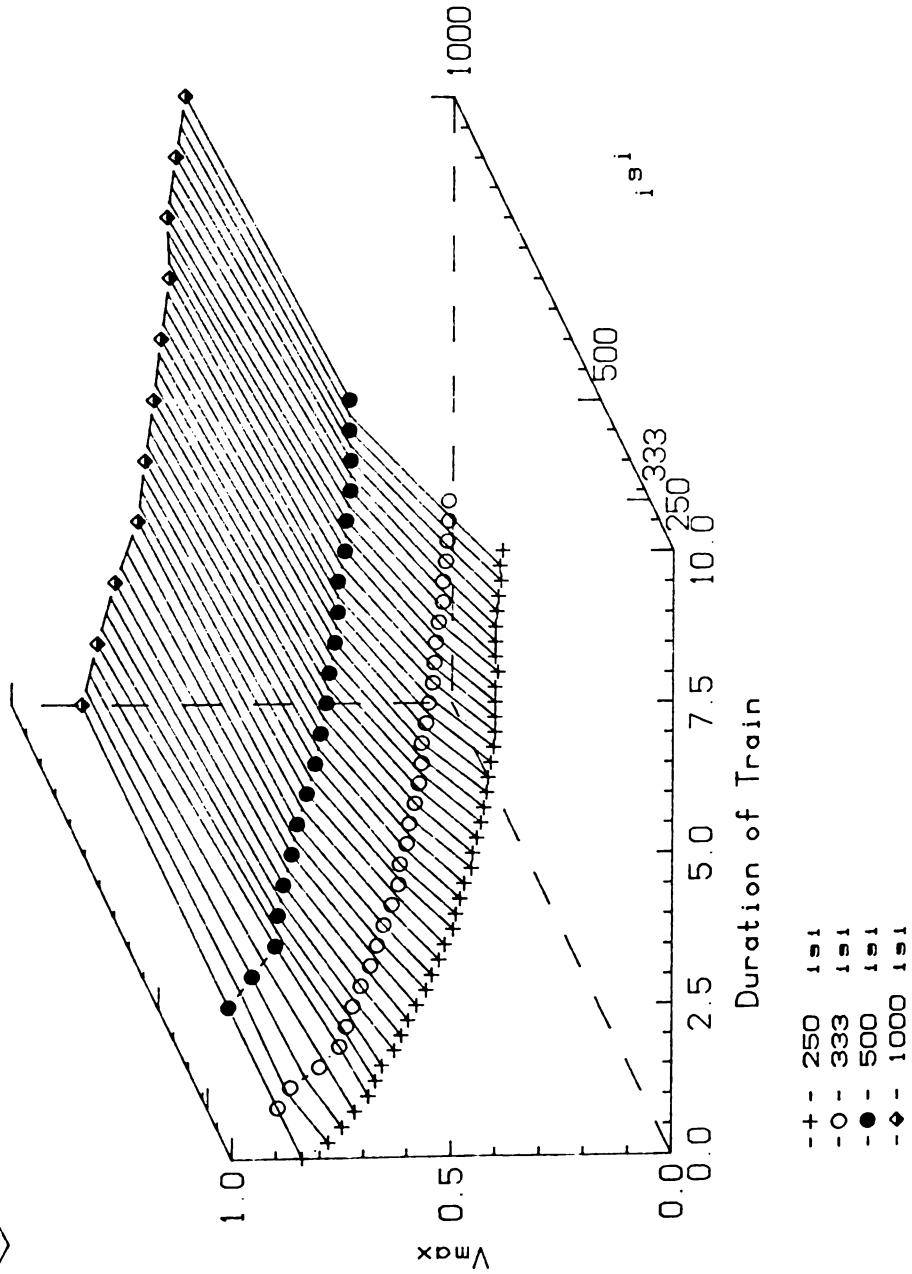


Figure 3.13 Use dependence of B-1401

The effects of 3.0 µg/ml [7.73 µM] B-1401 are shown. The first beat in each train is 84% of Control. Steady state level at 250 ISI is 0.40.

was reached with a beat constant of 1.02 beats. In another experiment 10 $\mu\text{g/ml}$ [24.88 μM] had a beat constant of 0.68 beats at 2 Hz.

3.3. Summary of use-dependence

A summary of the use dependent experiments is shown in Table 3.1.

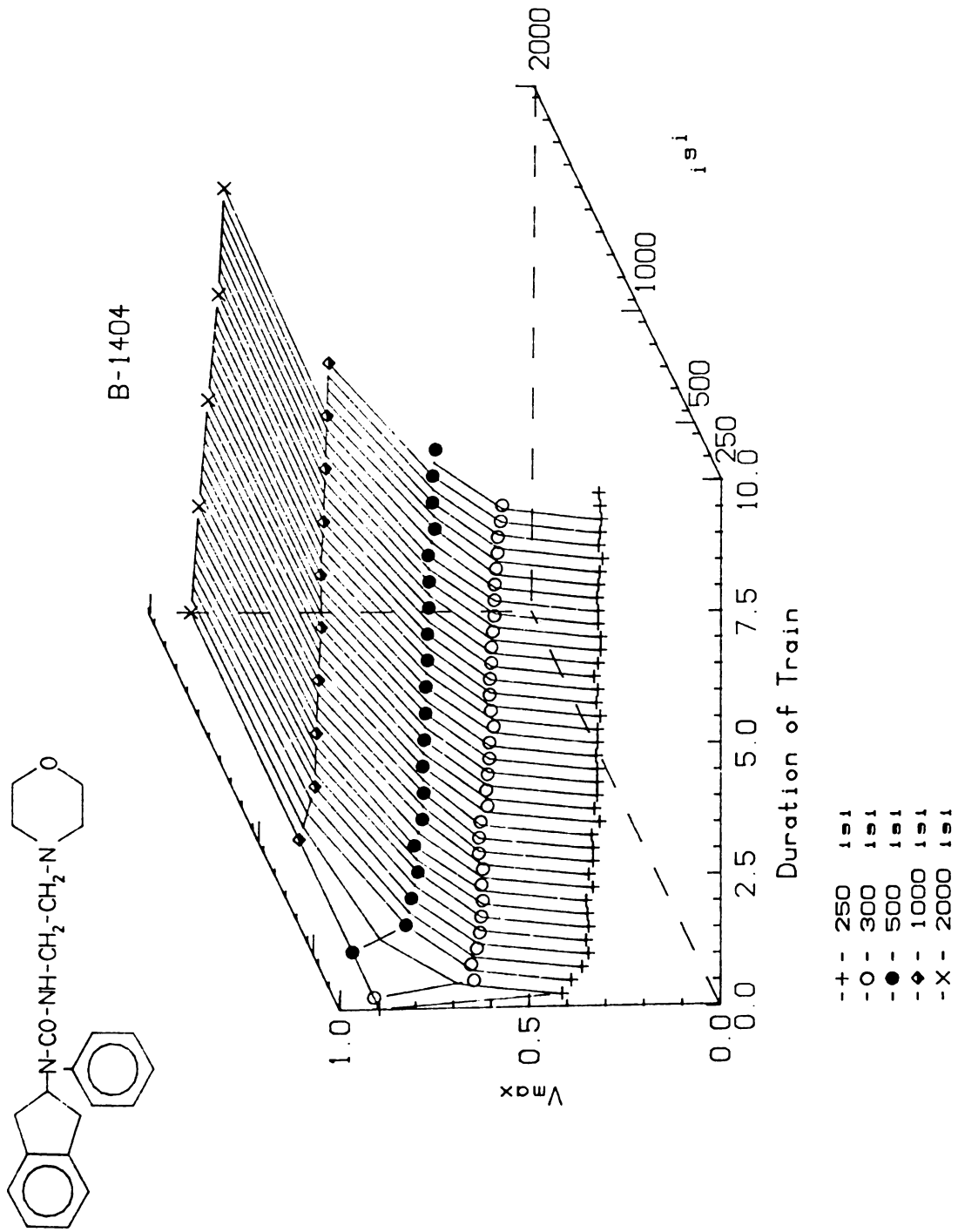


Figure 3.14 Use dependence of B-1404

The effects of 20 µg/ml [49.8 µM/l] of B-1400 are shown. The first beat is unchanged from control. Steady-state ISI is 26% of control.



EXPERIMENTAL RESULTS

	Beat Constants (beats)			
	300	500	1000	2000
2	8.90	8.12	125	<1
2	7.89	6.42	2.03	2.17
1	9.81*	7.88	4.95	
74	4.46*	2.04	2.06	
82	.615	1.02	1.53	
702	1.62	1.35	1.36	16.2
.96	2.77	.652		
0.8	15.2	11.5	1.10	3.08
1.31	13.9	10.6	4.50	3.45
12.3	17.0	6.91	1.39	3.67
4.16	6.16	2.54	1.97	1.53
4.24	4.42	2.78	2.23	1.95
3.62	3.71	2.97	1.00	<1
3.22	2.99	4.82	5.92	10.8
.025	.521		.826	<1
1.29	.967	1.27	1.17	
.995	1.29	1.41	.913	<1
	1.07	1.08	.712	
3	1.23	.872	1.26	.014
0	1.05	1.15	1.81	1.10
90	1.49	1.25	1.57	1.18
90	.535	1.06	1.18	
.36 mg			2.45	3.54
1.00	10.8	7.71	6.44	3.48
2.79	3.76	3.93	2.94	1.59
2.79	6.92	5.58	4.63	3.84
7.71	7.10	6.45	6.29	5.79
12.9	5.56	5.17	4.41	3.24
7.71	3.64	4.50	3.84	3.77

Table 3.1 Summary of use-dependent experiments. Time constant (number of beats for V_{max} to decline to 1/e) at different stimulus rates.

control (no drug)
= 333 msec

Time constant for this recovery process approximately 50 msec in this experiment. The recovery from drug induced block appears to consist of a

CHAPTER 4

RECOVERY RESULTS

As shown in the previous section aprindine and its derivatives produce a beat-by-beat decline in V_{max} as a function of driving rate and dose. Recovery from this block occurs in an exponential fashion when the preparation is rested. This recovery process has been shown to be insensitive to the dose of the drug used (Courtney 1980, Sada et al. 1981).

Figure 4.1 shows a composite picture of an experiment demonstrating the recovery process. In the figure a steady-state level of block has been induced with a 300 msec ISI train. A test pulse is then given at variable durations following the train. Test pulses which occur at a time less than the diastolic time of the train produce more block than the steady-state level. Longer rest periods result in a progressively smaller levels of block.

Figure 4.2 (page 60) shows this recovery process for aprindine derivative B-1704. The figure also shows the characteristic fast recovery of the control (no drug) preparation. The time constant for this recovery process is approximately 50 msec in this experiment. The recovery from drug induced block appears to consist of a

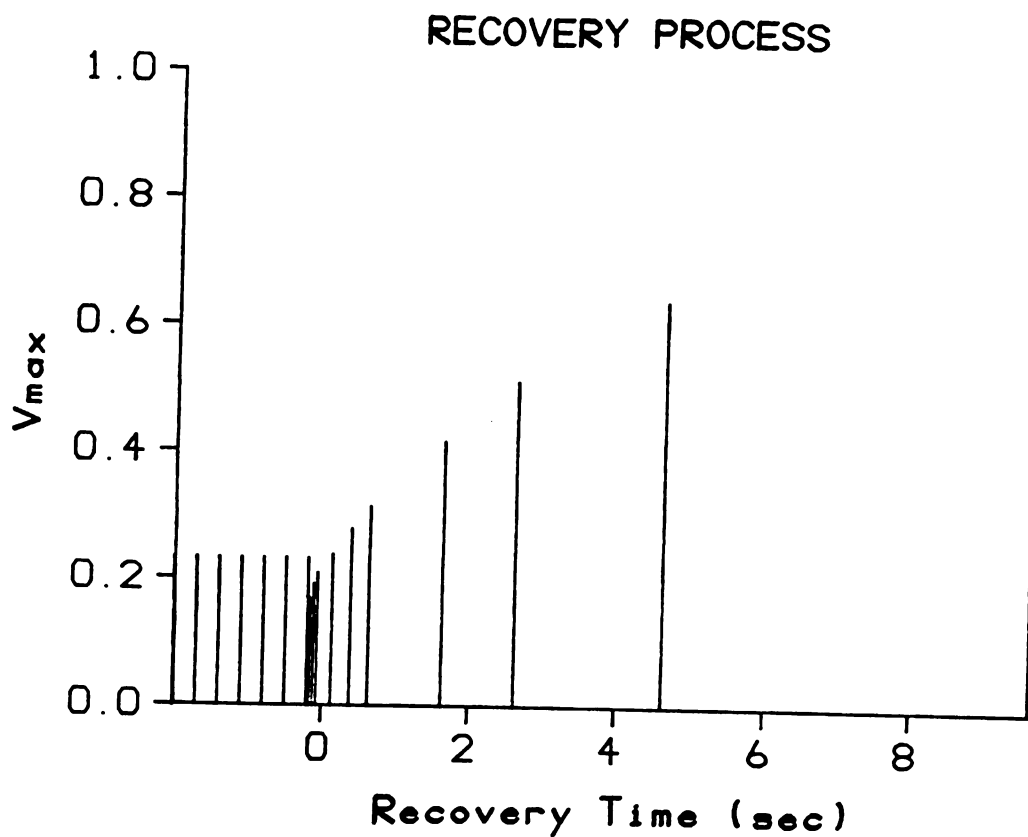


Figure 4.1 Recovery Process

A steady-state level of block was produced by a 300 msec ISI train. V_{max} of extra beats after the end of the train are shown. Recovery time varies from 20 to 9800 msec.

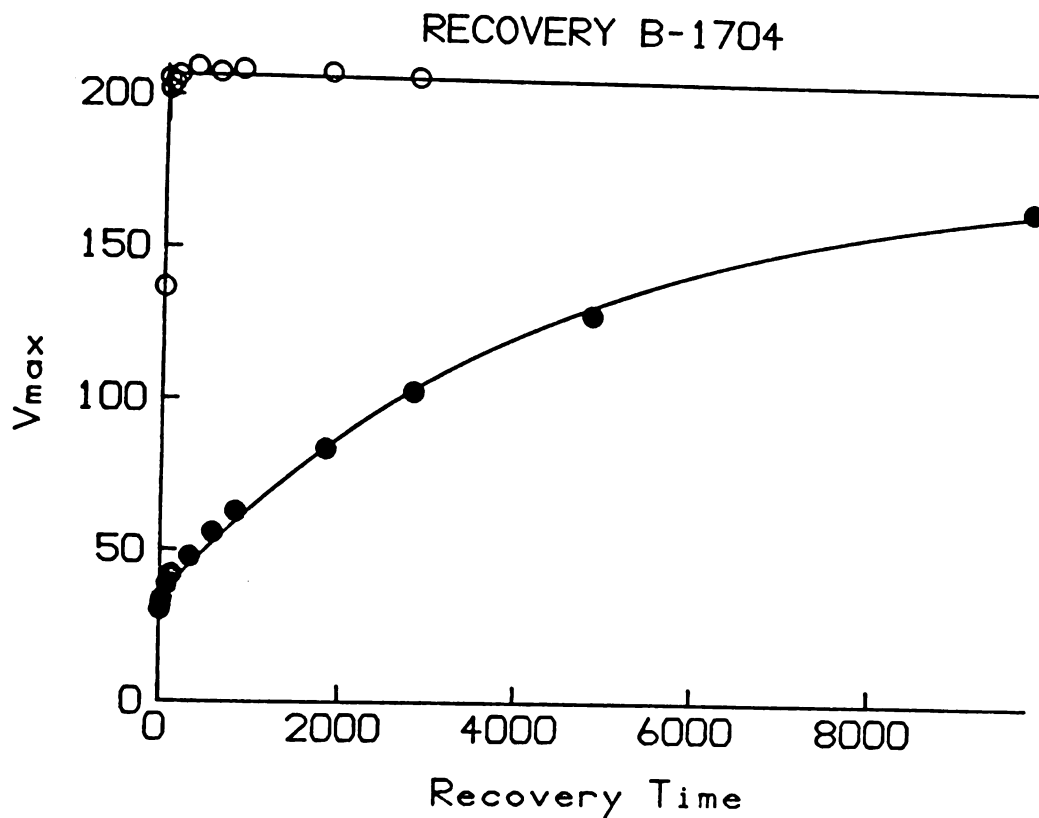


Figure 4.2 Recovery of B-1704

Filled circles show recovery from steady state block for 5.0 µg/ml B-1704. A single exponential fit with a time constant of 4.4 sec is drawn through the points. Open circles show the drug free recovery process in the same preparation.

fast initial component, similar to the control, followed by a much slower exponential process (Figure 4.3, page 62). The fast component of the recovery process was not seen in all preparations in the presence of drug.

A summary of recovery data is shown in Table 4.1 (page 63). The time constants of recovery varied over an order of magnitude from 0.37 sec for compound A-777 to 4.9 sec for moxaprine.

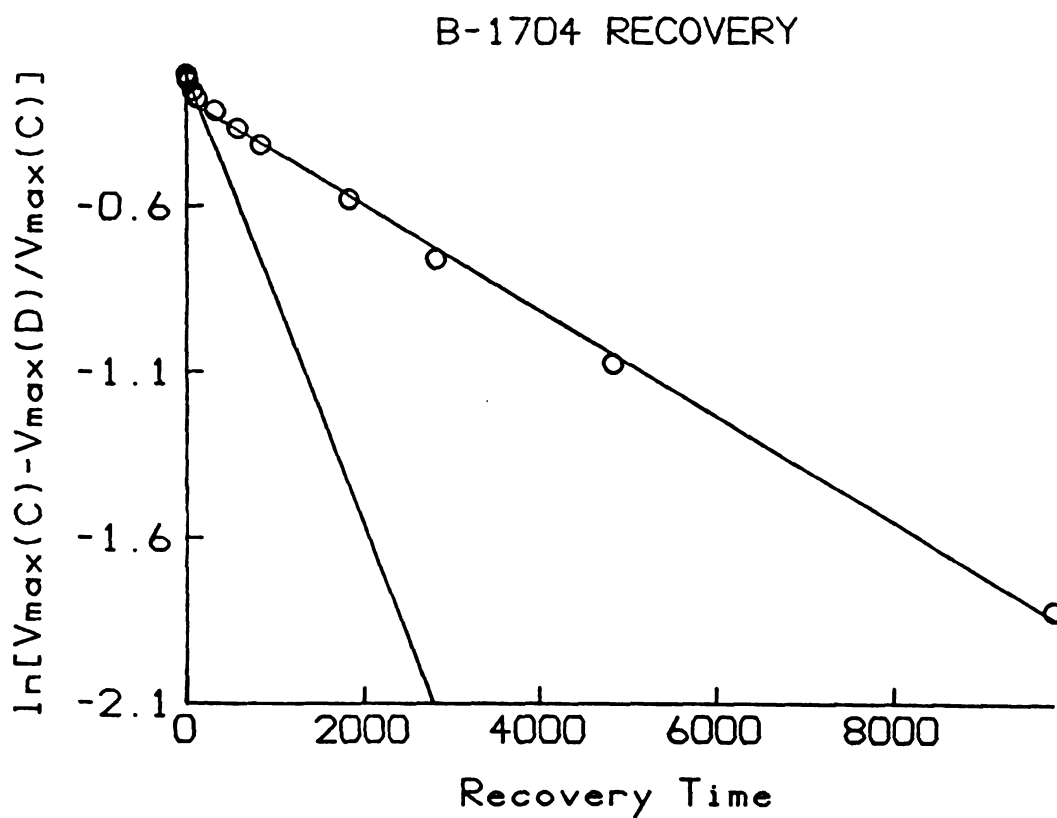


Figure 4.3 The two processes of Recovery

The recovery in the presence of 5 $\mu\text{g/ml}$ of B-1704 show two distinct processes present: a fast process with a time constant of 55 msec and a slower process with a time constant of 4.4 sec.

COMPOUND	TIME CONSTANT (sec \pm SEM)	n	MOL. WT.
B-1404	0.35 \pm 0.08	4	365.47
A-777	0.39 \pm 0.02	2	308.47
A-2077	0.43 \pm 0.05	2	281.40
A-1800	0.58 \pm 0.10	2	322.49
C-1622	2.6	1	336.52
B-1401	2.8 \pm 0.8	2	351.49
B-1400	3.2 \pm 0.7	2	365.42
A-1704	3.7 \pm 0.8	2	338.49
Aprindine	4.6 \pm 0.02	2	322.49
Moxaprine	4.9 \pm 0.5	3	352.52

Table 4.1 Recovery time constants.

CHAPTER 5

VOLTAGE CLAMPED EXPERIMENTS

The ideal experiment to test the blocking effects of antiarrhythmic drugs should control the voltage of the preparation through each part of the action potential. The physical limitations of cardiac preparations prevents this ideal experiment from being performed under normal conditions because the sodium current is too large and fast to be adequately and accurately controlled. The development of computer controlled voltage clamp circuits however, has allowed us to voltage clamp the preparation during portions of the action potential where smaller currents are flowing. With this approach we were able to control the shape and resting potential of the action potential and thus obtain a more consistent experimental preparation.

5.1. Slow inactivation

The protocol used in this series of experiments consisted of a square pulse of variable duration (10-2000 msec), a return to resting level for 50 msec, followed by an unclamped test pulse. The action potential was allowed to free run during the upstroke of the prepulse and the upstroke of the test pulse. Upstrokes were evoked by a 1

Clamp Voltage (mV)	Time Constant (sec) ± SEM	Estimated Steady-state	Block at 2 sec ± SEM	n
-20	4.26 ± 3.05	0.75 ± .10	0.89 ± .02	6
0	4.82 ± 1.37	0.61 ± .10	0.86 ± .02	10
+20	2.32 ± 1.13	0.79 ± .08	0.87 ± .02	8
+40	4.33 ± 1.81	0.59 ± .16	0.85 ± .04	6

Note: Time constants and estimated steady-state levels are not significantly different ($p=0.74$, $p=0.51$).
SEM = Standard Error of the Mean

Table 5.1 Slow Inactivation

msec current clamp pulse. Switching between current clamp, free-run, and voltage clamp was done by the computer. Only preparations where the voltage could be controlled within 10 msec of the upstroke were used in these studies. The cell was clamped to the resting level (-85 mV) for 2 seconds prior to the prepulse and remained unclamped between experimental protocols.

Under control (no drug) conditions we found that a slow component of inactivation developed with an exponential time course. This process of slow inactivation had a time constant of 2.3 ± 1.1 sec ($n = 8$) at a clamp potential of +20 mV. The time constant of slow inactivation was not voltage-dependent over the range of -20 to +40 mV (see Table 5.1). Time constants similar to these have recently been reported (Clarkson et al. 1984). The estimated steady-state level of slow inactivation at each potential were also not significantly different. This is in contrast to the results of Clarkson et al. However, since the maximum duration of clamps used in this study were less than one time constant in length, extrapolation to steady-state may have resulted in erroneous estimates.

A 2000 msec maximum clamp duration was chosen to minimize the effect of slow inactivation on block development in the presence of drug. The average of 30 control experiments produced a $13 \pm 1\%$ depression of V_{max} for a

clamp of 2000 msec.

Clarkson et al. also reported an "ultra slow" component of inactivation with a time constant of several minutes. The ultra slow component of inactivation is expected to contribute very little (< 1%) to the clamps of 2000 msec or less used in the present work.

5.2. Plateau clamps in the presence of drug

Plateau clamps in the presence of aprindine derivatives produced in each case an exponential decline of test pulse V_{max} with increasing clamp duration. An attempt was made in each preparation to clamp to -20, 0, 20, 40 mV . However, it was not possible to adequately clamp the highest and lowest potential in every preparation . The V_{max} values reported were normalized to the largest V_{max} seen during control conditions.

In each of the ten experiments a 2000 msec clamp produced at least a 50% decline in V_{max} from control. In almost all cases the time constant of V_{max} depression was much shorter than that of control. A dose of 3.0 $\mu\text{g/ml}$ was used for each experiment in this section.

5.2.1. Aprindine Plateau Clamp

Figure 5.1 shows a typical plateau clamp experiment in the presence of aprindine (8.4 μM). A least-square

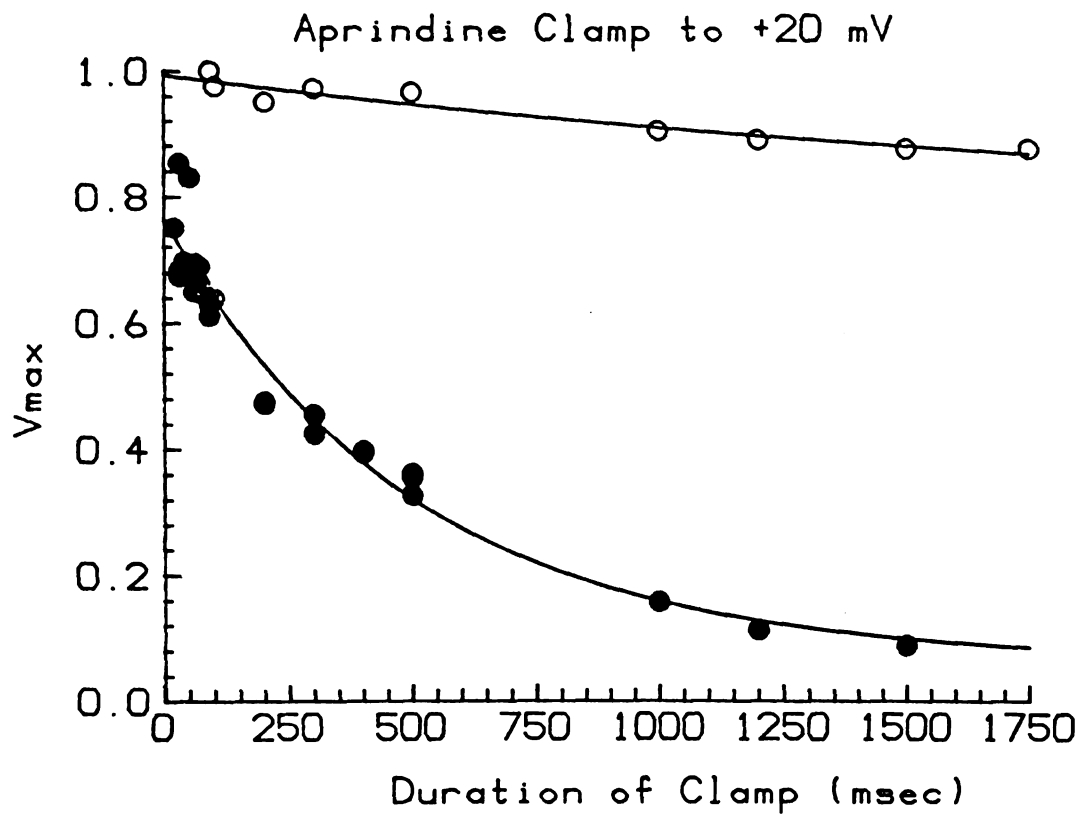


Figure 5.1 Aprindine Plateau Clamps

Open symbols represent control test response following a plateau clamp. Closed symbols show the response in the presence of $8.4 \mu\text{M}$ aprindine. The smooth line through the points is a least-square exponential fit of the points.

estimate of a single exponential of the form:

$$V_{max} = A \exp(-\text{time}/\text{Tau}) + \text{Const.}$$

has been fitted through the points. The time constant (Tau) in the drug condition in this figure is 500 msec. The value of V_{max} extrapolated to zero clamp duration is 0.77.

The difference between V_{max} at time zero in control conditions and V_{max} at time zero with drug is an indicator of the importance of activation block to the overall blocking behavior of the drug. The amount of block seen during the test pulse of a two pulse protocol will depend on:

- (1) Drug induced inactivation at the holding potential prior to the clamp step.
- (2) The block produced during the upstroke of clamp step.
- (3) The block occurring during the depolarizing clamp (plateau).
- (4) The recovery from block during the 50 msec rest period preceding the test upstroke.
- (5) The block occurring before the time of V_{max} in the test pulse.

Local anesthetics appear to shift the inactivation kinetics of drug associated channels in the hyperpolarizing direction (Weidmann 1955). A large voltage shift can

trap drug-associated channels in the inactivated state (Figure 1.1, page 7). This block will be seen as part of the tonic block in the presence of drug.

When an action potential is evoked, sodium channels open rapidly. Many sodium channel blocking drugs have a high affinity for this short lived channel state. These drugs can be termed "activation" or "open channel" blockers.

Drug free channels recover rapidly ($\tau =$ about 10 msec at -85 mv) from inactivation when the membrane potential returns to resting levels (Weidman 1955). Drugs that show use-dependent block at a particular holding potential do so in part because the time constant of recovery is slowed in the presence of drug. The recovery time constants of the aprindine derivatives vary over an order of magnitude (Table 4.1, page 63). The fastest drug (B-1404) would be expected to recover 13% during the 50 msec between the clamp and the test upstroke. The slowest drug (moxaprine) should recover only about 1% during this period.

Channels must be opened in order to assess the level of block. In the Hodgkin-Huxley model of the sodium channel about 10% of the channel open time occurs before the time of V_{max} . It follows that 10% of the full activation block can occur before the V_{max} of the test pulse.

In the experiment shown in Figure 5.1, and most others, the largest V_{max} value in the presence of drug is not the first time point (10 msec) but occurs some time after. The reason for this delayed peak is unknown but it makes the extrapolation to zero time uncertain.

As mentioned above, zero time block greater than tonic block indicates that the drug blocks during activation. However even a small block per activation, which might not show up on extrapolation to zero time, can be important to overall blocking behavior and produce significant levels of block during a train of action potentials. In the experiment shown in Figure 5.1 "tonic block", non-clamped V_{max} after a long rest, was depressed very little (< 5%) from control. This suggests that activation as well as the inactivation block apparent in the figure may be important in aprindine's blocking behavior.

5.2.2. A-1800 Plateau Clamp

The aprindine derivative A-1800 [11.4 μM] showed the fastest development of block during the inactivated state. An example of an experiment with clamps to +20 mV is shown in Figure 5.2 (page 73). In this experiment the V_{max} of the test pulse declined to a steady-state level within 300 msec ($\tau = 89$ msec). The zero intercept in this experiment was estimated to be 0.82. A fast inactivation blocker like A-1800 will be very sensitive to changes in action potential shape. Drugs such as A-1800 will preferentially act on portions of the heart with longer action potentials.

5.2.3. A-1622 Plateau Clamp

A much different profile is seen with compound C-1622 shown in Figure 5.3 (page 74). This drug produces a large zero time depression and a slow decline in V_{max} ($\tau = 623$ msec) to a steady-state level of 0.19.

5.2.4. A-777 Plateau Clamp

Figure 5.4 (page 75) shows the effects of the two pulse protocol in the presence of 8.7 μM A-777. The time constant of block is 333 msec. The zero time intercept is 0.98 .

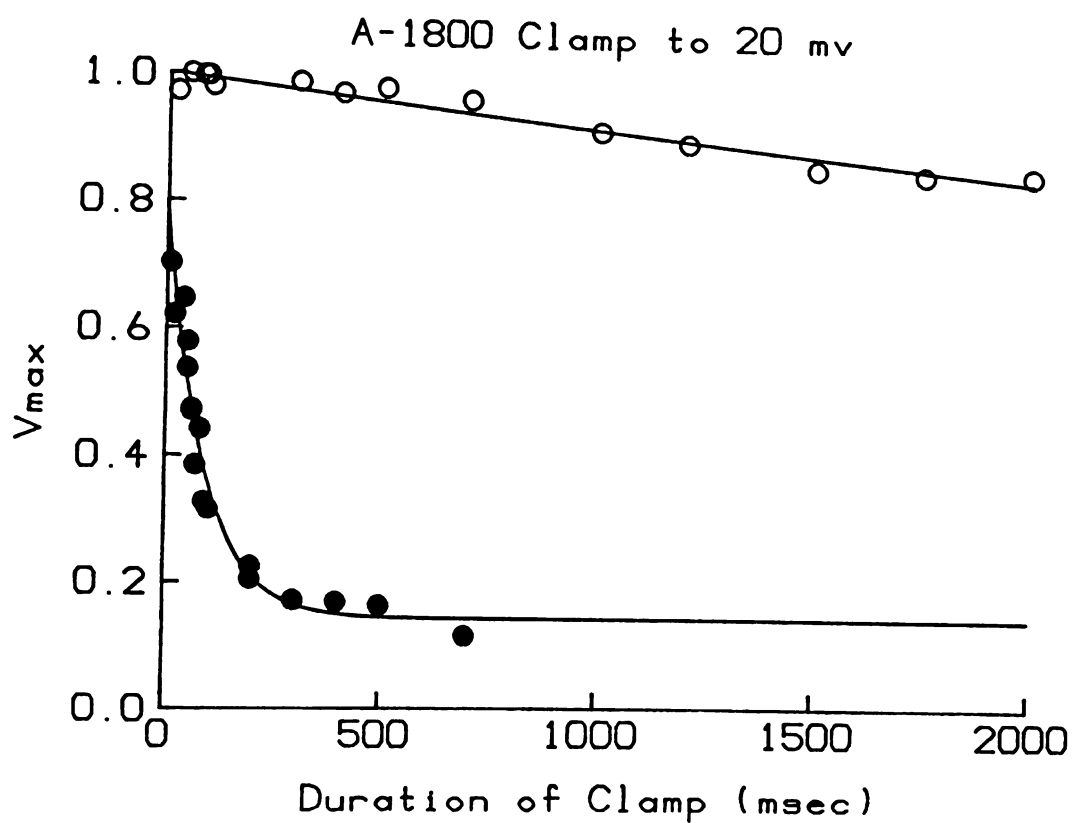


Figure 5.2 A-1800 Plateau Clamps

Open symbols represent control test response following a plateau clamp. Closed symbols show the response in the presence of $11.4 \mu\text{M}$ A-1800. The smooth line through the points is a least-square exponential fit of the points.

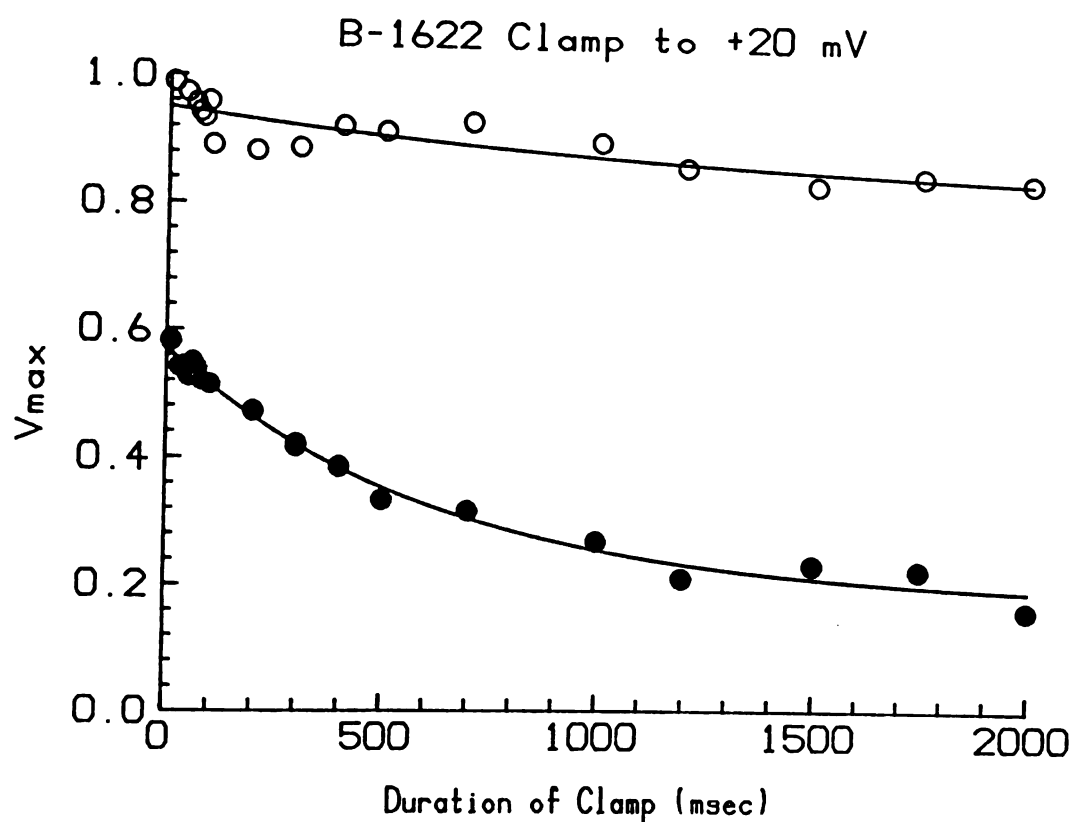


Figure 5.3 B-1622 Plateau Clamps

Open symbols represent control test response following a plateau clamp. Closed symbols show the response in the presence of 7.33 μ M B-1622. The smooth line through the points is a least-square exponential fit of the points.

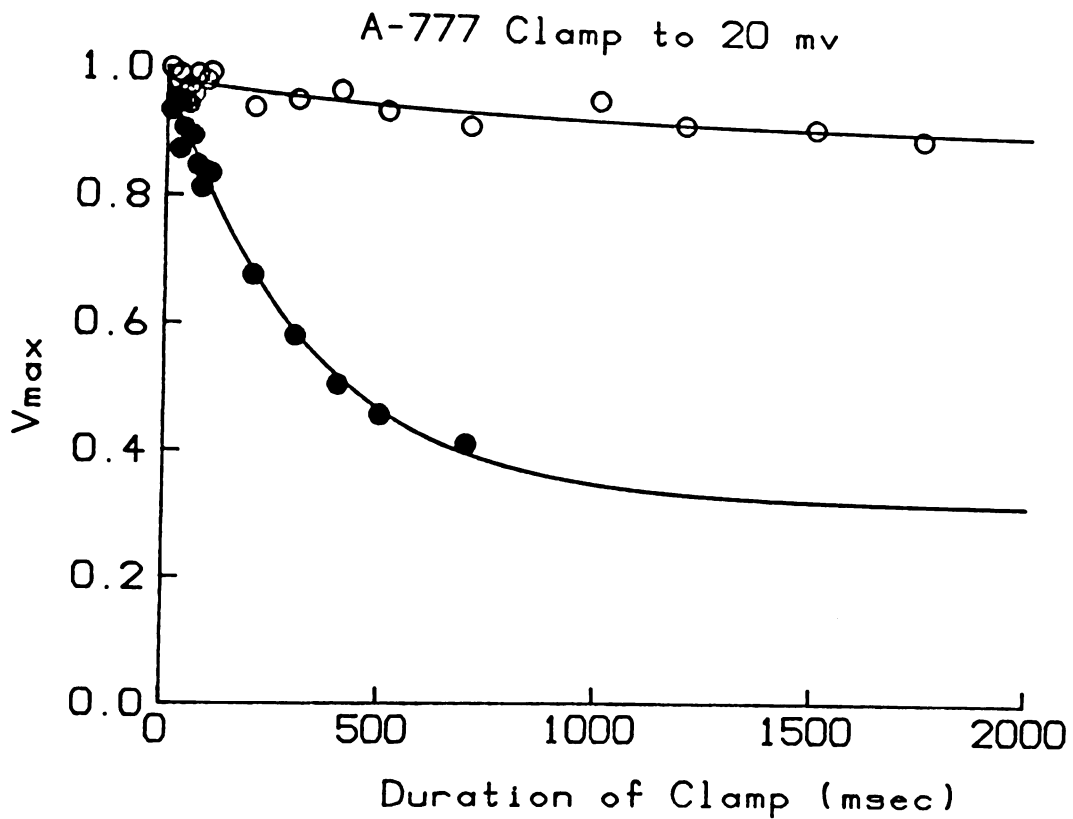


Figure 5.4 A-777 Plateau Clamps

Open symbols represent control test response following a plateau clamp. Closed symbols show the response in the presence of $8.7 \mu\text{M}$ A-777. The smooth line through the points is a least-square exponential fit of the points.

5.2.5. B-1704 Plateau Clamp

B-1704 [8.0 μM] is shown in Figure 5.5 (page 77). The time constant of block is 770 msec with a steady-state value of 0.45 and a zero time intercept of 0.87.

5.2.6. Moxapridine Plateau Clamp

The effects of 7.7 μM moxapridine are shown in Figure 5.6 (page 78). The time constant of block was 1000 msec with a zero time intercept of 0.68.

5.2.7. B-1400 Plateau Clamp

B-1400 is shown in Figure 5.7 (page 79). The time constant of block was 714 msec and the zero time intercept was 0.67.

5.2.8. B-1401 Plateau Clamp

B-1401 is shown in Figure 5.8 (page 80). The time constant of block was 2500 msec and the zero time intercept was 0.80.

5.2.9. B-1404 Plateau Clamp

B-1404 is shown in Figure 5.9 (page 81). The time constant of block was 320 msec and the zero time intercept was 0.84.

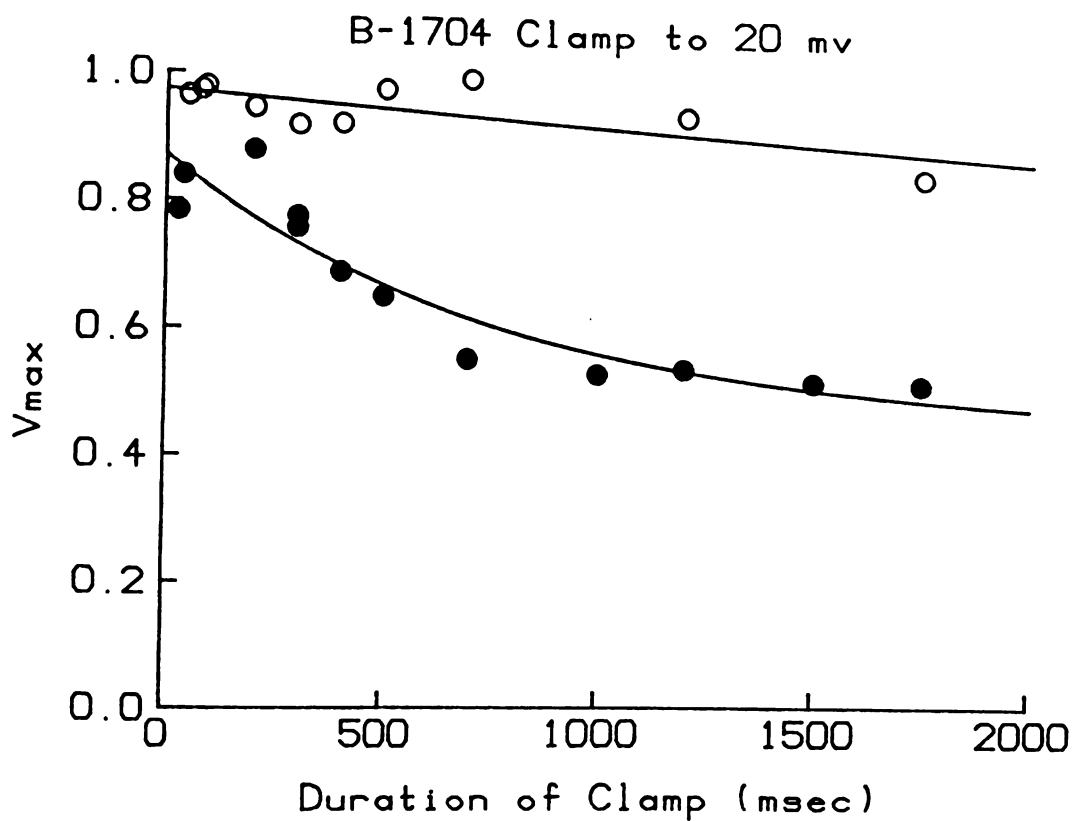


Figure 5.5 B-1704 Plateau Clamps

Open symbols represent control test response following a plateau clamp. Closed symbols show the response in the presence of $8.0 \mu\text{M}$ B-1704. The smooth line through the points is a least-square exponential fit of the points.

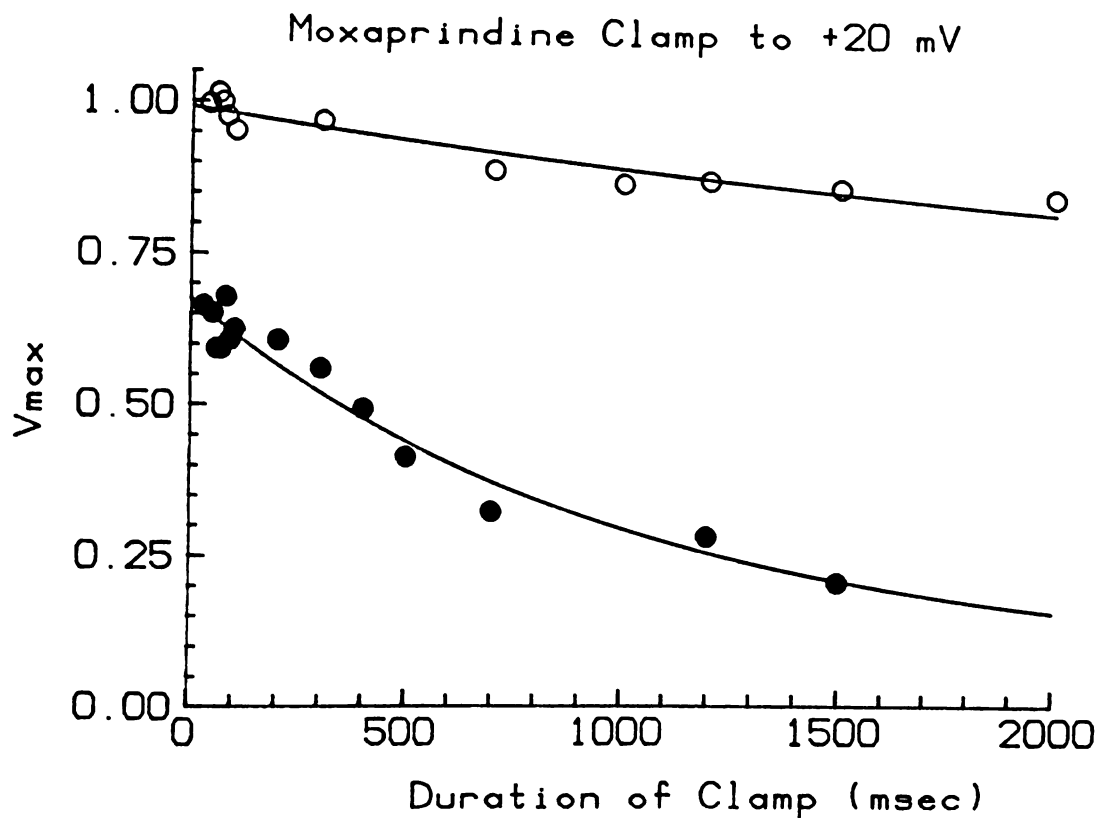


Figure 5.6 Moxaprine Plateau Clamps

Open symbols represent control test response following a plateau clamp. Closed symbols show the response in the presence of $7.7 \mu\text{M}$ moxaprine. The smooth line through the points is a least-square exponential fit of the points.

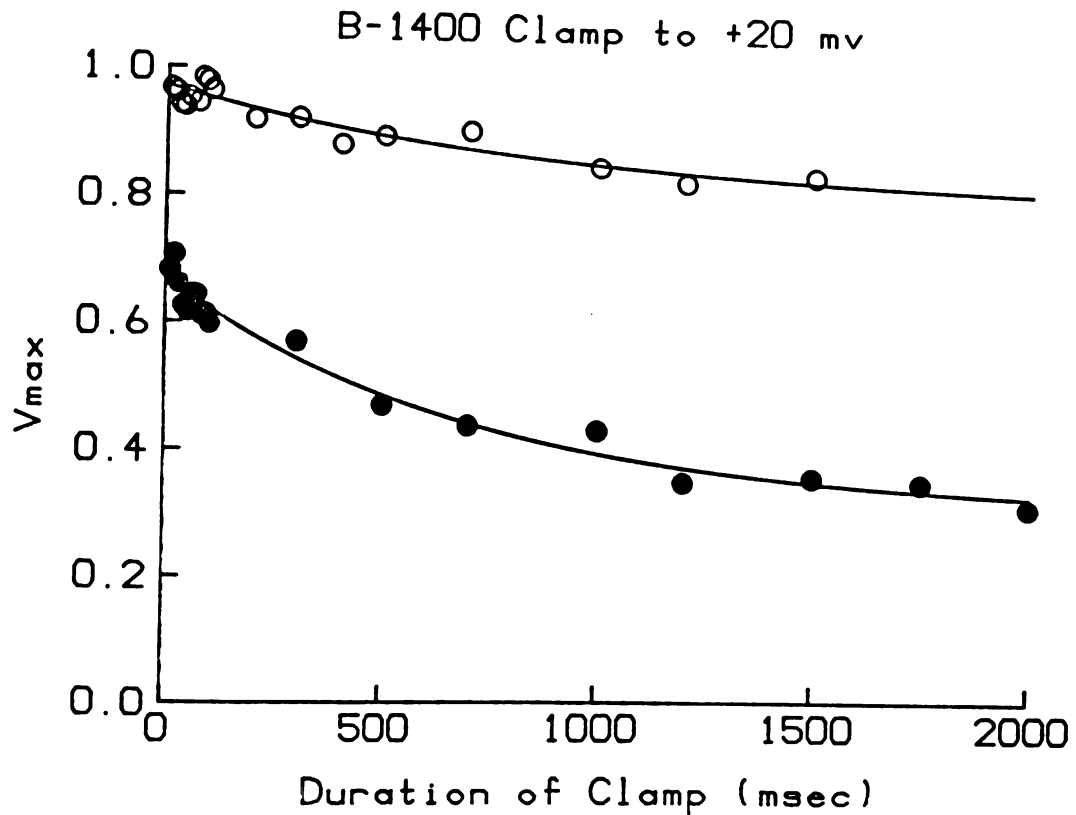


Figure 5.7 B-1400 Plateau Clamps

Open symbols represent control test response following a plateau clamp. Closed symbols show the response in the presence of 7.46 μM B-1400. The smooth line through the points is a least-square exponential fit of the points.

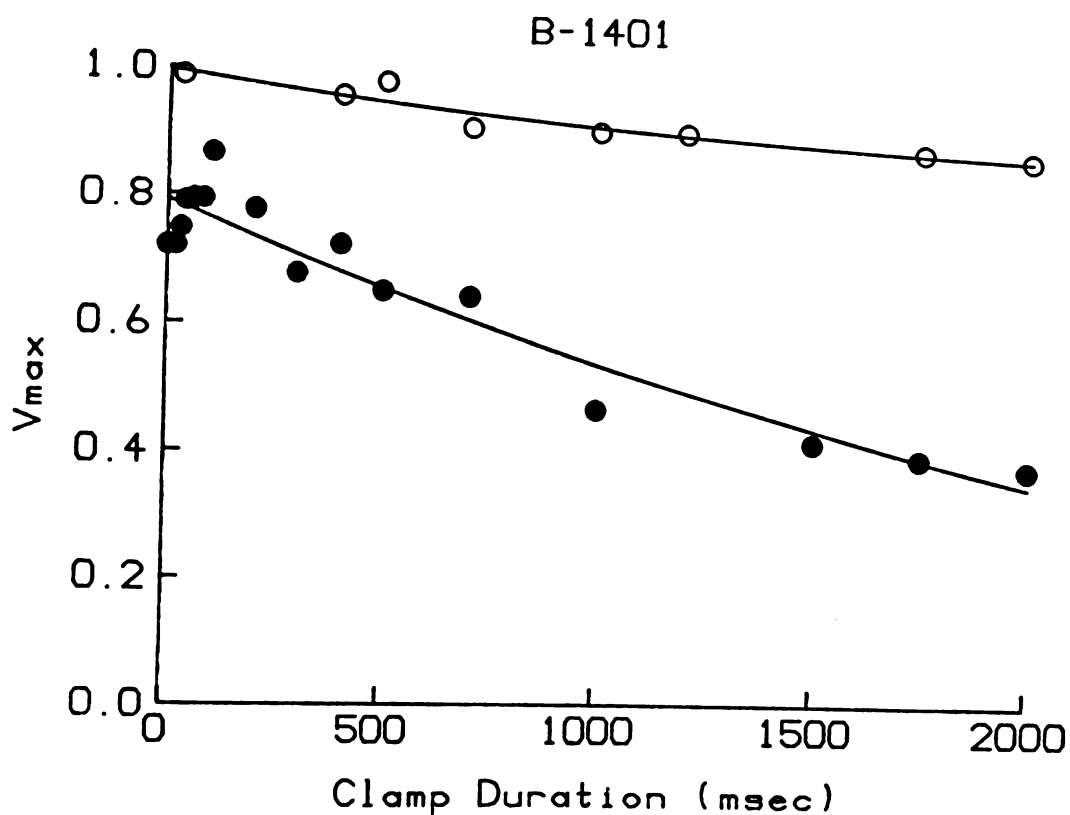


Figure 5.8 B-1401 Plateau Clamps

Open symbols represent control test response following a plateau clamp. Closed symbols show the response in the presence of $7.73 \mu M$ B-1401. The smooth line through the points is a least-square exponential fit of the points.

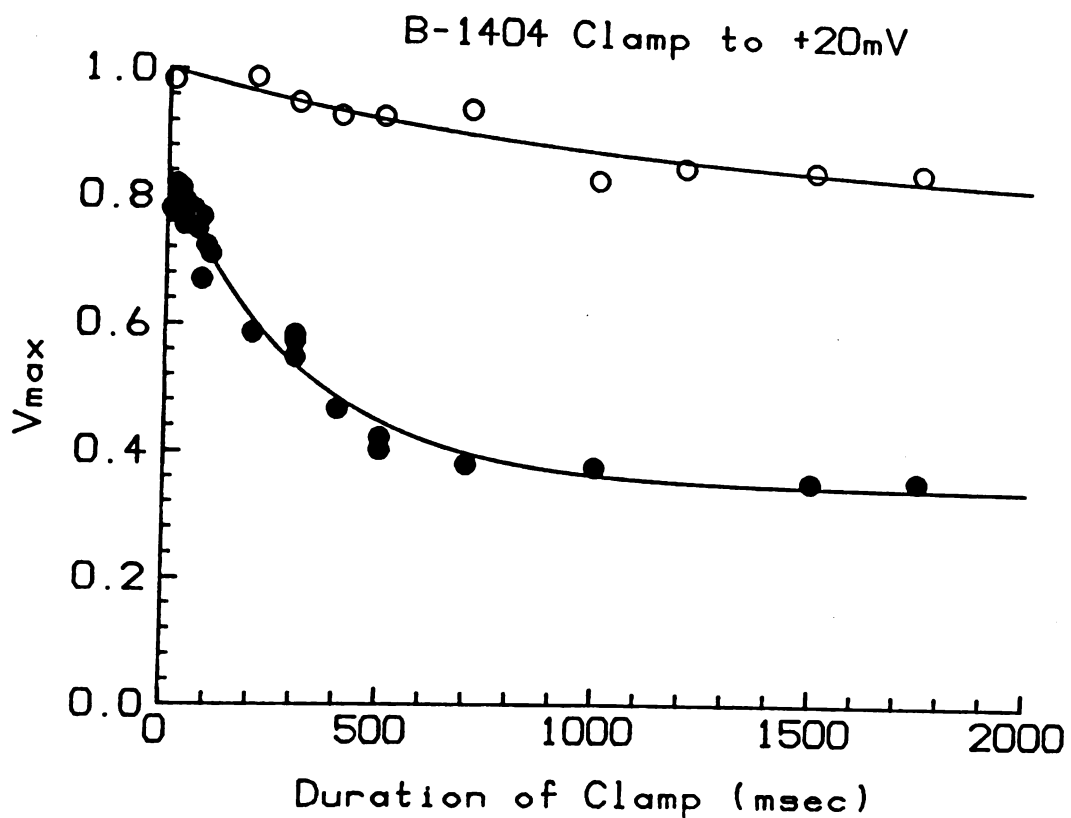


Figure 5.9 B-1404 Plateau Clamps

Open symbols represent control test response following a plateau clamp. Closed symbols show the response in the presence of 7.46 μ M B-1404. The smooth line through the points is a least-square exponential fit of the points.

A summary of the time constants of inactivation block is shown in Table 5.2 (page 84).

5.3. Voltage dependence of plateau

None of the compounds studied was clearly voltage dependent in the range of -20 mV to +40 mV. Figure 5.10 shows inactivation block at four clamp potentials in the presence of A-2077.

Deviations in the exponential fit from one voltage to another were always accompanied by a large difference in the estimated steady-state level of block. The estimated steady-state value is very sensitive to scatter of the data, particularly for drugs with longer time constants. When the fits used to generate the data in Table 5.2 were forced to a common steady-state level large differences between time constants disappeared. It is clear from these experiments that if there is voltage dependence at depolarized potentials it is not very large.

In contrast to inactivation block activation block has been shown to be voltage dependent (Yeh & Narahashi 1977, Cahalan & Almers 1979). The pooled mean zero time block for all the drugs increased from .20 at 0 mV to .25 at +40 mV (Table 5.3, page 85).

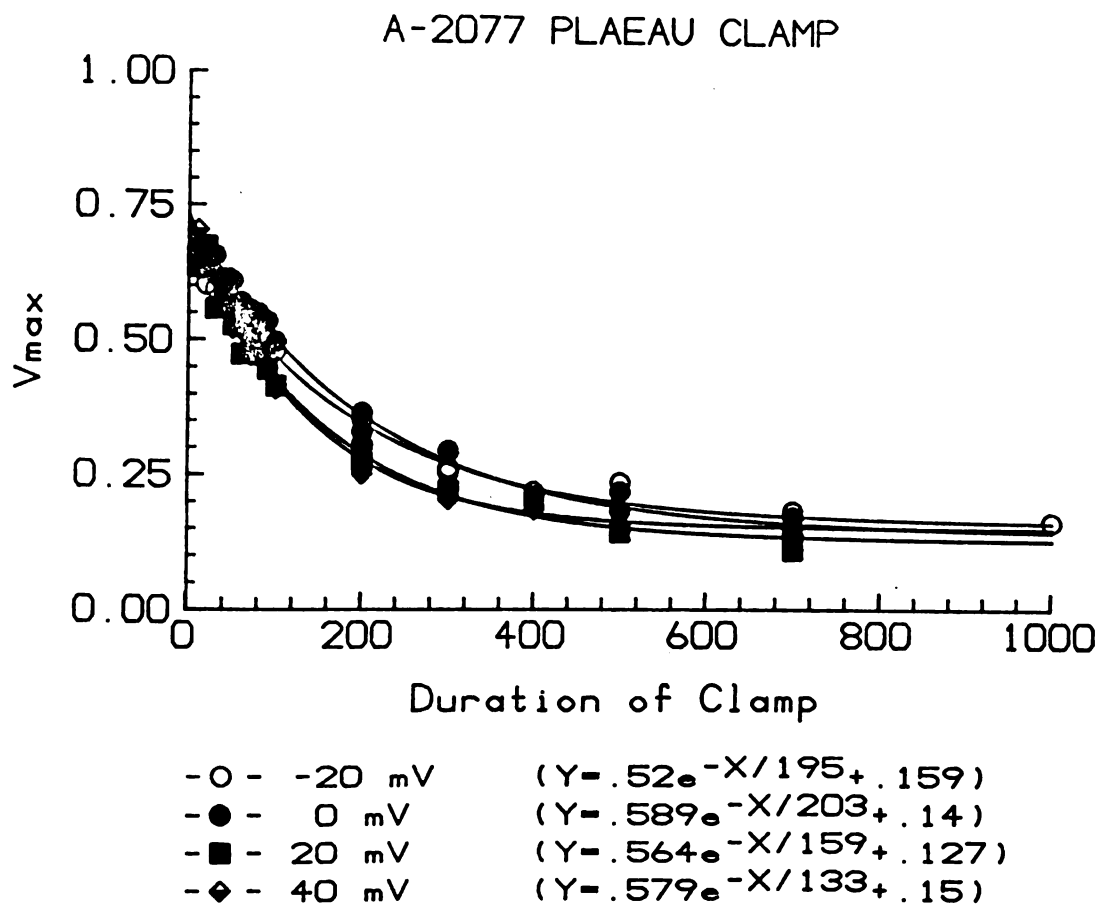


Figure 5.10 A-2077 Plateau Clamps

Plateau clamps to -20, 0, +20, +40 mV in the presence of $9.43 \mu\text{M}$ A-2077. The smooth line through the points is a least-square exponential fit of the points.

Time Constants (msec)				
Compound	Plateau Voltage			
	-20 mV	0 mV	+20 mV	+40mv
Moxaprine	592	792	1005	1244
Aprindine		512	499	
777		431	333	390
2077	195	204	159	132
1800	97.2	122	88.9	82.6
1704	1950	3896	769	
B-1400		1703	714	2660
1622	627	1025	623	650
1404		838	320	481
1401	4339	2170	2527	1923

Table 5.2 Plateau Clamp Protocol Time Constants

Shown are the time constants for the rate of development of block during the plateau. The protocol used is described in the text.

Compound	Plateau Voltage		
	0 mV	+20 mV	+40mv
Moxaprine	.71	.68	.66
Aprindine	-	.76	.72
777	.71	.68	.66
2077	.73	.69	.73
1800	.88	.82	.88
1704	.84	1.0	-
1400	.69	.67	.62
1622	.63	.57	.62
1404	.88	.84	.87
1401	.89	.81	.84

Table 5.3 Plateau Clamp Zero Time Intercepts

Shown are Vmax values for a plateau clamp extrapolated to zero time. Values are normalized to control Vmax.

CHAPTER 6

DISCUSSION

6.1. Physical properties and use-dependence

6.1.1. Rate of development of block

The use-dependent block of the aprindine compounds shown in Chapter 3 all demonstrated beat-by-beat decline in Vmax until a steady state was reached. The rate of decline depended on the rate of stimulation and dose. The rate of decline (beat constant) varied from 0.65 beats for the fastest drug (B-1404) to 11.5 for the slowest (C-1622) (see Table 6.1).

The rate of block is a global description of use-dependent block composed of the block occurring during the action potential and the unblocking occurring during diastole. Courtney (1980) and others have correlated the rate of block with the size (molecular weight) of sodium channel blockers.

Table 6.1 ranks the 10 drugs used in this study in the order of their beat constants at 2 Hz. In Figure 6.1 the beat constant of depression is plotted against the

Compound	Beat Constant	Mol. Weight	Log Q	pKa
B-1404	1.01 (1)	366 (10)	2.61 (9)	6.38 (1)
A-2077	1.26 (2)	281 (1)	2.07 (3)	8.43 (3)
A-777	1.32 (3)	309 (2)	2.21 (6)	8.80 (5)
A-1800	3.90 (4)	323 (3)	3.54 (10)	8.13 (2)
A-1704	4.08 (5)	339 (6)	2.08 (4)	8.73 (4)
Aprindine	4.12 (6)	323 (4)	2.41 (8)	9.18 (7)
Moxapridine	4.85 (7)	353 (8)	2.09 (5)	9.63 (10)
B-1401	6.17 (8)	352 (7)	1.92 (2)	8.82 (6)
B-1400	8.12 (9)	365 (9)	.966 (1)	9.45 (9)
C-1622	11.5 (10)	337 (5)	2.36 (7)	9.26 (8)

Table 6.1
Physical characteristics of the compounds studied.
Numbers in parenthesis indicate relative ranking in each column.

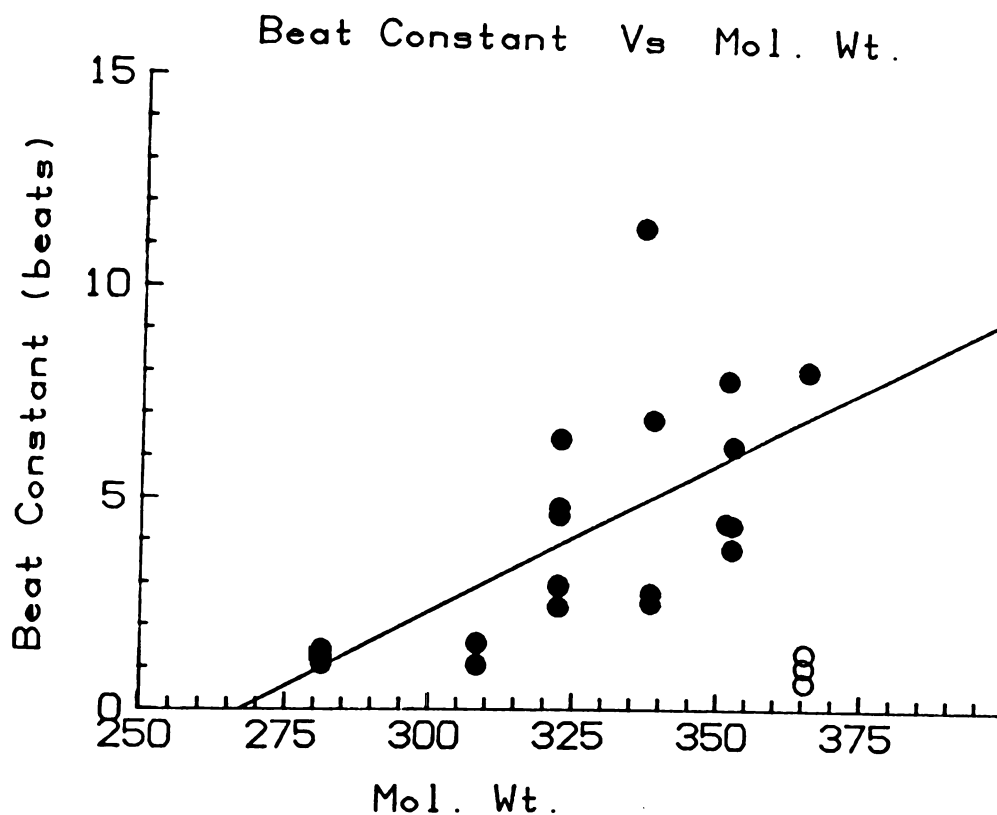


Figure 6.1 Beat constant vs molecular weight

Beat constant at 2 Hz is plotted against molecular weight of the base. Filled circles are included in the regression line shown. Open circles are compound B-1404 not included in the regression (see text). Numeric values are listed Table 6.1 .

molecular weight of the 10 compounds. A linear correlation calculation using all experimental points was not significant at the 95% confidence level ($p=0.07$, $r=0.36$). However, if we repeat the correlation with compound B-1404 excluded (open circles in Figure 6.1), we get a significant correlation ($p=0.0007$, $r=0.67$). This regression line is shown in the figure and is given by the formula:

$$\text{Beat Constant} = 0.710 (\text{Mol. Wt.}) - 18.99$$

The compound B-1404 is unique in several respects. It has the highest molecular weight (365.5), the lowest pKa (6.38), and the fastest block onset. Structurally, it is the only compound in the series with a terminal morpholine group.

The relationship between the beat constant and pKa is shown in Figure 6.2. The regression line shown in the figure is given by the equation:

$$\text{Beat Constant} = 1.56 \text{ pKa} - 9.63$$

$$(r=0.52, p=0.007)$$

Interestingly, if we include all the points, pKa is more strongly correlated with beat constant than any other of the physical properties (Mol. Wt, Log Q, Log P) tested. As noted above the only compound with a pKa below 7.4 is B-1404.

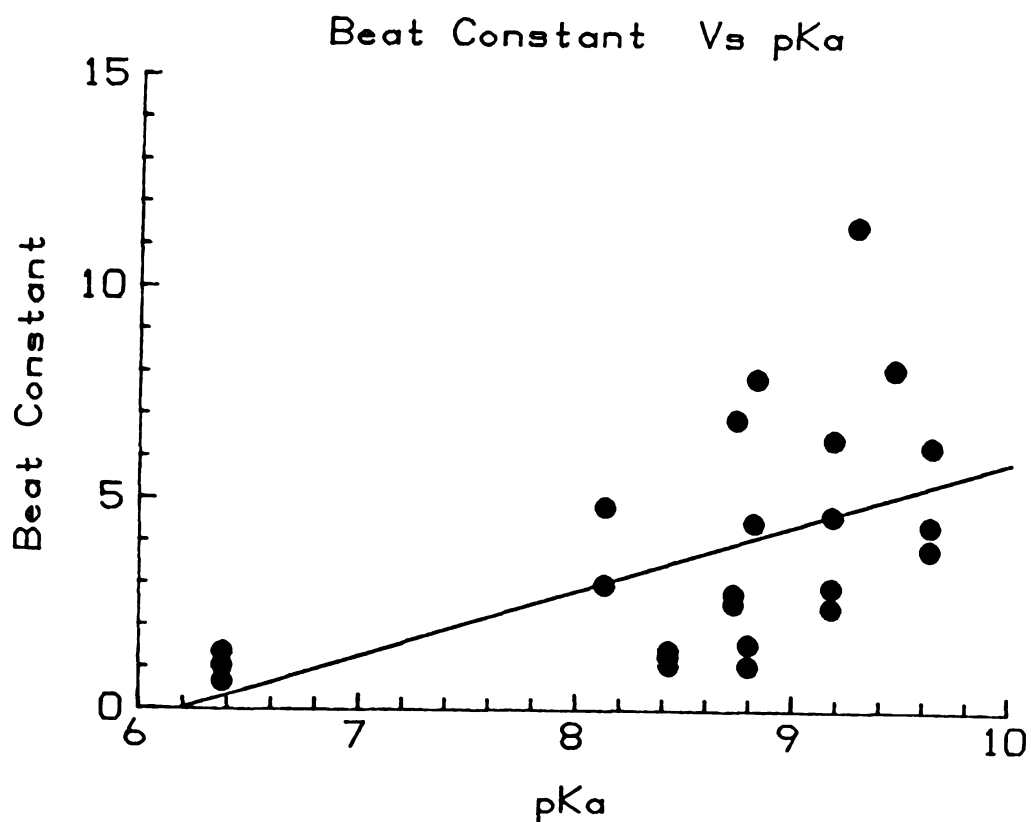


Figure 6.2 Beat constant vs pKa

Beat constant at 2 Hz is plotted against pKa for each compound. The equation of the regression line is described in the text. Numeric values are listed in table 6.1 .

A stepwise regression with the parameters mol. wt., pKa, and Log Q is best fitted by the following formula:

$$\begin{aligned} \text{Beat Constant.} &= 1.91 (\text{pKa}) + 0.048 (\text{Mol. Wt.}) \\ &+ 0.499 (\text{Log Q}) - 29.7 \end{aligned}$$

The coefficient of determination for this regression is 0.49 ($p = 0.002$). The coefficient of determination expresses the proportion of total variability attributable to the dependence on all the variables (Wonnacott & Wonnacott 1977). The variables are listed in the equation in the order of their importance to the regression.

6.1.2. Recovery from block

The blocking rate reflects both the the rate of drug induced blocking and the rate of unblocking. The correlations shown above may reflect a dependence of only one of these processes (blocking or unblocking) on the physical properties of the compounds studied.

In Chapter 4 the rates of unblocking during rest were determined. The rates of channel unblocking determined by the method of chapter 4 will be independent of the blocking behavior of the compounds except for the small amount of block occurring before the time of V_{\max} on the test pulse. Courtney and others have shown that rates of unblocking are insensitive to drug dose and are correlated

with lipid solubility and with size.

Figure 6.3 shows the average tau recovery plotted against pKa of the compounds. The linear fit to the data gives a regression formula:

$$\text{Recovery Tau} = 1.32 (\text{pKa}) + 9.14 \quad (r = 0.69, p = 0.028)$$

The relationship between pKa and recovery time constant was again the most significant of the physical parameters followed by molecular weight and lipid solubility. Multiple correlation of recovery time constant with these parameters produced the following formula:

$$\begin{aligned} \text{Recovery Tau} = & 1.23 (\text{pKa}) + .03 (\text{Mol. Wt.}) \\ & + .45 (\text{Log P}) - 20.7 \end{aligned}$$

The correlation coefficient for this formula is 0.70 ($p = 0.05$). The expected values using this formula are shown in Table 6.2 (page 94). In Table 6.2 the ratio of the measured recovery time constant and the predicted value is shown in the third column. We see from this ratio that the compounds with the largest deviation from unity are the compounds with the fastest recovery.

The results presented here differ from the report by Courtney (1981) that molecular weight was the most important factor in determining unblocking rates. Here pKa

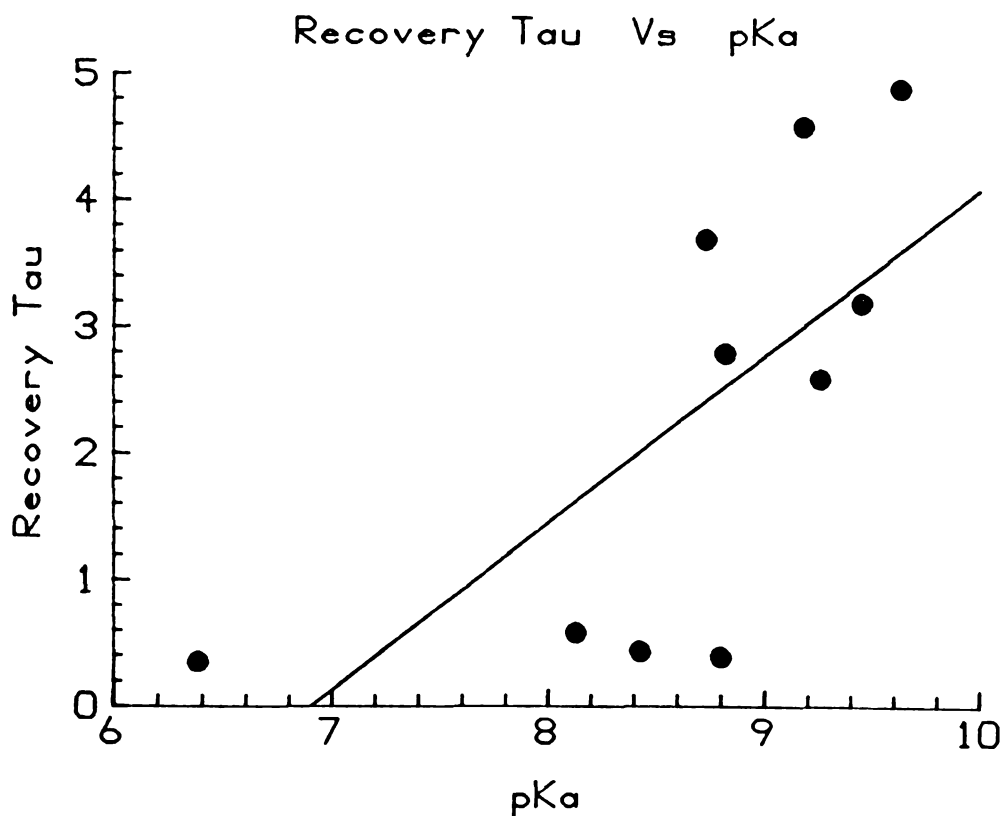


Figure 6.3 Recovery Tau vs pKa

The time constant of recovery (Tau) in seconds is plotted against pKa . The equation of the regression line is described in the text. PKa values are listed in Table 6.1.

Compound	Tau Recovery (sec.)	Predicted Tau (sec.)	Ratio
B-1404	.35	.08	4.3
A-777	.39	1.7	.25
A-2077	.43	.11	3.8
A-1800	.58	1.6	.36
C-1622	2.6	3.4	.76
B-1401	2.8	3.0	.95
B-1400	3.2	4.0	.80
A-1704	3.7	2.5	1.5
Aprindine	4.6	2.8	1.6
Moxaprine	4.9	4.4	1.1

Table 6.2 Time constant of recovery (Tau) and values of Tau predicted from the equation shown in the text. The ratio of measured to predicted is shown in the last column (Ratio).

seems to correlate most strongly both with recovery time and rates of block onset. Lipid solubility (Log P) was the least important parameter to both recovery tau and beat constant. Log P was positively correlated with blocking rates and negatively correlated with recovery time constant.

The modulated receptor hypothesis includes the idea that hydrophobic pathways are important determinants of removal of drug from closed channels (Hille 1977). Presumably this requires the diffusion of the uncharged species through the membrane. We recall that permanently charged molecules such as QX-314 have slow recovery from block whereas permanently neutral molecules such as benzocaine are very rapid. For ionizable compounds such as the ones in this study the rate of loss of a proton, which may be a required step in closed channel unblocking, is a function of pKa and external pH. All the drugs in this study are very lipophilic in the unionized form. It may be that under these circumstances pKa becomes the most important parameter determining closed channel unblocking.

6.1.3. Block during the plateau

Since channels are closed during most of the plateau we would expect some of the same physical properties that affect closed channel unblocking during rest to be

involved with the rates of blocking seen during the plateau phase of the action potential. The relationship between molecular weight and plateau blocking constants (time constant of blocking during plateau clamp) is shown in Figure 6.4. The correlation coefficient for this relationship is 0.54. The physical property most strongly correlated with block during the plateau is Log Q. This relationship is shown in Figure 6.5 (page 98). The correlation coefficient for this relationship is -0.56. PKa was not significantly correlated with the plateau time constant.

It is clear that physical properties are important in determining the rates of blocking and unblocking seen with aprindine derivatives. Low pKa is associated with rapid unblocking and with the global blocking parameter beat constant. Larger size is associated with slower rates of blocking and unblocking. On the other hand higher lipid solubility seems to be associated with more rapid block during the plateau.

6.2. Models of sodium channel block

It is clear from the results presented here that the global behavior of sodium channel blockers is a complicated function of blocking and unblocking rates. These rates may be modified by pH, action potential duration,

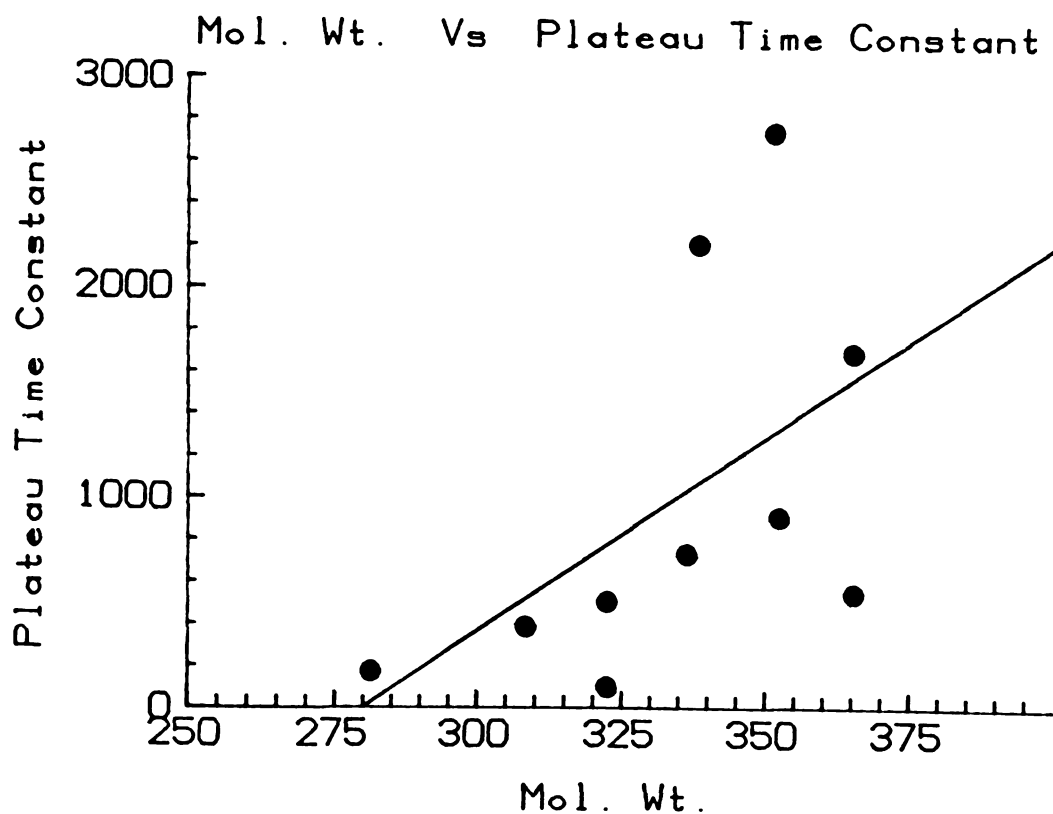


Figure 6.4 Molecular weight vs plateau block

Molecular weight is plotted against the time constant of block during the plateau (msec). The regression line shown is described in the text. Molecular weights are listed in Table 6.1.

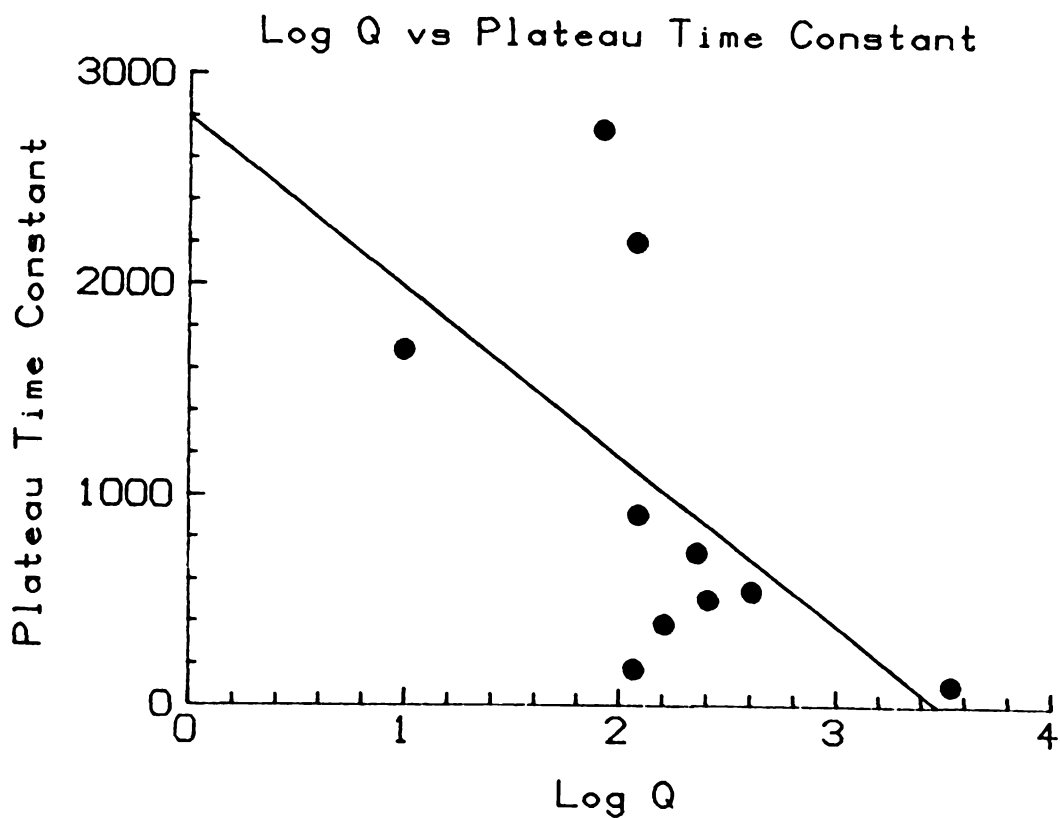


Figure 6.5 Log Q vs plateau block

Log Q is plotted against the time constant of block during the plateau (msec). The regression line shown is described in the text. Log Q values are listed in Table 6.1.

and resting potential. An understanding of how a compound's properties affects its usefulness as a clinical antiarrhythmic agent requires knowledge of how a drug interacts with sodium channels during each phase of an action potential under a variety of external conditions. Many of the proposed drug-receptor interactions are not directly measurable and must be inferred. The development of a model of sodium channel blocking has allowed inferences about these more fundamental processes to be made from measurements of the kinetics of sodium channel block.

Sodium channel kinetics can be described in terms of three states of the channel (Hodgkin & Huxley 1955). In the rested state (R), which is most prevalent at negative membrane potentials, the channels are closed but they can be opened by depolarization. Upon depolarization, rested channels can briefly open (O) before becoming inactivated (I). During the inactivated state, which is most prevalent at depolarized membrane potentials, channels are closed and cannot be opened by further depolarization.

Ideas about the mechanism of transition between these three states have changed in light of recent measurements of single sodium channels. Nevertheless, the kinetic behavior of large populations of sodium channels can be well described in terms of the rested, open, and inactivated states.

6.2.1. Modulated receptor model

Hille (1977) and Hondeghem & Katzung (1977) proposed that each of the sodium channel states has characteristic association and dissociation rate constants for any particular sodium channel blocker. Thus the action of sodium channel blockers would be modulated by the state of the sodium channel, and the receptor modulation would provide the basis for the voltage- and time-dependent action of these drugs. This hypothesis has been called the modulated receptor hypothesis (MRH) (Hille 1977). According to this hypothesis, drug-associated channels behave similarly to drug free channels with two exceptions:

- (1) They do not conduct sodium, even when open.
- (2) Drug binding stabilizes the inactivated state of the channel.

At normal resting potentials drug-free channels are mostly in the rested state, while drug-associated channels remain mostly in the inactivated state.

The development of this model makes it possible to characterize drug behavior in terms of affinities of the drug to the three states of the sodium channel.

6.3. Computer Implementation of the MRH

Hondeghem and Katzung (1977) published a set of differential equations for the modulated receptor theory in ventricular myocardium. They translated these equations into a program, written in the BASIC language, which they ran on a laboratory computer. This program, even after extensive optimization could simulate only 3 action potentials per hour. A small experimental protocol of 10 action potentials required more than 3 hours of computation. Checking only 10 different estimates of the 7 model parameters with a database of only 10 points would take more than a thousand years of computation time.

As part of this dissertation research the model was rewritten in a higher level computer language "C". Although this produced substantial improvements in speed it still took over a minute to simulate a single action potential. Speeds several orders of magnitude greater than this are required to make least square error estimates of model parameters practical. Moreover, in order to quantitatively unravel the structure activity relationship of sodium channel blockers in terms of MRH it will be necessary to determine model parameters for a large number of drugs. With this goal in mind we undertook the development of a simplified model which, while duplicating most of the features of the full MRH model allows analyti-

cal solution (and thus rapid calculation) of the differential equations embodied in the model.

6.4. Simplification of the model

The analytical solution to the MRH model was made possible by making two assumptions about the behavior of common sodium channel blockers. These assumptions were based on our present knowledge of the kinetics of sodium channel block. It is possible that drugs may be found and conditions altered such that these assumptions are no longer valid. Nevertheless we shall show that the simplified (fast) model produces simulations very similar to the full model under a variety of conditions.

6.4.1. Rested state equilibrium

All sodium channel blockers produce block in a tonic and use-dependent fashion. The tonic block is responsible for the reduction of the sodium current observed after an infinitely long rest period, whereas use-dependent block is the additional reduction of the sodium conductance that is observed only when the channels are being opened and inactivated by depolarizations.

In terms of the modulated receptor hypothesis tonic block can result from binding of the drug to any of the three states:

(i) Binding to rested channels will result in tonic reduction of sodium conductance.

(ii) Any block of open channels that occurs during the first action potential after a long rest period, but prior to the measured peak will also appear as tonic block. Also, at potentials where channels are noisy and exhibit random openings, open channel block will appear as tonic block.

(iii) The combination of slow recovery of block from the inactivated state with a voltage shift of inactivation to more negative membrane potentials will trap channels in the ID state (Figure 1.1, page 7). This too would appear as tonic block.

Use-dependent block results when the time between depolarizations is too short for recovery from block to proceed to equilibrium (Hondeghe & Katzung 1984). For most drugs studied so far, use dependence can be progressively reduced as the membrane potential between depolarizations is made more negative (Hondeghe and Katzung 1980). One interpretation of these results is that as more of the channels are clamped into the R and RD states, distribution between the drug-free and drug-associated channels occurs progressively more quickly. Thus, one only needs to know the dissociation constant (K_{dR}) in order to compute the distribution between the R and RD

states. The modified model assumes equilibrium between the R and RD states.

It is unlikely that the transitions between the R and RD states occur truly instantaneously. Therefore, it is to be expected that as the time in the rested states is progressively shortened one might reach a point where using the dissociation constant is no longer satisfactory to accurately compute the distribution between the R and RD states. Even if the equilibrium between R and RD isn't fast it is known that the O - OD equilibrium is fast. Upon depolarization channels may partition between these two states according to their affinity regardless of the distribution in R and RD.

6.4.2. Modification of the open state model

The open state has a very short duration (Yeh & Narahashi, 1977). Drug interactions with the open state must be very rapid for any significant block to occur. Direct measurement of the open state interactions have been performed in nerve and in all instances an equilibrium is reached in a few hundred μ sec (Hondeghe & Katzung, 1984). It is doubtful however, that this is fast enough to reach a steady state during one upstroke. In heart the equivalent open channel time at 37°C has been estimated to be only 0.3 msec (Hondeghe & Katzung 1977),

and even at 22°C the mean channel open time was measured to be only 1 msec (Lo & Shrager 1981). Thus, it unlikely that for all drugs open state equilibrium would be reached during a single upstroke.

In the original description of open channel block (Strichartz 1973, Courtney 1975) open channel block was treated as a discrete event: during each upstroke a fraction of the rested channels blocked/unblocked. Although this may not be fully correct, postulating a fixed fractional block for a fixed open time is one practical simplification. Recent evidence from single sodium channel recordings suggest that open time may indeed be a constant for a given condition (Aldrich et al, 1983). If this result is confirmed our assumption of fixed fractional block per activation becomes even more realistic.

6.4.3. Derivation of analytical solution

The above simplifications to the original MRH model (i.e. equilibrium of rested and open drug binding) allow the new model to be decomposed into two discrete state models both of which have an analytical solution.

6.4.3.1. The Closed States Model

The closed states model describes the movement of channels between blocked and unblocked states during rest or the plateau of an action potential. Since no channels are in the open state, all channels are distributed between the rested and inactivated states:

$$(1) \quad R + RD + I + ID = 1$$

where R and I represent the fractions of channels that are in the drug-free rested and inactivated states respectively; while RD and ID represent these respective drug-associated channels. Since the transitions between the rested states are assumed to be at equilibrium at all times it follows that:

$$(2) \quad (R \times [D]) / RD = KdR$$

where [D] is the drug concentration and KdR is the rested state dissociation constant.

The transition between the rested and inactivated states is controlled by Hodgkin-Huxley variables α -h and β -h, and α' -h and β' -h in the same way as in the original model. These rate constants are voltage-dependent functions and are described in the Hondeghem and Katzung paper (1977, equations 15-18).

The transitions between the I and ID pools are governed, as in the original model, by the rate constants k_i and l_i . The modified model is shown schematically in Figure 6.6. The above assumptions can be translated into a set of simultaneous differential equations:

$$(3) \quad (dR/dt + dRD/dt) = (\alpha-h * I) + (\alpha'-h * ID) \\ - (\beta-h * R) - (\beta'-h * RD) .$$

$$(4) \quad dI/dt = (\beta-h * R) + (l_i * ID) \\ - (\alpha-h * I) - (k_i * [D] * I) .$$

$$(5) \quad dID/dt = (\beta'-h * RD) + (k_i * [D] * I) \\ (\alpha'-h * ID) - (l_i * ID) .$$

Equations 1-5 can be solved as shown in appendix A.

6.4.3.2. Open State Model

The open state model operates only at the instant of depolarization. All channels in the rested states (R and RD) are distributed between the O and OD states according to the open state affinities (Figure 6.6). The O and OD pools are then added to the I and ID pools respectively.

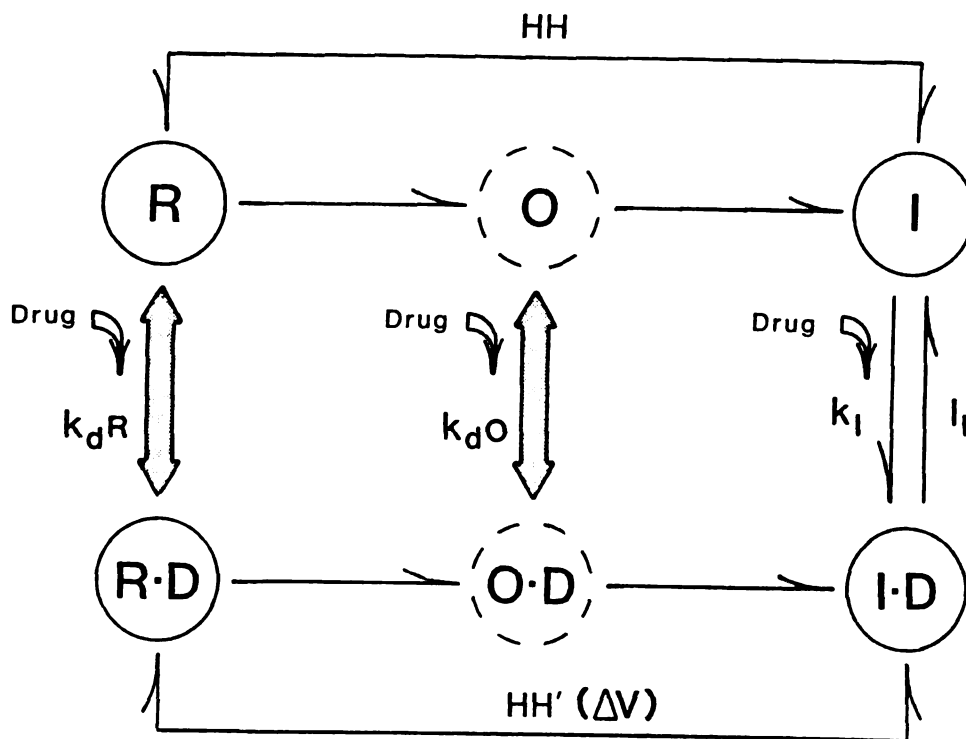


Figure 6.6 Modified MRH model

Drug-free channels (R , O , I) bind drug (D). Drug associated channels (RD , OD , ID). The $R \leftrightarrow RD$ transition and $O \leftrightarrow OD$ are always at equilibrium defined by K_{dO} and K_{dR} . Channel gating (HH) is shifted in the hyperpolarizing direction for drug associated channels (HH').

The formulation of the open state model is given in the two equations below where the subscript "b" denotes a pool just before activation and "a" just after activation.

$$(6) \quad I_a = I_b + (R_b + RD_b) * 1 / (1 + [D]/KdO) .$$

$$(7) \quad ID_a = ID_b + (R_b + RD_b) * 1 / (1 + KdO/[D]) .$$

6.4.4. Least square error search

The analytical solution provided by the simplified model makes it feasible to search for parameter values that minimize the difference between experiment and model. Using a PDP11/34 running the UNIX operating system each action potential is computed in about 1.5 msec. A full 10 point parameter grid least square error search against 10 experimental points for 5 parameters of the analytical version of the model (KdR , KdO , ki , li and voltage-shift (DV)) requires approximately 1/2 hour of computation.

Although the simplification to the model speeds up model simulation by many orders of magnitude, use of the "grid" method of search still requires large computation times. Of the various searching strategies possible we have opted to use the "Pattern search" algorithm (Hook & Jeeves, 1961). Pattern search is a direct search routine for minimizing a function of several variables. This

method searches for patterns of parameter changes which are successful in reducing the error. These changes are then repeated until they fail to decrease the error. A new pattern is then found and the process repeats itself. The process ends when no successful pattern can be found. This method has been found to be successful with many non-linear curve fitting problems involving minimization of the sum of the squares (Wilde 1964).

In the simulations to be presented here an average of about 3000 separate simulations of an experiment with about 60 action potentials are performed with an average total run time of about 20 min.

6.4.5. Comparison of MRH models

In order to evaluate to what extent the simplified model can reproduce the full model, we used data derived from the full model as input for the simplified model. The rate constants reported by Hondeghem & Katzung (1980) for quinidine and lidocaine were used to generate these points. Quinidine and lidocaine differ considerably in their kinetics of block much as the aprindine derivative do.

For this search we constrained the voltage shift, k_i , and l_i to the same values as the full model, i.e., only values for K_dR and K_dO were searched. Such optimization

is required since the full model was not constrained to select values for k_r , l_r and k_o , l_o that yielded time constants that are short enough to always reach steady state. These rested and open state dissociation constants are shown in Table 6.3. For lidocaine the K_{dO} found by the simplified model was 9×10^{-5} compared to the value of 3×10^{-5} used by the full model. This discrepancy points up the differences between the two models. The values of k_o and l_o used in the full model produce block of open channels with a time constant 0.3 msec at the dose used. This compares with a mean open time (the amount of time the average channel is open) of 0.3 msec found in the full model. Thus the duration of the open state is too brief for equilibrium to occur. In the simplified model equilibrium is assumed to occur and thus the affinity found by the search was smaller in the simplified model. In general the affinity for the open state found by the simplified model will always be less than or equal to the full model. At the present time our knowledge of how drugs interact with open channels is too scanty to choose which of the models is a more accurate description of reality.

Comparisons between the two models are shown for quinidine (Figures 6.7 and 6.8) and lidocaine (Figures 6.9 and 6.10). Input to the simplified MRH consisted of four rate trains at 4, 2, 1 and .5 Hz, four trains at 3.3 Hz at

Lidocaine Model Parameters

	ki (M ⁻¹ ms ⁻¹)	li (M ⁻¹ ms ⁻¹)	V-shift (mV)	KdR (M)	KdO (M)
Full Model	50	.002	30	2.5	3x10 ⁻⁵
Simplified Model	50*	.002*	30*	.08	9x10 ⁻⁵

Quinidine Model Parameters

	ki	li	V-shift	KdR	KdO
Full Model	0	6x10 ⁻⁵	40	>>1	1x10 ⁻⁴
Simplified Model	0*	6x10 ⁻⁵ *	40*	1.08	2x10 ⁻⁴

* Parameter constrained to this value.

Table 6.3 Parameters used in the simulations shown in Figures 6.7 to 6.10. The full MRH model was used to generate 152 data points which were used as input to the simplified model.

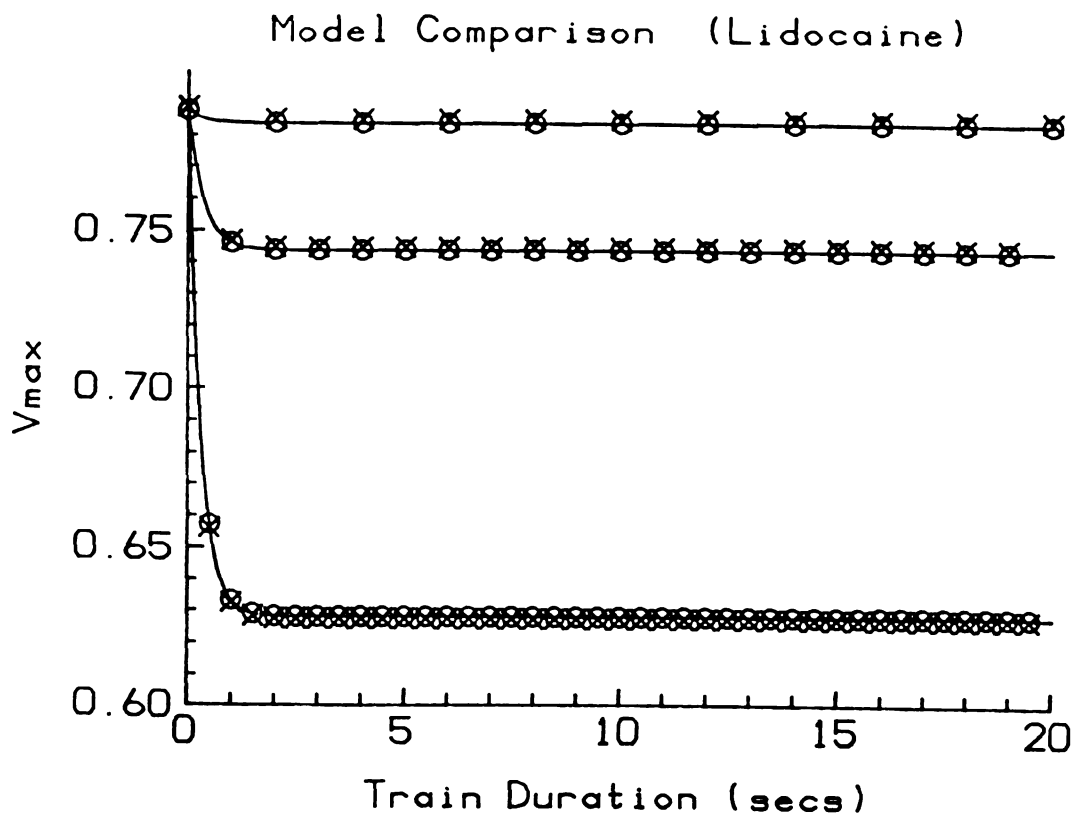


Figure 6.7 Model comparison of lidocaine rate trains

Comparison of trains of action potentials at 2, 1, and .5 Hz in the presence of lidocaine ($30 \mu\text{M}$). Circles are points generated by the full MRH model. Crosses are output of the simplified model after a search for model parameters. Parameters used in both simulations are shown in Table 7.3.

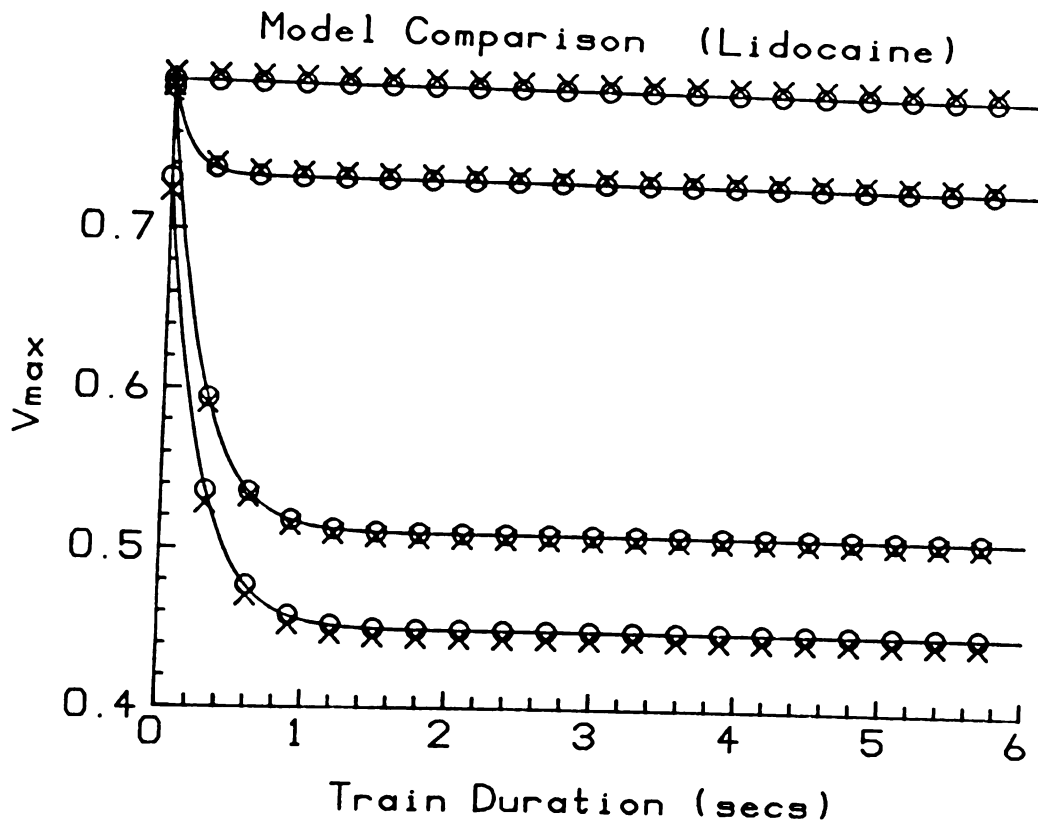


Figure 6.8 Model comparison of lidocaine rate trains

Comparison of 3.3 Hz trains of action potentials at -75, -85, -100, and -120 mV in the presence of lidocaine (30 μM). Circles are points generated by the full MRH model. Crosses are output of the simplified model after a search for model parameters. Parameters used in both simulations are shown in Table 6.3 .

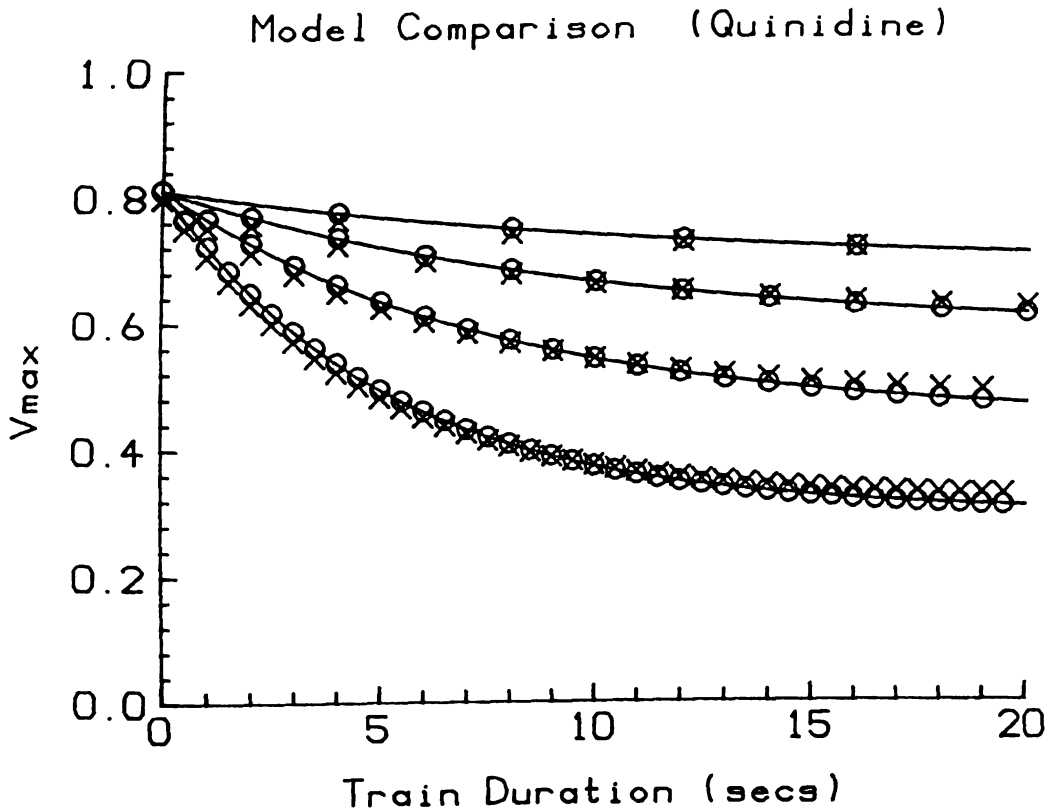


Figure 6.9 Model comparison of quinidine rate trains

Comparison of trains of action potentials at 4, 2, 1, and .5 Hz in the presence of quinidine ($15 \mu\text{M}$). Circles are points generated by the full MRH model. Crosses are output of the simplified model after a search for model parameters. Parameters used in both simulations are shown in Table 6.3 .

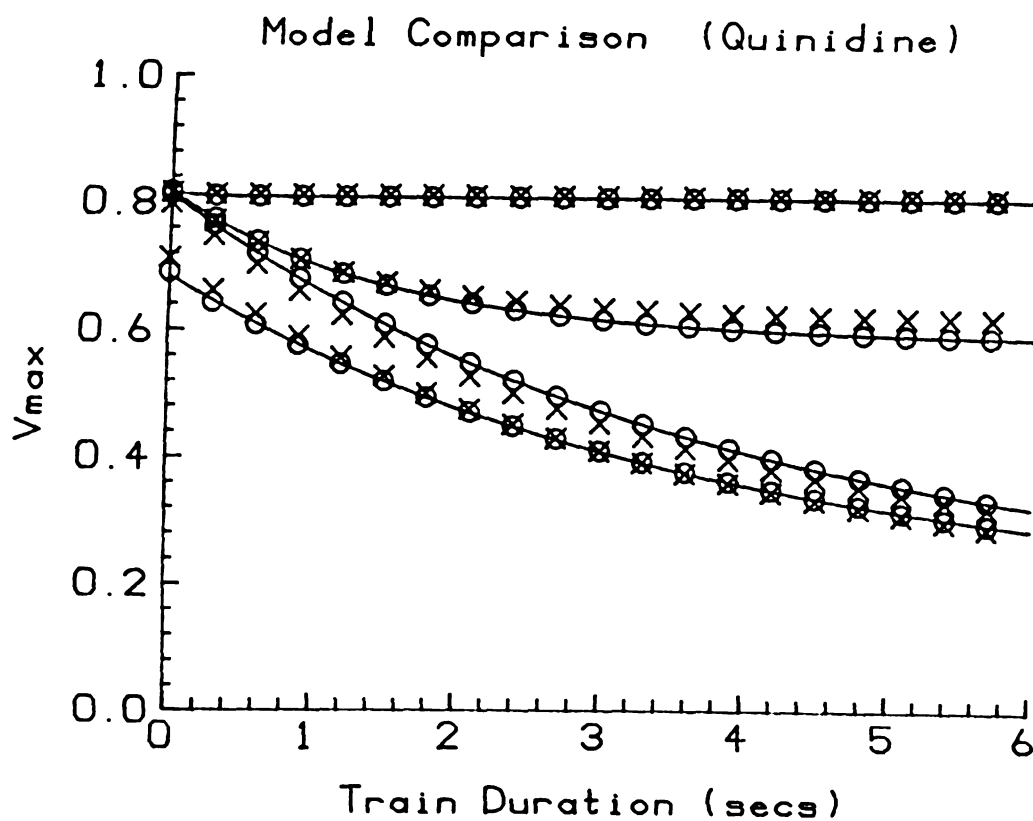


Figure 6.10 Model comparison of quinidine rate trains

Comparison of 3.3 Hz trains of action potentials at -75 , -85 , -100 , and -120 mV in the presence of quinidine ($15 \mu\text{M}$). Circles are points generated by the full MRH model. Crosses are output of the simplified model after a search for model parameters. Parameters used in both simulations are shown in Table 6.3.

-75, -85 -100, and -120 mV resting potential, and 5 recovery points for a total of 152 points. The rate and voltage drug effects are compared for the full model (circles) and simplified model (crosses) in each of the figures. From these figures we can conclude that the simplified model is quite successful in duplicating the behavior of the full model with drugs of differing kinetics under a variety of conditions.

6.5. Fit of experimental data

To further classify the kinetic properties of the aprindine derivatives we used the data obtained in the results section as input to the simplified MRH model.

Since single experiments showed different levels of tonic block, only results of a single experiment were used for these fits. The same fitting procedure was applied to each drug.

A global fit, using the pattern-search method to find parameters that minimize the least-square error, was used on data obtained from plateau clamp experiments. These data were expected to contain the greatest amount of information on the rate of block during the action potential after the upstroke. The MRH parameters that determine the rate and steady state level of block during the plateau are the rate constants k_i and l_i . The values of

k_i and l_i obtained from the model fit of the plateau data were used as starting values for k_i and l_i in subsequent model simulations, thus biasing further fits to these values.

Further model simulations were done on a set of data consisting of four trains at different rates and 10-20 recovery points occurring after a 3.3 Hz train. This data was used in a "grid" search for least square error parameters. In this grid search K_dO and K_dR were allowed to vary from 1 to 10^{-6} and V -shift between 10 and 100 Volts. k_i and l_i , constrained by the results of the plateau fits, were allowed to vary only one order of magnitude in either direction. The constraints on k_i and l_i were applied to minimize the number of model evaluations required. If these values were allowed to vary greatly they invariably fell within these bounds. The "grid" search evaluated every combination of about 10 possible values for each parameter. Thus approximately 50,000 separate model simulations were done. In the "grid" method a single simulation with a set of parameters was terminated when the accumulated error exceeded the minimum error found so far. In this manner the rate of simulations increased as the search progressed and the minimum error decreased. The 50,000 simulations with 90 experimental points took approximately one hour. The grid search method also had

the ability to report model parameters that had an error within 50 % of the current minimum. This served as a check so that greatly differing parameter combinations with about the same error could be evaluated in greater detail. In practice however, as the search progressed only one value of V-shift and l_i were found that produced an error within 50% of the minimum. In contrast, several combinations of K_dR , K_dO , and k_i were often found that could produce errors within these rather wide boundaries.

The set of parameters that the grid search found to produce the minimum error was used as starting values for a pattern search of the same data. Our implementation allows weighting of individual points as well as the weighting of trains. This weighting was important in causing the pattern search to converge from random starting values but made little difference when the fit was started from values obtained from the grid search.

The results of model fits to the data are shown in Table 6.4. From this table we note that none of the compounds had a significant affinity for rested state (K_dR). Any affinity for the rested state in the presence of a voltage shift would result in significant tonic block. In most experiments tonic block was less than 10 %. In contrast the affinity for open channels (k_dO) and inactivated channels (K_dI) varied over several orders of magnitude.

Compound	KdR	KdO	ki	li	DV	KdI	Sq.Err. *
1400	1.0*	3.6e-4	4.33	2.22e-5	34.1	5.12e-6	2.38e-3
1401	.89	.42	64.4	2.47e-4	57.0	3.84e-6	1.10e-3
1404	1.0*	4.1e-5	5.0e-4	2.36e-7	25.4	4.72e-4	5.18e-3
1622	1.0*	1.2e-3	56.2	7.00e-6	31.5	1.25e-7	2.79e-4
1704	.60	6.6e-4	40.4	1.51e-4	47.8	3.74e-6	2.26e-3
1800	1.0*	1.3e-4	5.05	2.00e-4	30.1	3.95e-5	1.16e-3
2077	.009	6.9e-5	122	2.06e-3	40.1	1.69e-5	7.19e-4
777	.022	.040	1190	7.38e-4	25.4	6.19e-7	1.22e-3
Aprindine	.73	2.9e-5	67.3	2.63e-4	53.6	3.91e-6	7.61e-3
Moxapridine	.046	1.2e-4	15.6	9.14e-5	34.7	5.84e-6	6.13e-4

* Parameter reached boundary of search.

** Sq. Err. = average square error per point.

Table 6.4 Parameters obtained using the modified MRH described in the text.

6.6. Model parameters and Physical Properties In order to determine which physical parameters might determine the model constants we calculated the correlation of all the model constants and K_{dI} against the physical constants pK_a , $\log P$, $\log Q$ and molecular weight. Of the various combinations the only significant correlations were between K_{dI} and pK_a , and between molecular weight and l_1 .

K_{dI} , the dissociation constant of the inactivated state was negatively correlated with pK_a . The coefficient of correlation for this was -0.89 ($p=0.0005$). This correlation corresponds to our finding that higher pK_a is associated with slower recovery from use-dependent block.

The other significant relationship was between molecular weight and l_1 ($r = -0.84$, $p=0.002$). Recovery from block in terms of the MRH requires movement of channels from the drug-associated inactivated pool ID into the R pool. An important route in this recovery is the movement from ID to I and thence to R. l_1 is the model constant that describes the initial step of this movement. Thus since our data showed a relationship between recovery time constant and molecular weight this is reflected in a relationship between molecular weight and the rate constant l_1 .

6.7. Conclusions

The results of MRH fits shown in Table 6.4 show that all the aprindine derivatives have a high affinity for the inactivated state and a low affinity for rested channels. The affinity for the open channel is less than for the inactivated state for all drugs except for the fast drug B-1404. Whether this difference between open and inactivated affinity is real or an artifact of considering open block instantaneous cannot be answered with our data. One thing that is clear is that inactivation block is an important mechanism for all these compounds. Kinetic experimental protocols that do not either control or accurately measure the action potential duration on a beat to beat basis will yield data that are subject to many inaccuracies. From the results presented here it is clear that many of the kinetic differences can be accounted for by considering physical properties, at least within a family of compounds. It is also clear that many more drugs and more rigorously controlled experimental data will be required to answer detailed questions about the role of molecular structure in determining rates of sodium channel block. The modified MRH model presented here may be a tool useful to that end.

Bibliography

- Akerman B (1973). Uptake and retention of the enantiomers of a local anesthetic in isolated nerve in relation to different degrees of blocking of nervous conduction. *Acta Pharmacol. Toxicol.* 32:225-236.
- Akerman SBA, Camougis G, Sandberg RA (1969). Stereoisomerism and differential activity in excitation block by local anaesthetics. *Eur. J. Pharmacol.* 8:337-347.
- Aldrich RW, Corey DP, Stevens CF (1983). A reinterpretation of mammalian sodium channel gating based on single channel recording. *Nature* 306:436-441.
- Anderson WG (1983). An improved model for assessment of positive inotropic activity in vitro. *Drug Development Res* 3:443-451.
- Armstrong CM, Gilly WF (1979). Fast and slow steps in the activation of sodium channels. *J. Gen. Physiol.* 74:691-711.
- Attwell D, Cohen I, Eisner DA (1981). The effects of heart rate on the action potential of guinea pig and human ventricular muscle. *J. Physiol.* 313:439-461.
- Buchi J, Perlia X (1971) Structure-activity relations and physico-chemical properties of local anesthetics. In: *International Encyclopedia of Pharmacology and Therapeutics: Local Anesthetics (vol I)*, Ed. Lechat P, Pergamon Press, Oxford pp 39-130.
- Cahalan MD (1978). Local anesthetic block of sodium channels in normal and pronase-treated squid giant axons. *Biophys J* 23:285-311.
- Cahalan MD, Almers W (1979). Interactions between quaternary lidocaine, the sodium channel gates, and tetrodotoxin. *Biophys. J.* 27: 39-56.

- Campbell TJ, VaughanWilliams EM (1983). Voltage- and time-dependent depression of maximum rate of depolarisation of guinea pig ventricular action potentials by two new antiarrhythmic drugs, flecainide and lorcainide. *Cardiovasc Res* 17:251-258.
- Campbell TJ (1983). Kinetics of onset of rate-dependent effects of Class I antiarrhythmic drugs are important in determining their effects on refractoriness in guinea pig ventricle, and provide a theoretical basis for their subclassification. *Cardiovasc Res* 17:344-352.
- Carmeliet EP, Verdonck F (1974). Effects of aprindine and lidocaine on transmembrane potentials and radioactive K efflux in different cardiac tissues. *Acta Cardiologica Supplementum XVIII* 73-90.
- Chen C-M, Gettes LS (1976). Combined effects of rate, membrane potential, and drugs on maximum rate of rise (V_{max}) of action potential upstroke of guinea pig papillary muscle. *Circ. Res.* 38:464-469.
- Chen C-M, Gettes LS, Katzung BG (1975). Effect of lidocaine and quinidine on steady state characteristics and recovery kinetics of $(dv/dt)_{max}$ in guinea pig ventricular myocardium. *Circ. Res.* 37:20-29.
- Clarkson CW, Mason JW, Matsubara T, Moyer JW, Hondeghem LM (1983). Slow inactivation in guinea pig ventricular myocardium. *Biophys J* 41:309a.
- Colatsky TJ (1982). Quinidine block of cardiac sodium channels is rate- and voltage-dependent. *Biophys. J.* 37:343a.
- Colatsky TJ (1982). Mechanisms of action of lidocaine and quinidine on action potential duration in rabbit cardiac Purkinje fibers. *Circ. Res.* 50:17-27.
- Courriere H, Paubel JP, Niviere P, Foussard-Blanpin O (1978). Structure activity study in a series of local anesthetic agents. *Eur. J. Med Chem.* 13:121-126.

- Courtney KR (1980). Interval-dependent effects of small antiarrhythmic drugs on excitability of guinea-pig myocardium. *J. Molec. Cell. Cardiol.* 12:1273-1286.
- Courtney KR (1980). Antiarrhythmic drug design: Frequency-dependent block in myocardium. *Molecular Mechanisms of Anesthesia (Progress in Anesthesiology, Vol. 2)*, edited by BR Fink, Raven Press, New York, pp 111-118.
- Courtney KR, Kendig JJ, Cohen EN (1978). Frequency-dependent conduction block: The role of nerve impulse pattern in local anesthetic potency. *Anesthesiology* 48:111-117.
- Courtney KR (1975). Mechanism of frequency-dependent inhibition of sodium currents in frog myelinated nerve by the lidocaine derivative GEA 968. *J. Pharmacol. Exp. Ther.* 195:225-236.
- Courtney KR (1981). Comparative actions of mexiletine on sodium channels in nerve, skeletal and cardiac muscle. *Eur. J. Pharmacol.* 74:9-18.
- Courtney KR, Etter EF (1983). Modulated anticonvulsant block of sodium channels in nerve and muscle. *Europ J Pharmacol* 88:1-9.
- Courtney KR (1983). Comments on "Mechanisms of quinidine-induced depression of maximum upstroke velocity in ovine cardiac Purkinje fibers" (Letters to the Editor). *Circ Res* 52:232.
- Courtney KR (1981). Slow sodium channel inactivation and the modulated receptor hypothesis :Application to phenobarbital. *B.B.A.* 642:.
- Courtney KR (1983). Quantifying antiarrhythmic drug blocking during action potentials in guinea-pig papillary muscle. *J Mol Cell Cardiol* 15:749-757.
- Dangman KH, Hoffman BF (1981). In vivo and in vitro antiarrhythmic and arrhythmogenic effects of N-Acetyl procainamide. *J. Pharmacol. Exp. Ther.* 217:851-862.

- Draper MH, Weidmann S (1951). Cardiac resting and action potentials recorded with an intracellular electrode. *J. Physiol.* 115:74-94.
- Ehring GR, Hondeghem LM (1980). Structural similarities and cardiac electrophysiological differences between lidocaine and procainamide. *Proc West Pharmacol Soc* 23:163-166.
- Eisner DA, Lederer WJ, Vaughan-Jones RD (1981). The dependence of sodium pumping and tension on intracellular sodium activity in voltage-clamped sheep Purkinje fibres. *J. Physiol.* 317:163-187.
- Gettes LS, Reuter H (1974). Slow recovery from inactivation of inward currents in mammalian myocardial fibres. *J. Physiol.* 240: 703-724.
- Gilmour RF Jr, Chikharev VN, Jurevichius JA, Zacharov SI, Zipes DP, Rosenshtraukh LV (1981). Effect of aprindine on transmembrane currents and contractile force in frog atria. *J Pharmacol Exp Ther* 217:390-396.
- Gintant GA, Hoffman BF, Naylor RE (1983). The influence of molecular form of local anesthetic-type antiarrhythmic agents on reduction of maximum upstroke velocity of canine cardiac Purkinje fibers. *Circ Res* 52:735-746.
- Gliklich JI, Hoffman BF (1978). Sites of action and active forms of Lidocaine and some derivatives on cardiac Purkinje fibers. *Circ Res* 43(4):638-651.
- Glitsch HG (1973). An effect of the electrogenic sodium pump on the membrane potential in beating guinea-pig atria. *Pflugers Arch.* 344:169-180.
- Grant AD, Trantham JL, Brown KK, Strauss HC (1982). pH-dependent effects of quinidine on the kinetics of dV/dt -max in guinea pig ventricular myocardium. *Circ. Res.* 50:210-217.
- Grant AO, Strauss LJ, Wallace AG, Strauss HC (1980). The influence of pH on the electrophysiological effects of lidocaine in guinea pig ventricular myocardium. *Circ. Res.* 47:542-550.

- Hauswirth O, Singh BN (1979). Ionic mechanisms in heart muscle in relation to the genesis and the pharmacological control of cardiac arrhythmias. *Pharmacol Rev* 30:5-63.
- Heistracher P (1971). Mechanism of action of antifibrillatory drugs. *Naunyn-Schmiedeberg's Arch. Pharmacol.* 269:199-212.
- Hille B, Courtney KR, Dum R (1975). Rate and site of action of local anesthetics in myelinated nerve fibers. book: *Molecular Mechanisms of Anesthesia*, edited by B.R.Fink, *Progress in Anesthesiology* vol 1. Raven Press New York.
- Hille B (1966). Common mode of action of three agents that decrease the transient change in sodium permeability in nerves. *Nature* 210:1220-1222.
- Hille B (1977). Local anesthetics: Hydrophilic and hydrophobic pathways for the drug-receptor reaction. *J gen Physiol* 69:497-515.
- Hodgkin AL (1951). The ionic basis of electrical activity in nerve and muscle. *Biol. Rev* 26:339-409.
- Hondeghem LM, Katzung BG (1984). Antiarrhythmic agents: The modulated receptor mechanism of action of sodium and calcium channel-blocking drugs. *Ann. Rev. Pharmacol. Toxicol.* 24:387-423.
- Hondeghem LM, Ehring GR, Moyer JW (1978). Observations on the nature of the voltage shift of antiarrhythmic drugs. *Proc West Pharmacol Soc* 21:67-69.
- Hondeghem LM, Katzung BG (1977). Time- and voltage-dependent interactions of antiarrhythmic drugs with cardiac sodium channels. *Biochim. Biophys. Acta* 472:373-398.
- Hondeghem LM, Katzung BG (1980). Test of a model of antiarrhythmic drug action. Effect of quinidine and lidocaine on myocardial conduction. *Circulation* 61:1217-1224.

- Hooke R, Jeeves TA (1961). Direct Search Solution of Numeric and Statistical Problems. J. Assoc Comp. Mach. , 8:212-229.
- Johnson EA, McKinnon MG (1957). The differential effect of quinidine and pyrilamine on the myocardial action potential at various rates of stimulation. J Pharmacol Exp Ther 120:460-468.
- Khodorov B, Shishkova L, Peganov E, Revenko S (1976). Inhibition of sodium currents in frog Ranvier node treated with local anesthetics. Role of slow sodium inactivation. Biochim. Biophys. Acta. 433:409-435.
- Kline RP, Cohen I, Falk R, Kupersmith J (1980). Activity-dependent extracellular K⁺ fluctuations in canine Purkinje fibres. Nature 286(5768):68-71.
- Kojima M, Ban T, Sada H (1982). Effects of disopyramide on the maximum rate of rise of action potential (V_{max}) in guinea-pig papillary muscles. Japan J Pharmacol 32:91-102.
- Lo M-VC, Shrager P (1981). Block and inactivation of sodium channels in nerve by amino acid derivatives. II. Dependence on temperature and drug concentration. Biophys J 35:1-16.
- Lofgren N (1948). Studies on Local Anesthetics: Xylocaine, a New synthetic Drug. Ivar Haeggströms Boktryckeri A.B., Stockholm.
- Lucchesi BR, Gibson JK, Patterson E (1982). Pharmacology of Antiarrhythmic drugs. In: Modern Pharmacology, Eds: Craig and Sitzel, Pub: Little, Brown & Co.
- Mason JW, Hondeghem LM, Katzung BG (1983). Amiodarone blocks inactivated cardiac sodium channels. Pflugers Arch. 396:79-81.
- Matsubara T, Hondeghem LM (1984). Activation versus inactivation block of sodium channels by quinidine in guinea pig papillary muscle. Proc West Pharmacol Soc 27:19-21.

- Matsubara T, Hondeghem LM (1983). Activation versus inactivation block of sodium channels in guinea pig ventricular muscle by lidocaine. *Circulation* 67:II-1000.
- Meyer H (1901). Zur Theorie der Alkolnarkose. Der Einfluss wechselnder Temperatur auf Wirkungsstärke und Theilungscoefficient der Narcotica. *Arch. Exp. Pathol. Pharmacol.* 46:338-346.
- Mirro MJ, Watanabe AM, Bailey JC (1981). Electrophysiological effects of the optical isomers of disopyramide and quinidine in the dog. Dependence on stereochemistry. *Circ. Res.* 48:867-874.
- Moyer J, Ehring G, Hondeghem L (1982). Kinetics of Interaction of a series of Aprindine Derivatives with the Cardiac Sodium Channel. *Fed. Proc.*
- Moyer JW, Hondeghem L (1978). Rate rhythm and voltage dependent effects of aprindine: a test model of the mechanisms of action of antiarrhythmic drugs. *Proc West Pharmacol Soc* 21:57-61.
- Narahashi T, Frazier DT, Yamada M (1970). The site of action and active form of local anesthetics. I. Theory and pH experiments with tertiary compounds. *J. Pharmacol. Exp. Ther.* 171:32-44.
- Nelson PH, Strosberg AM, Untch KG (1980). Mono- and Diaryl-2-quinuclidinylcarbinols with Local Anesthetic and Antiarrhythmic activity. *J. Med. Chem.* 23:180-184.
- Overton E (1896). Über die osmotischen Eigenschaften der Zelle in ihrer Bedeutung für die Toxikologie und Pharmakologie. *Z. Phys. Chem.* 22:189-209.
- Pisciotta AV, Cronkite C (1983). Aprindine induced Agranulocytosis. *Arch. Inter. Med.* 143:241-243.
- Ritchie JM, Ritchie B, Greengard P (1965). The active structure of local anesthetics. *J. Pharmacol. Exp. Ther.* 150:152-159.

- Ritchie JM (1975). Mechanism of action of local anaesthetic agents and biotoxins. *Br. J. Anaesth.* 47:191-198.
- Ritchie JM, Ritchie B (1968). Local anesthetics: Effects of pH on activity. *Science* 162:1394-95.
- Sada H, Ban T (1981). Frequency - dependent block of nerve conduction by b-adrenergic blocking agents. *Arch int Pharmacodyn* 254:134-144.
- Sada H (1978). Effect of phentolamine, alprenolol and prenylamine on maximum rate of rise of action potential in guinea-pig papillary muscles. *Naunyn-Schmiedeberg's Arch. Pharmacol.* 304:191-201.
- Sada H, Ban T (1981). Time independent effects on cardiac action potential upstroke velocity (resting block) and lipid solubility of beta adrenergic blockers. *Experientia* 37:171-172.
- Sada H, Ban T (1981). Effects of various structurally related beta-adrenoceptor blocking agents on maximum upstroke velocity of action potential in guinea pig papillary muscles. *Naunyn-Schmiedeberg's Arch. Pharmacol.* 317:245-251.
- Sada H, Ban T (1980). Effects of acebutolol and other structurally related beta adrenergic blockers on transmembrane action potential in guinea-pig papillary muscles. *J. Pharmacol. Exp. Ther.* 215:507-514.
- Sanchez-Chapula J, Tsuda Y, Josephson IR (1983). Voltage- and Use- Dependent effects of lidocaine on sodium current in rat single ventricular cells. *Circ Res* 52:557-565.
- Seeman P (1972). The membrane action of anesthetics and tranquilizers. *Pharmacol Rev* 24:583-655.
- Staessen J, Kesteloot H (1981). Moxapridine in the acute treatment of ventricular arrhythmias in patients with cardiovascular disease. *Eur. J. Clin. Pharmacol.* 19:167-172.

- Starmer CF, Grant AO, Strauss HC (1983). A model of the interaction of local anesthetics with Na channels. *Biophys J* 41:145a.
- Steinberg MI, Greenspan K (1976). Intracellular electrophysiological alterations in canine cardiac conducting tissue induced by aprindine and lignocaine. *Cardiovas Res* 10:236-244.
- Strichartz GR (1973). The inhibition of sodium currents in myelinated nerve by quaternary derivatives of lidocaine. *J. Gen. Physiol.* 62:37-57.
- Strobel GE, Bianchi CP (1970). Effects of pH gradients on action procaine and lidocaine in intact and desheathed nerves. *J. Pharmacol. Exp. Ther.* 172:1-17.
- TenEick RE, Yeh JZ, Robertson L (1980). Cellular electrophysiological effects of aprindine on cat papillary muscle. *Fed Proc* 39:966.
- VanLeeuwen R, Meyboom RHB (1976). Agranulocytosis and Aprindine. *Lancet* 1976;2:1137.
- Verdonck F, Vereecke J, Vlengels A (1974). Electrophysiological effects of aprindine on isolated heart preparations. *Eur J Pharmacol* 26:338-347.
- Weidmann S (1955). The effect of the cardiac membrane potential on the rapid availability of the sodium-carrying system. *J. Physiol* 127:2130224.
- Weidmann S (1955). Effects of calcium ions and local anesthetics on electrical properties of purkinje fibres. *J Physiol* 129:568-582.
- Weld FM, Coromilas J, Rottman JN, Bigger JT Jr (1982). Mechanism of quinidine-induced depression of maximum upstroke velocity in ovine cardiac Purkinje fibers. *Circ. Res.* 50:369-376.
- Wilde DJ (1964). *Optimum Seeking Methods*. PUB: Prentice Hall CITY: Englewood Cliffs, N.J.

- Yeh JZ (1980). Blockage of sodium channels by stereoisomers of local anesthetics. Mol. Mech. of Anes. (Prog. in Anesthesiol. Vol 2) ed. B. Raymond Fink, Raven Press.
- Yeh JZ, TenEick RE (1980). Voltage dependent block of Na channels in cat papillary muscle and squid axon produced by aprindine. Fed Proc 39:966.
- Yeh JZ, Narahashi T (1977). Kinetic analysis of pancuronium interaction with sodium channels in squid axon membranes. J Gen Physiol 69:2293-323.
- Zipes DP, Troup PJ (1978). New antiarrhythmic agents. Amiodarone, aprindine, disopyramide, ethmozin, mexiletine, tocainide, verapamil. Am. J. Cardiol. 41:1005-1024.

Appendix

The equations for the modified model are given in chapter 6. The following symbols are used throughout this derivation.

- R = Channels in the rested drug-free state.
- RD = Drug associated resting channels.
- O = Open channels.
- OD = Drug associated open channels.
- I = Inactivated drug-free channels.
- ID = Drug associated inactivated channels.
- [D] = Drug concentration.
- KdR = Rested state dissociation constant.
- KdO = Open state dissociation constant.
- A = Hodgkin-Huxley rate constant alpha-h.
- B = Hodgkin-Huxley rate constant beta-h.
- A' = alpha-h modified by the voltage shift.
- B' = beta-h modified by the voltage shift.
- li = Inactivated state dissociation rate constant.
- ki = Inactivated state association rate constant.

A.1 The closed states model

KdR is defined as:

$$(1) \quad (R \times [D]) / RD = KdR$$

Since R and RD are always at equilibrium:

$$(2) \quad RD = RX \quad \text{Where,} \quad X = [D]/KdR$$

From chapter 6 :

$$(3) \quad \frac{dR}{dt} + \frac{dRD}{dt} = AI + A'ID - BR - B'RD$$

Combining (2) and (3):

$$(4) \quad \frac{dR}{dt} = \frac{A * I}{(1+X)} + \frac{A' * ID}{(1+X)} - \frac{(B + B'*X) * R}{(1+X)}$$

The sum of all channels is equal to unity.

$$(5) \quad R + RD + I + ID = 1$$

Or,

$$(6) \quad ID = 1 - I - R(1+X)$$

Substituting (6) into (4) gives:

$$(7) \quad \frac{dR}{dt} = \frac{A-A'}{1+X} * I - A' + \frac{B+B'X}{1+X} * R + \frac{A'}{1+X}$$

and,

$$(8) \quad \frac{dR}{dt} = aI - bR + c \quad \text{where,}$$

$$a = A-A' \quad b = A' + \frac{B+B'X}{1+X} \quad c = \frac{A'}{1+X}$$

The change in the inactivated pool can be written as:

$$(9) \quad \frac{dI}{dt} = BR + (li * ID) - AI - (ki*[D]*I)$$

Substituting (6) into (9):

$$(10) \quad \frac{dI}{dt} = (B-li-li*X)*R - (li+ki*[D]+A)*I + li$$

Or,

$$(11) \quad \frac{dI}{dt} = f*R - g*I + h \quad \text{where,}$$

$$f = (B-li-li*X) \quad g = (li+kiD+A) \quad h = li$$

Equations (8) and (11) together with (6) define the movement of channels during the closed states. To solve (8) and (11) we perform a Laplace transform and obtain:

$$(12) \quad s*i(s) - I_0 = f*r(s) - g*i(s) + h/s \quad \text{and,}$$

$$(13) \quad s*r(s) - R_0 = a*i(s) - b*r(s) + c/s$$

Where R_0 and I_0 are the initial values of I and R .

Rearranging (12) and (13) give :

$$(14) \quad r(s) = \frac{a \cdot i(s) + c/s + R_0}{(s + b)}$$

$$(15) \quad i(s) = \frac{f \cdot r(s) + h/s + I_0}{(s + g)}$$

Substituting (14) into (15) :

$$(16) \quad i(s) = \frac{I_0 \cdot s + (c+hb)/s + (R_0 + gh)}{s^2 + (b+g) \cdot s + (bg - fa)}$$

Similarly,

$$(17) \quad r(s) = \frac{R_0 \cdot s + (h+cg)/s + (I_0 + bc)}{s^2 + (b+g) \cdot s + (bg - fa)}$$

We note that the denominator of these expressions are in quadratic form and use the quadratic formula to extract the roots. Thus,

$$(18) \quad -z_1 = \frac{(b+g) - \sqrt{(b+g)^2 - 4(bg - fa)}}{2}$$

and,

$$(19) \quad -z_2 = \frac{(b+g) + \sqrt{(b+g)^2 - 4(bg - fa)}}{2}$$

The denominator in (16) and (17) can be written:

$$(s + z_1)(s + z_2)$$

Now (16) can be rewritten:

$$(20) \quad i(s) = \frac{I_0 \cdot s}{(s+z_1)(s+z_2)} + \frac{(c+hb)/s}{(s+z_1)(s+z_2)} + \frac{(R_0 + gh)}{(s+z_1)(s+z_2)}$$

Noting that the reverse transform with respect to t is:

$$1/(s+z_1)(s+z_2) = (\exp(-z_1 \cdot t) - \exp(-z_2 \cdot t)) / (z_2 - z_1)$$

The reverse Laplace transform of (20) becomes:

$$(21) \quad I(t) = \frac{d}{dt} \left[\frac{\exp(-Z_1 t) - \exp(-Z_2 t)}{(Z_2 - Z_1)} \right] * I_0$$

$$+ (c+hb) \int_0^t \frac{\exp(-Z_1 t) - \exp(-Z_2 t)}{(Z_2 - Z_1)} dt$$

$$+ (Ro+gb) \frac{\exp(-Z_1 t) - \exp(-Z_2 t)}{(Z_2 - Z_1)} .$$

Or,

$$(22) \quad I(t) = \frac{(-Z_1 \exp(-Z_1 t) + Z_2 \exp(-Z_2 t)) * I_0}{(Z_2 - Z_1)}$$

$$+ (c+hb) * \frac{((\exp(-Z_1 t) - 1) / -Z_1) - ((\exp(-Z_2 t) - 1) / -Z_2)}{(Z_2 - Z_1)}$$

$$+ (Ro+gb) * \frac{\exp(-Z_1 t) - \exp(-Z_2 t)}{(Z_2 - Z_1)} .$$

By a similar methods (17) can be transformed into:

$$(23) \quad R(t) = \frac{(-Z_1 \exp(-Z_1 t) + Z_2 \exp(-Z_2 t)) * R_0}{(Z_2 - Z_1)}$$

$$+ (h+cg) * \frac{((\exp(-Z_1 t) - 1) / -Z_1) - ((\exp(-Z_2 t) - 1) / -Z_2)}{(Z_2 - Z_1)}$$

$$+ (I_0+bc) \frac{\exp(-Z_1 t) - \exp(-Z_2 t)}{(Z_2 - Z_1)} .$$

Equations (22) and (23) together with (5) allow the computation of all the channel pools at any time t.

A.2 The active state model

In the activated state channels in the rested state distribute themselves according to a fixed fraction into the I and ID pool.

$$(24) \quad F = (OD) / (OD + O)$$

and ,

$$(25) \quad O * [D] / OD = KdO$$

combining (24) and (25) gives the fraction in terms of KdO:

$$(26) \quad F = 1 / (1 + (KdO/[D]))$$

The "block" occurring during activation is:

$$(27) \quad \text{block} = F*(R+RD)$$

Therefore at the end of activation:

$$(28) \quad ID = IDo + \text{block}$$

Or,

$$(29) \quad ID = IDo + F*(R+RD)$$

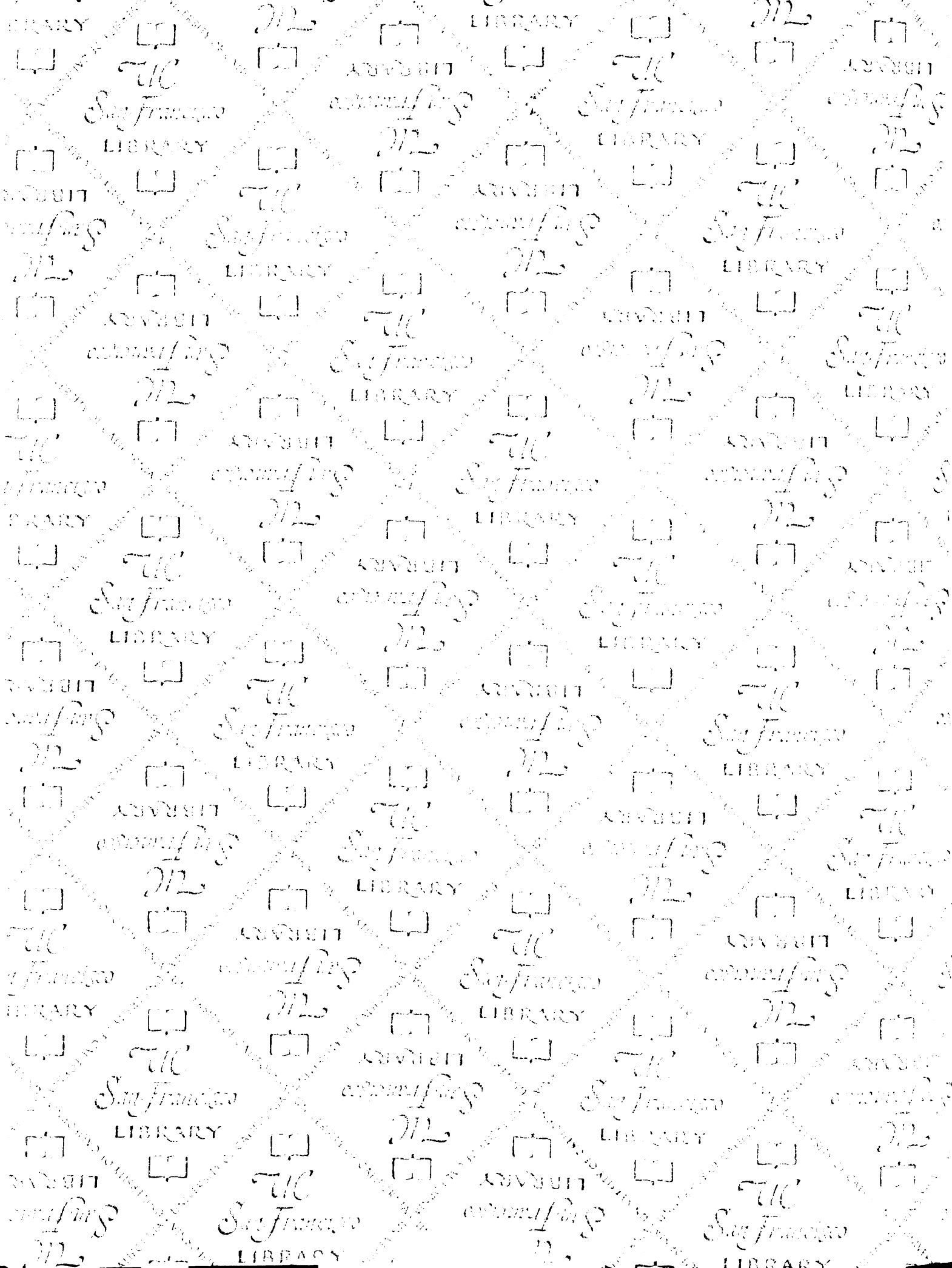
and,

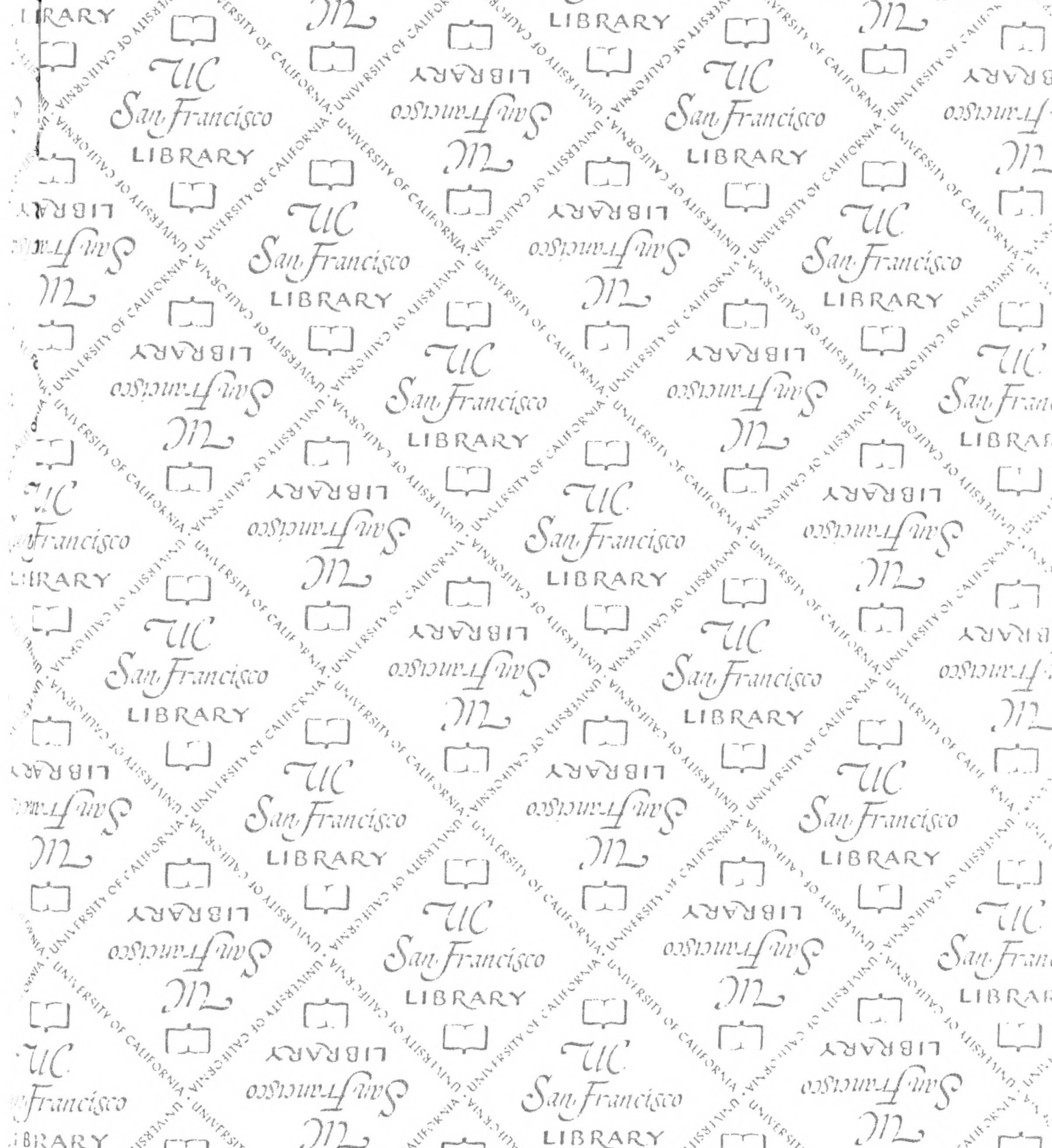
$$(30) \quad I = Io + (1-F)*(R+RD) = 1 - ID$$

Vmax is proportional to the channels in R before activation minus the block occurring before the time of vmax.

$$(31) \quad Vmax = R - ((R/(RD+R))*C*\text{block})$$

Where C is the fraction of open time before the time of Vmax. In our modeling we set C to 0.11 .





FOR REFERENCE

NOT TO BE TAKEN FROM THE ROOM



CAT. NO. 23 012

PRINTED
IN U.S.A.

